

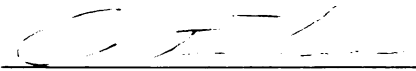




This is to certify that the  
dissertation entitled  
THE RETINO-HYPOTHALAMO-SPINAL PATHWAY WHICH  
MEDIATES GONADAL RESPONSES TO PHOTOPERIOD  
IN SYRIAN HAMSTERS  
presented by

TIMOTHY GRANT YOUNGSTROM

has been accepted towards fulfillment  
of the requirements for  
PH.D. Neuroscience/  
degree in Psychology



Major professor

Date DECEMBER 18, 1989



PLACE IN RETURN BOX to remove this checkout from your record.  
TO AVOID FINES return on or before date due.

DATE DUE	DATE DUE	DATE DUE
MAR 10 1994		

MSU Is An Affirmative Action/Equal Opportunity Institution

c:\circ\dtedue.pm3-p.1

**THE RETINO-HYPOTHALAMO-SPINAL PATHWAY WHICH MEDIATES  
GONADAL RESPONSES TO PHOTOPERIOD IN SYRIAN HAMSTERS**

**By**

**Timothy Grant Youngstrom**

**A DISSERTATION**

**Submitted to  
Michigan State University  
in partial fulfillment of the requirements  
for the degree of**

**DOCTOR OF PHILOSOPHY**

**Department of Psychology and Neuroscience Program**

**1989**



**ABSTRACT****THE RETINO-HYPOTHALAMO-SPINAL PATHWAY WHICH MEDIATES  
GONADAL RESPONSES TO PHOTOPERIOD IN SYRIAN HAMSTERS****by****Timothy Grant Youngstrom**

The reproductive system of the Syrian hamster is sensitive to changes in photoperiod. The pineal hormone, melatonin, is involved in many of the changes observed in the reproductive system. However, the interpretation of functional data obtained in the study of the multisynaptic pathway mediating the circadian rhythm of melatonin production and photoperiodism has relied on anatomical data obtained from the nonphotoperiodic rat. The present study examined the anatomical features of two segments of this circuit at the light microscopic level in hamsters.

Intraocular injections of horseradish peroxidase conjugated to Cholera toxin (CT-HRP) stained retinal ganglion cell (RGC) efferents in a number of structures of the hypothalamus (including the suprachiasmatic nuclei [SCN]), anterior thalamus and piriform cortex. Retinal input to selected sites was confirmed by retrograde labeling of RGCs following injections of fluorescent dye-labeled latex microspheres aimed at these targets. Not all effects of photoperiod in the hamster are mediated by pineal melatonin. Some extra-SCN sites receiving retinal input may participate in the expression of pineal-independent photoperiodism.

A second segment of the circuit is thought to involve the hypothalamic paraventricular nuclei (PVN). Iontophoretically applied *Phaseolus vulgaris*-leucoagglutinin labeled efferent fibers of PVN neurons with apparent terminal fields in the spinal cord, including the intermediolateral cell column. Spinal cord injections of CT-HRP or wheat germ agglutinin-HRP were employed to retrogradely label PVN neurons; these injections labeled fibers of PVN origin that organized themselves into four tracts on their path to the spinal cord.

Electrolytic lesions of one of these tracts at an extra-hypothalamic site failed to prevent gonadal regression in short-day male hamsters, in contrast to the effects of lesions made in the hypothalamus. Thus, PVN fibers in the dorsal midline tract do not appear to be involved in mediating the effects of photoperiod on the reproductive system of the male Syrian hamster. Bilateral parasagittal knife cuts made lateral to the PVN are effective in preventing gonadal regression in Syrian hamsters suggesting that the lateral PVN-spinal cord efferents labeled by HRP conjugates are involved in the control of photoperiodism in this species.

**To my best love MARTHA,**

**I'M DONE!**

**NOW we may go.**

## **ACKNOWLEDGEMENTS**

I would like to thank the members of my committee, Drs. Antonio A. Nunez, Cheryl L. Sisk, John I. Johnson and Charles D. Tweedle for their assistance and suggestions. The author would like to thank Dr. Nunez for his support and the use of his facilities. The assistance of a number of people was essential for the completion of these projects and the author is grateful for each person's many hours of participation. Special thanks to those graduate students I have often turned to with questions and were able to provide me with useful comments, assistance and support, Ken Smithson and Barb Modney. A significant contribution to those studies employing CT- and WGA-HRP was made by Dr. Mark L. Weiss of M.S.U. who made most of the conjugates with me and Dr. Richard R. Miselis of the University of Pennsylvania who provided laboratory facilities to create some of these conjugates. Mark has also been a valuable source of information and help in several of these projects. The author is grateful to Betti Weiss for her skillful drawing of one of the figures used in this paper. The author also thanks Dr. Glenn I. Hatton for permitting the use of his equipment for the evaluation of fluorescent dye labeled tissue and his service on the dissertation committee. This work was supported in part by NIMH Grant MH 37877 to Dr. A.A. Nunez and by Biomedical Research Funds from Michigan State University.

## TABLE OF CONTENTS

LIST OF TABLES . . . . .	v
LIST OF FIGURES . . . . .	vi
LIST OF ABBREVIATIONS . . . . .	xiii
INTRODUCTION . . . . .	1
EXPERIMENT Ia-Retinal Efferent Projections to the Hypothalamus and Basal Forebrain Identified by Anterogradely Transported CT-HRP. . . . .	7
METHOD . . . . .	9
RESULTS . . . . .	11
EXPERIMENT Ib-Retinal Efferent Projections to the Hypothalamus and Basal Forebrain: Retinal Neurons Retrogradely Labeled by Fluorescent Dye. . . . .	33
METHOD . . . . .	34
RESULTS . . . . .	37
DISCUSSION . . . . .	43
EXPERIMENT IIa-The PVN Efferent Pathway to the Spinal Cord Identified by Iontophoretically Applied Phaseolus vulgaris- Leucoagglutinin. . . . .	51
METHOD . . . . .	53
RESULTS . . . . .	54
EXPERIMENT IIb-The PVN Efferent Pathway to the Spinal Cord: Retrograde labeling of Neurons and Fibers in the PVN and LHA. . . . .	66
METHOD . . . . .	69
RESULTS . . . . .	71

DISCUSSION . . . . .	84
EXPERIMENT III-Do Extrahypothalamic Lesions of a PVN to Spinal Cord Pathway (Tract 1) Block the Testicular Response to Photoperiod? . . . . .	89
METHOD . . . . .	91
RESULTS . . . . .	94
DISCUSSION . . . . .	94
GENERAL DISCUSSION . . . . .	100
PHOTOPERIODISM . . . . .	100
RGC INPUT TO THE BASAL FOREBRAIN . . . . .	102
PARAVENTRICULO-SPINAL CORD CONNECTIONS . . . . .	103
NEURAL CONTROL OF THE CIRCADIAN RHYTHM OF PINEAL MEL SYNTHESIS . . . . .	105
SPECIES SPECIFIC ANATOMY . . . . .	107
BIBLIOGRAPHY . . . . .	110

## LIST OF TABLES

<b>Table 1. Sites Receiving Retinal Ganglion Cell Efferents in the Syrian Hamster . . . . .</b>	<b>.12</b>
<b>Table 2. Areas of the CNS Containing PHA-L Stained PVN Efferents . . . . .</b>	<b>.62</b>
<b>Table 3. Areas of the Brain Containing Retrogradely Labeled Neurons Following Injections of CT- and WGA-HRP into the Spinal Cord. . . . .</b>	<b>.73</b>
<b>Table 4. Final Mean Width (<math>\pm</math> sem) of Right Testis of Male Syrian Hamsters in Experiment III . . . . .</b>	<b>.95</b>

## LIST OF FIGURES

- Figure 1.** Camera lucida drawings of coronal sections through the brain of a Syrian hamster that received a unilateral intraocular injection of CT-HRP (3  $\mu$ l) into the left (L) eye. The distribution of staining was asymmetrical with the highest density of label in the hemisphere contralateral (viewer's left) to the injected eye. All of the illustrations are drawn to the same scale (Bar [A & E]= 500  $\mu$ m). For a definition of the abbreviations used in this and subsequent figures refer to the *List of Abbreviations*, p. xlii. . . . . 13
- Figure 2.** Photomicrograph (A) of a coronal section (50  $\mu$ m) through the caudal half of the SCN of an animal that received a unilateral injection of CT-HRP into the left eye. Labeling was present throughout each nucleus, including the dorso-medial crescent (arrows) adjacent to the ventral wall of the third ventricle which was relatively less densely labeling. Some labeled fibers continued dorsally through and around the SCN terminating in the overlying anterior hypothalamic area (AHA; darkfield illumination; Bar = 200  $\mu$ m). The box in (B) outlines the area depicted in (A). . . . 16
- Figure 3.** Schematic drawing (A) of a coronal section through the hypothalamus depicting the area (BOX) shown in (B). B - CT-HRP labeled fibers passed dorsally through the SCN and AHA to terminate in the AHA ventral to the PVN, while other fibers coursed along the ventral PVN. Some fibers ended along the ventral border while others ended in the PVN or continued dorsally into the ZI. Photomicrograph of a coronal section (50  $\mu$ m) through the middle of the PVN. (darkfield illumination; Bar = 200  $\mu$ m) . . . . . 19



**Figure 4. Photomicrograph of the same coronal section shown in Figure 2. Labeled fibers emerged from the lateral OC and coursed dorso-medially. Some fibers approached the fornix and PVN but could not be traced into the PVN. (darkfield illumination; Bar = 100  $\mu$ m) . . . . . 21**

**Figure 5. Photomicrograph of a coronal section through the OVLT. CT-HRP labeled fibers emerged from the OC contralateral to the injected eye near the SCN and turned rostrally to enter the POA. Some fibers continued rostrally into the horizontal band of the DBB, ending in the vicinity of the OVLT. A few continued dorsally in the vertical limb of the DBB and ended near the MS (darkfield illumination; Bar = 100  $\mu$ m). The location of the fibers shown in (A) is outlined in the schematic drawing (B). . . . . 23**

**Figure 6. Camera lucida drawing of a tissue section cut in a horizontal plane and stained for CT-HRP. Some labeled fibers emerged from the lateral half of the optic chiasm and coursed rostro-medially to the level of the OVLT. (Bar = 200  $\mu$ m) . . . . . 26**

**Figure 7. A fascicle of CT-HRP labeled RGC efferents emerged from the lateral OC at the level of the caudal SCN and turned ventro-laterally, entering layer 1 $\alpha$  of the Pyr (A; Bar = 200  $\mu$ m). At higher magnification (B) individual fibers with occasional varicosities along their length were seen turning dorsally and ending in small swellings in layer 1A (Bar = 20  $\mu$ m). (brightfield illumination) . . . . . 27**

**Figure 8. Photomicrograph (A) of a coronal section through the SON. In the rostral hypothalamus, CT-HRP labeled fibers emerged from the lateral OC and passed laterally over the SON where some fibers terminated in the dorsal SON.**

This bundle of fiber terminated in the dorsal SON. This bundle of fibers extended ventro-laterally into the Pyr (darkfield illumination; Bar = 20  $\mu$ m). The box in (B) indicates the location of the fibers shown in (A). . . . . 29

**Figure 9.** Photomicrograph of a coronal section through the rostral pole of the anterior thalamic nuclei. A small bundle of CT-HRP labeled fibers joined the stria terminalis (ST) as they continued from the LGN and ended in the TAM/TAV (darkfield illumination; Bar = 50  $\mu$ m; see Figure 1C for location of fibers) . . . . . 31

**Figure 10.** Photomicrograph of representative RGCs retrogradely labeled with RLM. The cells are from an animal that received a bilateral injection of RLM into the PVN (A) or POA (B) and represent the range in size of somata that were labeled. (epifluorescence illumination; Bar =20  $\mu$ m) . . .38

**Figure 11.** Camera lucida drawing of a coronal section through the hypothalamus at the level of bilateral RLM injections into the area of the PVN/ZI in a Syrian hamster. The center of each injection is marked by a dot. The total number of labeled cells counted in the retinae of each animal ranged between 2 and 12. . . . . 39

**Figure 12.** Schematic representation of the POA at the level of bilateral RLM injection into the brain of a hamster. The center of each injections is marked by a dot. The total number of cells labeled in each animal ranged between 3 and 15. (Illustration adapted from Maragos, *et al.*, 1989) . . .41

**Figure 13.** Schematic representation of the brain of a Syrian hamster at the level of bilateral RLM injections into the rostral thalamus. The center of each injection is marked

by a dot. The total number of cells labeled in each animal ranged between 2 and 9. (Illustration adapted from Maragos, <i>et al.</i> , 1989) . . . . .	42
Figure 14. Schematic drawings of the center of PHA-L injections to show their location in the brain. The numbers in the lower left corner refer to the case number (Cor -coronal section; Sag-sagittal section). . . . .	55
Figure 15 . Photomicrograph of a coronal section through the center of a PHA-L injection site confined to the PVN (G16). (brightfield illumination; Bar = 50 $\mu$ m) . . . . .	59
Figure 16. Camera lucida drawings of coronal sections through the brain of a hamster (G16) that received an iontophoretic injection of PHA-L into the lateral PVN. Some fibers emerging dorsally (1a & 1b) and ventro-laterally (2) from the PVN and formed tracts that followed separate trajectories to the periaqueductal grey (PAG). (Bar = 300 $\mu$ m) . . . . .	61
Figure 17. Schematic drawings of horizontal sections of the caudal brainstem and spinal cord (cervical and rostral thoracic) from an animal that received an iontophoretic injection of PHA-L into the left (L) PVN (G16). Drawings are arranged dorsal (A) to ventral (C) and are composites of 4 sections taken from each third of the spinal cord. . . . .	64
Figure 18. Schematic drawing demonstrating the vertebra, dorsal spines and spinal cord of the upper thoracic and cervical spinal column (a) of a Syrian hamster depicting the location of the glass pipette-tipped 1- $\mu$ l Hamilton syringe (b) used to inject the HRP conjugates into the lateral spinal cord (c). . . . .	70

**Figure 19.** Camera lucida drawings of coronal sections through the brain of a male Syrian hamster that received a unilateral injection of WGA-HRP into the spinal cord between vertebra C7 and T1. Labeling in the brain was predominantly ipsilateral to the injection site. Four tracts (labeled '1', '2', '3' & '4' in [B]) of stained fibers were seen to emanate from the PVN. (Bar [A & D] = 500  $\mu$ m) . . . . .74

**Figure 20.** Photomicrograph of a coronal section through the rostral PVN of a Syrian hamster. The dorsal and ventro-lateral PVN ipsilateral to an injection of WGA-HRP into the spinal cord contained retrogradely labeled neurons and fibers. Tract 3 was prominent as fibers from the PVN course ventro-laterally around the fornix. A few fibers were seen over the roof of the third ventricle (Tract 1), lateral to the PVN (Tract 2) and ventral to the PVN (Tract 4). Scattered labeled cells were also seen in the ipsilateral hypothalamus and contralateral PVN. (darkfield illumination; Bar = 200  $\mu$ m) . . . . .75

**Figure 21.** Photomicrograph of a coronal section near the middle of the PVN. A collection of retrogradely labeled cells were observed in the dorsal and ventro-lateral PVN. Fibers of Tract 3 remained evident around the fornix. Some fibers of the dorsal cell group were traced to the area over the third ventricle. (darkfield illumination; Bar = 200  $\mu$ m) . . . . .76

**Figure 22.** Photomicrograph of a coronal section through the caudal third of the PVN showing the nucleus ipsilateral to the injection site. The lateral parvocellular subdivision (as defined for the rat by Swanson & Kuypers[1980]) was intensely labeled and few individual cells could be seen distinctly from the background of labeling. The ventro-medial portion of the PVN contained fewer labeled cells than the lateral division while the fewest number of cells

were observed in the medial PVN. (darkfield illumination;  
 Bar = 200  $\mu$ m) . . . . .78

**Figure 23.** Photomicrograph of a coronal section through the caudal PVN. WGA-HRP labeled cells were present in the PVN and scattered through the LHA. At this level, fibers of Tract 2 split into two bundles. One fascicle turned ventrally (b) to join Tract 3 in the caudal hypothalamus while the second turned dorso-laterally over the CP (a). (darkfield illumination;Bar=200  $\mu$ m) . . . . .79

**Figure 24.** Photomicrograph of a coronal section near the level of Figure 21. The PVN is just out of the field depicted dorsally and to the viewer's left. Numerous fibers emerged from the ventral border of the PVN and surrounded or passed through the fornix. (darkfield illumination; Bar = 50  $\mu$ m) . . . . .81

**Figure 25.** Photomicrograph of a coronal section near the level of Figure 20, showing labeled fibers of Tract 4 near the wall of the third ventricle. (darkfield illumination; Bar = 50  $\mu$ m)  
 83

**Figure 26.** Mean width of the right testis (measured trans-scrotally) of animals receiving electrolytic lesions aimed at the PAG or sham-lesioned. Animals were lesioned (LES; n = 8) or sham lesioned (SDS; n = 7) and placed in a 8L:16D photoperiod, or sham lesioned and placed in a 16L:8D photoperiod (long-day sham [LDS]; n = 4). The mean testicular width for each short photoperiod housed groups was significantly smaller than that of the LDS group by the end of Week 8 and remained so until the end of the experiment. . . . . 96

**Figure 27. Mean body weight of animals receiving electrolytic lesions aimed at the PAG or sham-lesioned. Animals were lesioned (LES; n = 8) or sham lesioned (SDS; n = 7) and placed in a 8L:16D photoperiod, or sham lesioned and placed in a 16L:8D photoperiod (long-day sham [LDS]; n = 4). A nonsignificant decline in the mean body weight was observed in both short-photoperiod housed groups. Week zero represents the mean presurgical body weight of each group. . . . . 97**

## LIST OF ABBREVIATIONS

3V	Third Ventricle	MoV	Trigeminal Motor Nucleus
AC	Anterior Commissure	MPoA	Medial Preoptic Area
ADT	Anterior Dorsal Thalamic Nucleus	MPoN	Medial Preoptic Nucleus
AHA	Anterior Hypothalamic Area	MS	Medial Septum
AMB	Nucleus Ambiguus	MT	Mammillothalamic Tract
AP	Area Postrema	MTN	Medial Terminal Nucleus
BLX	Olfactory Bulbectomy	NST	Nucleus of the Solitary Tract
BNST	Bed Nucleus of the Stria Terminalis	OC	Optic Chiasm
C <sub>7</sub>	Cervical Vertebra 7	ON	Optic Nerve
Cor	Coronal	OT	Optic Tract
CP	Cerebral Peduncle	OVL	Organum Vasculosum of the Lamina Terminalis
CT-HRP	Cholera Toxin-Horseradish Peroxidase	PAG	Periaqueductal Grey
DBB	Diagonal Band of Broca	PB	Parabrachial Nucleus
DMN	Dorsomedial Nucleus	PC	Posterior Commissure
DMN <sub>pc</sub>	Dorsomedial Nucleus, <i>pars compacta</i>	PEG	Polyethylene Glycol
DMT	Dorsomedial Terminal Nucleus	PHA-L	<i>Phaseolus vulgaris</i> -leucoagglutinin
DNV	Dorsal Nucleus of the Vagus	Pn	Pons
DV	dorso-ventral	POA	Preoptic Area
F	Fornix	PRL	Prolactin
FR	Fasciculus Retroflexus	PT	Paratenial Nucleus
FSH	Follicle Stimulating Hormone	PVN	Hypothalamic Paraventricular Nucleus
H	Habenula	PVT	Thalamic Paraventricular Nucleus
IC	Internal Capsule	Pyr	Piriform Cortex
IGL	Intergeniculate Leaflet	Pyr <sub>I</sub>	Piriform Cortex, layer I
III	Third Ventricle	RC	rostral-caudal
IML	Intermediolateral Cell Column	RGC	Retinal Ganglion Cells
L	Left	RHT	Retino-Hypothalamic Tract
LC	Locus Coeruleus	RLM	Rhodamine Labeled Latex Microspheres
LD	Light-Dark	RPA	Raphe Pallidus Nucleus
LGN	Lateral Geniculate Nucleus	RPM	Raphe Magnus Nucleus
LH	Luteinizing Hormone	RPO	Raphe Obscurus Nucleus
LHA	Lateral Hypothalamic Area	Sag	Sagittal
LL	Lateral Lemniscus	SCG	Superior Cervical Ganglion
LOT	Lateral Olfactory Tract	SCN	Suprachiasmatic Nuclei
LPoA	Lateral Preoptic Area	SM	Stria Medullaris
LTN	Lateral Terminal Nucleus	SN	Substantia Nigra
MEL	Melatonin	SO	Subcommissural Organ
MFB	Medial Forebrain Bundle	SOL	Nucleus of the Solitary Tract
MH(a)	Medial Habenula	SON	Supraoptic Nucleus
ML	medio-lateral	ST	Stria Terminalis
		T <sub>2</sub>	Thoracic Vertebra 2

<b>TAM</b>	<b>Antero-Medial Thalamic Nucleus</b>
<b>TAV</b>	<b>Antero-Ventral Thalamic Nucleus</b>
<b>Tu</b>	<b>Olfactory Tubercle</b>
<b>V III</b>	<b>Vestibulocochlear Nerve</b>
<b>VMN</b>	<b>Ventromedial Nucleus</b>
<b>Vs</b>	<b>Trigeminal Sensory Tract</b>
<b>WGA-HRP</b>	<b>Wheat Germ Agglutinin-Horseradish Peroxidase</b>
<b>ZI</b>	<b>Zona Incerta</b>



## INTRODUCTION

The reproductive systems of a large number of seasonally breeding mammals are sensitive to changes in daylength (photoperiod). The response of the reproductive system to changes in photoperiod results from an interaction of the endogenous circadian system and the light-dark (LD) cycle (Elliot & Goldman, 1981; Bittman, 1984). In the Syrian hamster, prolonged exposure to short photoperiods (<12.5 hr) induces a marked alteration in the reproductive system expressed, in part, as gonadal regression and sexual quiescence (Gaston & Menaker, 1967; Seegal & Goldman, 1975). The pineal hormone, melatonin (MEL), is intimately involved in the control of these photoperiodic responses (Bittman & Karsch, 1984; Bittman, *et al.*, 1985; Carter & Goldman, 1983; Goldman & Darrow, 1983; Bartness & Goldman, 1988). The concentration of MEL in the pineal gland and in the systemic circulation displays a circadian rhythm with peak levels occurring during the dark phase (night) of the LD cycle (Tamarkin, *et al.*, 1979; Bittman, *et al.*, 1983; Rollag, *et al.*, 1978; Klein, 1979). The duration of elevated MEL is inversely proportional to the prevailing photoperiod. Long durations of elevated MEL are associated with short photoperiods while long photoperiods are associated with MEL elevated for shorter intervals (Rollag, *et al.*, 1978; Goldman, *et al.*, 1981; Illnerova & Vanecek, 1982b). Of the several parameters of MEL release that may provide information to the nervous system about photoperiod, duration of elevated MEL has been shown to be a critical factor determining the reproductive state of the Siberian hamster, a long photoperiod breeder (Carter & Goldman, 1983; Bartness & Goldman, 1988) and the sheep, a short photoperiod breeder (Bittman, *et al.*, 1985).

The effects of light on pineal MEL concentration appear to involve direct retino-hypothalamic tract (RHT) input to the hypothalamic suprachiasmatic nuclei (SCN; Tamarkin, *et al.*, 1985; Klein & Moore, 1979). The role of the SCN in the pathway controlling pineal MEL production is thought to be primarily that of a circadian oscillator, generating a circadian rhythm of neural activity that controls MEL synthesis and release (Goldman & Darrow, 1983; Klein, 1979). The SCN and the RHT also mediate the entrainment of the MEL rhythm to the prevailing photoperiod (Klein & Moore, 1979; Rollag & Niswender, 1976). Exposure of the animal to light at night, when MEL levels are normally elevated, results in a precipitous drop in both pineal gland and serum MEL concentrations to daytime levels (Tamarkin, *et al.*, 1979; Vanecek & Illnerova, 1982; Illnerova & Vanecek, 1982a,b). Depending upon the phase of the MEL rhythm at the time of light exposure, this manipulation results in a phase advance, a phase delay or no phase shifting of the MEL rhythm (Illnerova & Vanecek, 1982a,b) in animals released into constant dark conditions. The absence of phase shifts in the MEL rhythm at certain times in the cycle suggests that, independent of light's effect on the circadian oscillator, light also has a direct effect on the neural circuit mediating the elevated level of MEL production in the pineal gland. Recent work in the rat and hamster, using intraocular injections of Cholera toxin conjugated to horseradish peroxidase (CT-HRP), has revealed a more extensive distribution of retinal efferents in the brain than previously described (Levine, *et al.*, 1986; Johnson, *et al.*, 1988). Although the SCN of the hamster is the principal target of RHT input, the pattern of retinal input

to the remainder of the hypothalamus and forebrain (Johnson, *et al.*, 1988; Pickard & Silverman, 1981) deserves further attention.

A model of the neural circuit involved in the control of the pineal gland and MEL production has been proposed. It consists of a multisynaptic pathway connecting the SCN to the pineal gland by way of the hypothalamic paraventricular nuclei (PVN), intermediolateral cell column (IML) of the spinal cord and the superior cervical ganglion (SCG; Tamarkin, *et al.*, 1985). The efferent connections of the SCN have been examined in the rat using iontophoretic injections of *Phaseolus vulgaris*-leucoagglutinin (PHA-L). Projections of the SCN include a prominent group of fibers passing dorsally through the medial PVN where some of the fibers terminate (Watts, Swanson & Sanchez-Watts, 1987). In the Syrian hamster, horizontal knife cuts placed between the SCN and PVN abolish short-photoperiod-induced collapse of the reproductive system of males and females (Badura, *et al.*, 1987; Eskes & Rusak, 1985; Inouye & Turek, 1986; Nunez, *et al.*, 1985). Electrolytic or axon-sparing chemical lesions of PVN neurons block the nocturnal rise in MEL synthesis and photoperiodic responses (Bittman & Lehman, 1987; Brown, *et al.*, 1988; Eskes & Rusak, 1985; Lehman, *et al.*, 1984; Pickard & Turek, 1983; Hastings & Herbert, 1986). The available evidence suggests that the PVN is a relay nucleus in the pathway mediating photoperiodism, and that the pertinent information is sent through PVN descending projections to the spinal cord. In rats, PHA-L labeled fibers are found in the IML of the spinal cord following injections of this lectin into the PVN (Luiten, *et al.*, 1985). In hamsters, injections of wheat germ agglutinin conjugated to horseradish peroxidase (WGA-HRP) into the spinal cord between cervical vertebra 7 (C<sub>7</sub>) and thoracic

vertebra 2 (T<sub>2</sub>) label neurons throughout the rostro-caudal extent of the PVN (Don Carlos & Finkelstein, 1987). However, functional evidence supporting the direct involvement of a mono-synaptic PVN-spinal cord connection in the neural circuit mediating the circadian rhythm of pineal MEL synthesis and release is currently unavailable. Thus, brainstem nuclei receiving PVN efferents and projecting to the spinal cord may participate in the pathway, either partially or to the exclusion of PVN efferents terminating in the spinal cord. In hamsters, preganglionic fibers originating at the level of C<sub>8</sub>-T<sub>5</sub> in the IML terminate in the SCG (Reuss, *et al.*, 1989). Some fibers from SCG neurons, in turn, terminate in the pineal gland where sympathetic activation results in elevated MEL production (Bower & Zigmond, 1982; Wurtman, *et al.*, 1964; Kappers, 1960).

In the rat, two PVN-to-spinal cord pathways have been described (Luiten, *et al.*, 1985). One path exits the PVN dorsally (Tract 1), and projects caudally, running near the roof of the posterior hypothalamic portion of the third ventricle (III). The second set of PVN efferent fibers (Tract 2) exits the PVN laterally passing beneath the zona incerta (ZI) and dorsal to the internal capsule (IC) and medial forebrain bundle (MFB). In the mesencephalic Periaqueductal grey (PAG), and continuing caudally to the level of the area postrema (AP), fibers making up Tract 1 appear to turn ventro-laterally joining Tract 2 in the lateral lemniscus (LL) of the brain stem (Luiten, *et al.*, 1985). Recent evidence from experiments using Syrian hamsters indicates that male and female hamsters respond differently to horizontal knife cuts placed dorsal to the PVN. In the male hamster, these knife cuts, like cuts placed between the SCN and PVN, prevent gonadal regression perhaps by

disrupting Tract 1 (Nunez, *et al.*, 1985; Inouye & Turek, 1986). In contrast, similarly placed cuts in females do not prevent short-day-induced anestrus (Badura, *et al.*, 1989).

In male hamsters, horizontal knife cuts dorsal to the PVN are associated with increased levels of plasma follicle stimulating hormone (FSH; Badura, *et al.*, 1988). Similar changes in FSH levels have been observed following transection of the lateral olfactory tract (LOT) or removal of the olfactory bulbs (BLX) in the male Syrian hamster (Clancy, *et al.*, 1986; Pieper, *et al.*, 1989). Exposure of BLX hamsters to short photoperiods reduces both luteinizing hormone (LH) and FSH levels, but FSH levels remain above those of control animals and apparently at sufficiently high levels so as to maintain large testes. Thus, BLX and knife cuts dorsal to the PVN appear to remove a tonic inhibition on FSH secretion, but do not abolish the photoperiodic control of release of the hormone. A similar change in FSH concentrations, if present in the female, may not be sufficient for the production of estrous cycles during extended exposure to a short photoperiod. In the normal 4-day estrous cycle of the female hamster, serum FSH levels are low on diestrus 2 and early on proestrus (Lisk, 1985). A large surge in FSH secretion occurs on the afternoon of proestrus and is associated with increased LH release. A second surge in FSH release occurs on estrus, which is involved in initiating the development of the next set of follicles. LH and FSH levels have not yet been measured in female hamsters possessing horizontal knife cuts dorsal to the PVN, however, continuously elevated levels of FSH may be incapable of maintaining estrous cycles in the face of reduced levels of serum LH associated with exposure to short photoperiods.

Studies of the anatomical pathway mediating photoperiodism and the circadian rhythm of pineal MEL production in the Syrian hamster have had to rely upon anatomical data obtained from the nonphotoperiodic rat for the interpretation of the effects of lesions and knife cuts. While there is evidence to suggest that the pathways controlling MEL production are similar across species, it is, nevertheless, important that the anatomy of the pathway for the hamster be described and the postulated neural connections verified. The present series of experiments examined the anatomical features of two segments of this pathway for the hamster at the light microscopic level. First, the distribution of retinal ganglion cell efferents to the forebrain was examined. Second, the trajectory of PVN-spinal efferents through the brain was described and the location of neurons in the hypothalamus with projections that terminate in the spinal cord identified. A final experiment assessed the role played in photoperiodism by PVN efferent fibers that pass through the PAG in their way to the spinal cord.

## **EXPERIMENT 1a-Retinal Efferent Projections to the Hypothalamus and Basal Forebrain Identified by Anterogradely Transported CT-HRP.**

A RHT projecting primarily to the SCN has been found in a large number of mammalian species (Moore, 1978; Cassone, *et al.*, 1988). While the SCN is the principal recipient of RHT input, it is increasingly evident that other areas of the hypothalamus and basal forebrain receive direct retinal ganglion cell (RGC) input to varying degrees. Recent studies employing HRP as a tract-tracing tool have reported that the RHT projects to several areas of the hypothalamus, including the PVN, and suggest that the piriform cortex (Pyr), preoptic area (POA) and rostral thalamus are also targets of RGC efferents (Pickard & Silverman, 1981; Johnson, *et al.*, 1988; Levine, *et al.*, 1986; Itaya, *et al.*, 1981; Itaya, *et al.*, 1986).

Several pineal-independent effects of photoperiod have been found to occur in the Syrian hamster (see Bartness & Wade, 1985; Badura & Nunez, 1989) and some of the areas of the forebrain receiving direct retinal input may be involved in the control of these photoperiod-sensitive features. A recent report noted a pineal-independent decline in behavioral sensitivity to steroid hormones in females maintained in a short photoperiod (Badura & Nunez, 1989). In the female, the medial POA provides an inhibitory influence on reproductive behavior (Pfaff & Modianos, 1985), and in both male and female hamsters, the POA receives direct RGC input (Johnson, *et al.*, 1988). Also in both sexes, pineal-independent changes in feed efficiency and metabolism occur (Bartness & Wade, 1985) and some sites in the hypothalamus involved

in the control of energy balance, including the PVN and lateral hypothalamic area (LHA), have been found to contain RGC efferents.

Cholera toxin-HRP is a more sensitive neuroanatomical tract-tracer than free (unconjugated) HRP. In the rat and hamster, intraocular injections of CT-HRP have revealed a pattern of labeled RHT fibers more widely distributed than had previously been reported using other tract-tracing methods (Levine, *et al.*, 1986). The distribution of RGC efferents outside the SCN on the Syrian hamster remains controversial. For instance, Pickard & Silverman (1981) reported evidence of input to the diagonal band of Broca (DBB) rostrally, Pyr laterally and the dorsomedial (DMN) and ventromedial (VMN) nuclei caudally. More recently, a study using CT-HRP did not describe RGC input to some of these terminal sites for RGC efferents (e.g. - to the DMN; Johnson, *et al.*, 1988) or provided a different interpretation of their results (e.g. - input to the amygdala) compared to those of Pickard and Silverman (1981; e.g. - fibers in the piriform cortex). Johnson, *et al.*, (1988) also noted a direct projection to the anterior thalamus but could not detect the path taken by the retinal fibers to this site. The present experiment examined the RHT in the Syrian hamster, focusing on the extra-SCN projections using intraocular injections of CT-HRP. Experiment Ia, was completed shortly before the report of Johnson, *et al.* (1988), containing similar results, appeared in the literature.



## **METHOD**

### **Animals**

Adult male (n = 10) and female (n = 10) Syrian hamsters (*Mesocricetus auratus*; 120 - 200 g) were obtained from Charles Rivers Laboratories and group-housed (n = 6 males or females/cage; cage size- 16.5 x 30.5 x 36 cm) in a stimulatory photoperiod (16 hour/8 hour LD cycle). Food (Wayne Mouse Breeder Blox) and water were available *ad libitum*.

### **Surgery**

Animals were anesthetized with Equithesin (4.5 ml/kg) and received unilateral (n = 17) or bilateral (n = 3) intraocular injections (1.5 - 3.0  $\mu$ l) of CT-HRP (0.38-0.49%) using a 10- $\mu$ l Hamilton syringe. The conjugate was prepared in the laboratory of Dr. R.R. Miselis (University of Pennsylvania) using methods previously described (Shapiro & Miselis, 1985).

### **Perfusion and Histology**

Following survival periods of 12-48 hrs, the animals were deeply anesthetized with Equithesin and perfused transcardially (using an IV cannula) with heparinized (2 U/ml) 0.05 M phosphate buffered (pH 7.4) physiological saline rinse (250 ml over 10 min) followed by 0.05 M phosphate buffered (pH 7.4) fixative containing 0.5 % (w/v) paraformaldehyde and 1.25 % (v/v) gluteraldehyde infused at the same rate. All solutions were infused using a peristaltic pump (Master-flex; Cole-Parmer). The brains were post-fixed overnight at 4°C in the same fixative. Frozen coronal (n = 19) or horizontal (n = 1) sections (50  $\mu$ m) were collected in cold 0.1 M phosphate buffer (pH 7.4) and subsequently processed using the tetramethylbenzidine protocol of

Mesulam (1982). The sections were arranged into three sets of adjacent serial sections, each set consisting of every third section. All sections were mounted on previously gelatinized slides. Two sets were air dried, cleared in xylenes and coverslipped using Permount. One set of tissue was air dried and then counterstained with cresylecht violet prior to coverslipping.

### Evaluation

The uncounterstained tissue was evaluated immediately using brightfield and darkfield optics. Photographs of reaction product in areas of interest in the brain were made at this time. Subsequently, the labeled fibers were plotted on camera lucida drawings of sections from representative cases. Structures of the brain were identified by referring to the adjacent cresylecht violet stained sections.

### Criteria for evaluating alternate transport mechanisms

The tissue was examined for evidence of hemal or trans-synaptic transport of the CT-HRP. First, the magnocellular PVN and supraoptic nuclei (SON) were examined to determine if retrogradely labeled cells were present. In a number of species of rodents, magnocellular neurons within these two nuclei are retrogradely labeled when HRP is injected into the systemic circulation (Broadwell & Brightman, 1976; Youngstrom & Nunez, 1987). Second, the primary visual cortex was examined for evidence of orthogradely transported CT-HRP. Labeling in this area of cortex would be indicative of trans-synaptic transport in at least one target nucleus of the optic tract (Itaya & Van Hoesen, 1982).

## RESULTS

The distribution of labeling in the basal forebrain from the level of the organum vasculosum of the lamina terminalis (OVLT) through the posterior hypothalamus is depicted schematically in Figure 1 and listed in Table 1. There was no evidence of trans-synaptic transport of CT-HRP in the visual cortex of any animal and the distribution of CT-HRP staining was similar regardless of sex. The intensity of staining increased with longer survival but the pattern remained unchanged. Except for the SCN, this pattern of labeling was typified by the asymmetrical distribution of staining, with structures contralateral to the injected eye more intensely labeled than their ipsilateral counterparts following unilateral injections.

*SCN* - The SCN were the most densely labeled structures of the basal forebrain (Figures 1D-F & 2) and the pattern of staining was essentially the same as reported previously, so it will be reviewed briefly. Near the rostral pole of the SCN, each nucleus, separated from one-another by the third ventricle, possessed nearly equal amounts of stained fibers following a unilateral injection. Proceeding caudally, as the floor of the third ventricle separated from the optic chiasm (OC) the medial borders of the nuclei met at the midline. A less intensely stained dorso-medial crescent became evident in each nucleus (Figure 1E). At about the same level the intensity of stain in the ventral half of the nuclei increased and the pattern of labeling became slightly asymmetrical, the nucleus contralateral to the injected eye being more intensely stained. In the caudal one-third of the nucleus, the asymmetry persisted to a point near the caudal pole, where the

Table 1

Sites Receiving Retinal Ganglion Cell Efferents in the Syrian Hamster

AMYGDALA

Medial Amygdaloid  
Nucleus

CORTEX

Piriform Cortex, layer I

HYPOTHALAMUS/PREOPTIC

Anterior Hypothalamic  
Area  
Bed Nucleus of the Stria  
Terminalis  
Diagonal Band of Broca  
Dorsomedial Nucleus  
Lateral Hypothalamic  
Area  
Lateral Preoptic Area  
Medial Preoptic Area  
Paraventricular Nucleus  
Retrochiasmatic Area

Suprachiasmatic Nucleus  
Supraoptic Nucleus  
Ventromedial Nucleus

MESENCEPHALON

Dorsomedial Terminal  
Nucleus  
Lateral Terminal Nucleus  
Medial Terminal Nucleus  
Pretectum  
Superior Colliculus

THALAMUS/SUBTHALAMUS

Antero-Medial Thalamic  
Nucleus  
Antero-Ventral Thalamic  
Nucleus  
Lateral Geniculate  
Nucleus  
Zona Incerta

**Figure 1. Camera lucida drawings of coronal sections through the brain of a Syrian hamster that received a unilateral intraocular injection of CT-HRP (3  $\mu$ l) into the left (L) eye. The distribution of staining was asymmetrical with the highest density of label in the hemisphere contralateral (viewer's left) to the injected eye. All of the illustrations are drawn to the same scale (Bar [A & E]= 500  $\mu$ m). For a definition of the abbreviations used in this and subsequent figures refer to the *List of Abbreviations*, p. xiii.**

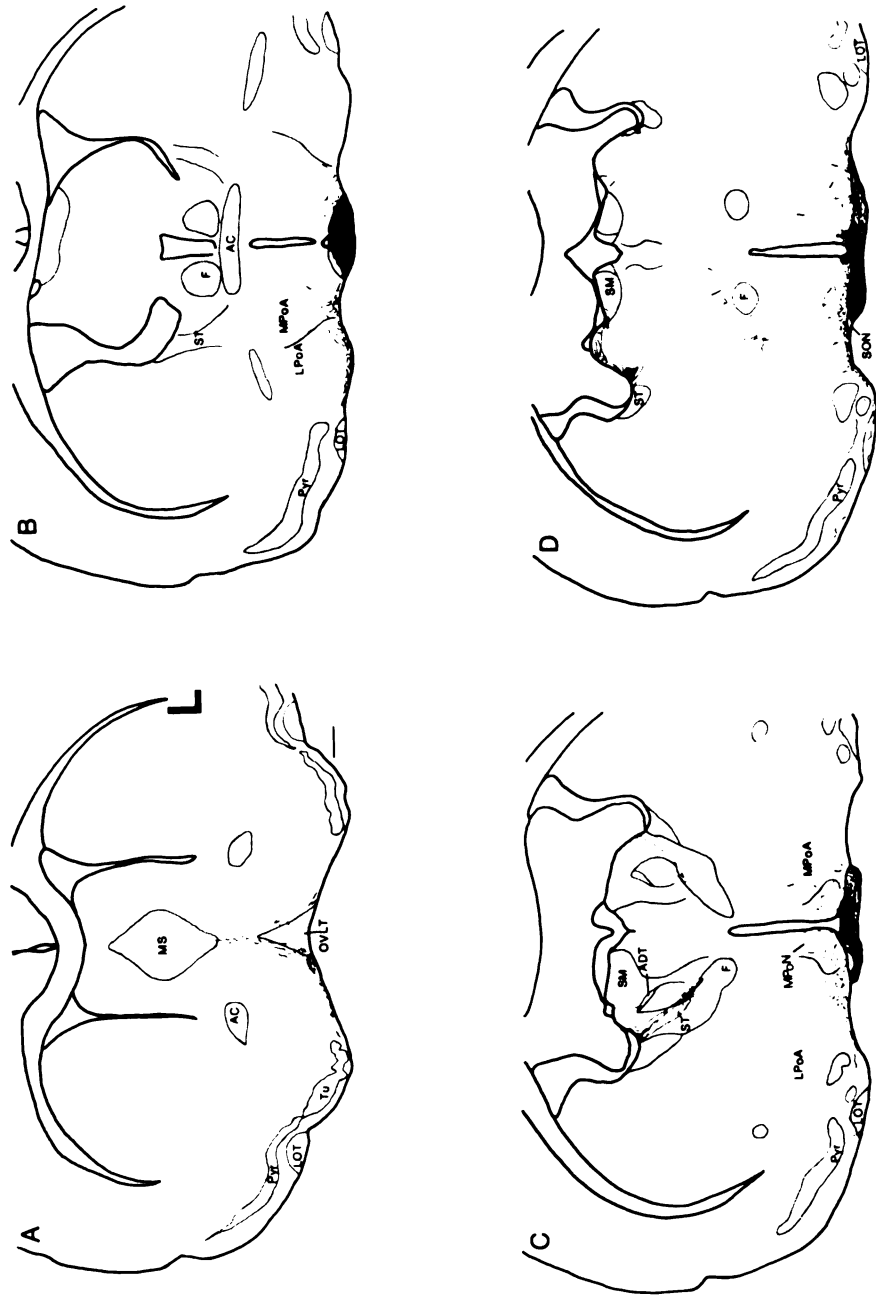


Figure 1



Figure 1 (Continued)

**Figure 2. Photomicrograph (A) of a coronal section (50  $\mu\text{m}$ ) through the caudal half of the SCN of an animal that received a unilateral injection of CT-HRP into the left eye. Labeling was present throughout each nucleus, including the dorso-medial crescent (arrows) adjacent to the ventral wall of the third ventricle which was relatively less densely labeling. Some labeled fibers continued dorsally through and around the SCN terminating in the overlying anterior hypothalamic area (AHA; darkfield illumination; Bar = 200  $\mu\text{m}$ ). The box in (B) outlines the area depicted in (A).**



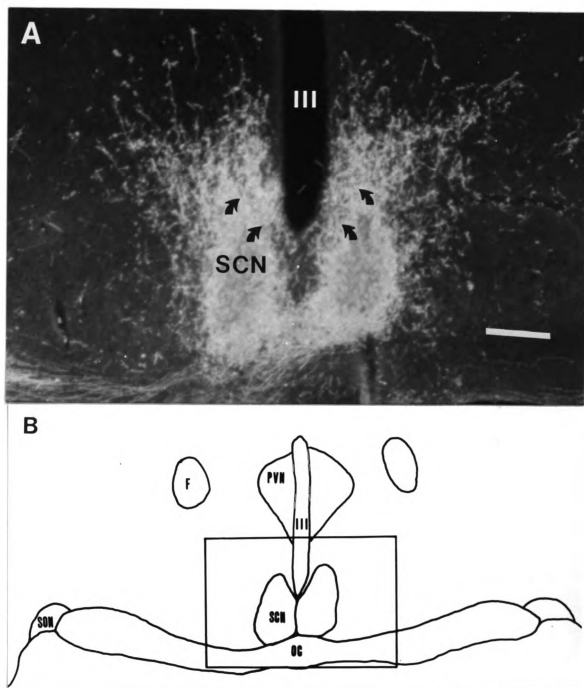


Figure 2

declining intensity of staining prevented identification of any asymmetry.

*Extra-SCN Hypothalamus* - A prominent feature of the RHT was a bundle of fibers passing through the SCN (Figures 1E,F & 2). This bundle first became evident as it emerged dorsally from the middle one-third of the SCN, increasing in prominence in the caudal one-third of the nuclei. After the SCN, the anterior hypothalamic area (AHA) possessed the highest density of stained fibers in the hypothalamus. Dorsal to the SCN, the fibers spread dorso-laterally into the AHA. At a level near the rostro-caudal mid-point of the PVN, some RHT fibers approached the nucleus ventrally (sub-PVN area) and traced a lateral path along the boundary (Figures 1E,F & 3). Other fibers penetrated the PVN, where a few fibers appeared to terminate, while the remainder continue dorsally into the ZI. Those fibers terminating in the PVN were located primarily in areas corresponding to the periventricular-, lateral- and dorsal-parvocellular regions of the PVN as described for the rat (Swanson & Kuypers, 1980) with the heaviest concentration of reaction product found in the ventro-lateral PVN. Additional fibers emerged from the lateral OC adjacent to the SCN and contributed to the RHT input to the lateral AHA (Figures 1E,F, 2 & 4).

At the level of the caudal SCN, stained fibers emerged from the lateral half of the optic tract (OT) coursing dorso-medially toward the fornix (F) and lateral PVN (Figures 1E,F & 4). It was not clear if these fibers penetrated the PVN or were restricted to the LHA. Caudally, at the level of the retrochiasmatic area, as the OT continued dorso-laterally, fibers emerged nearly horizontally from the tract,

**Figure 3. Schematic drawing (A) of a coronal section through the hypothalamus depicting the area (BOX) shown in (B). B - CT-HRP labeled fibers passed dorsally through the SCN and AHA to terminate in the AHA ventral to the PVN, while other fibers coursed along the ventral PVN. Some fibers ended along the ventral border while others ended in the PVN or continued dorsally into the ZI. Photomicrograph of a coronal section (50  $\mu$ m) through the middle of the PVN. (darkfield illumination; Bar = 200  $\mu$ m)**

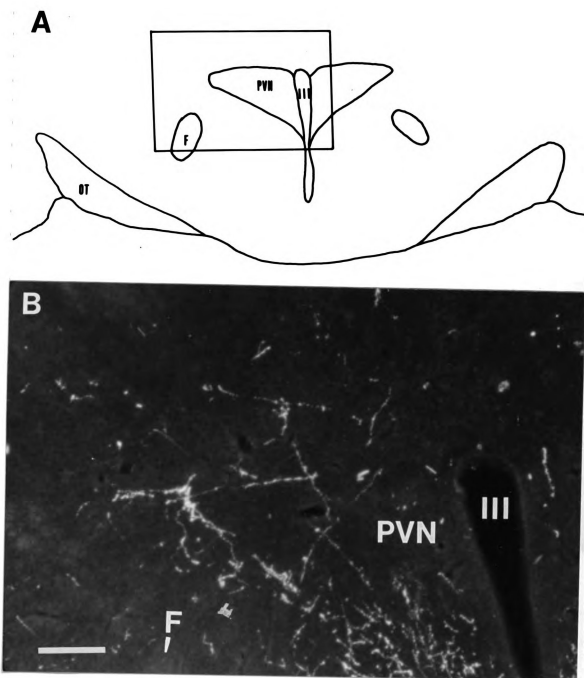


Figure 3

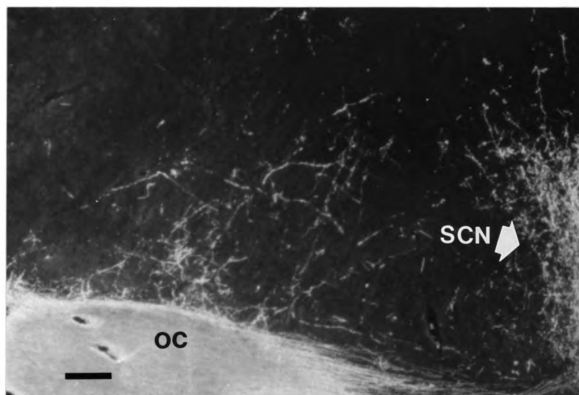


Figure 4. Photomicrograph of the same coronal section shown in Figure 2. Labeled fibers emerged from the lateral OC and coursed dorso-medially. Some fibers approached the fornix and PVN but could not be traced into the PVN. (darkfield illumination; Bar = 100  $\mu$ m)

coursing medially toward the ZI and PVN (Figures 1F,G). Some fibers passed through the dorsal half of the cerebral peduncle (CP) on their way to the dorsal hypothalamus. This input to the dorsal hypothalamus was quite sparse and was absent in the hypothalamus ipsilateral to the injected eye. At this same level stained fibers were also seen in the medial hypothalamus. The fibers were primarily confined to the region between the VMN and DMN bilaterally and the third ventricle (Figure 1G), although individual fibers were also evident in the lateral hypothalamus. A small plexus of fibers appeared to terminate in the DMN pars compacta (DMN<sub>pc</sub>; Figure 1H). The number of stained fibers in the hypothalamus declined rapidly in tissue caudal to this level.

*Preoptic Area* - At the level of the anterior SCN, a plexus of fibers emerged from the lateral OC and turned rostrally, entering the ventral POA contralateral to the injected eye (Figures 1C,D). Stained fibers were found in the medial and lateral POA and medial preoptic nucleus (Figures 1B,C). Continuing rostrally, some fibers were evident near the LOT and olfactory tubercle (Tu) but did not enter these structures. Most of the fibers reaching the level of the organum vasculosum of the lamina terminalis (OVLT), entered the horizontal limb of the DBB, and proceeded medially toward the OVLT (Figures 1A, 5). Of the fibers traced rostrally to this level, many ended in the transition area between the horizontal and vertical limbs of the DBB adjacent to the OVLT, while a few remaining fibers continued dorsally to end near the ventral boundary of the medial septum (MS). On the side ipsilateral to the injected eye, fibers entering the POA emerged from the OC at a point further rostral relative to contralateral fibers. The ipsilateral fibers

**Figure 5. Photomicrograph of a coronal section through the OVL. CT-HRP labeled fibers emerged from the OC contralateral to the injected eye near the SCN and turned rostrally to enter the POA. Some fibers continued rostrally into the horizontal band of the DBB, ending in the vicinity of the OVL. A few continued dorsally in the vertical limb of the DBB and ended near the MS (darkfield illumination; Bar = 100  $\mu$ m). The location of the fibers shown in (A) is outlined in the schematic drawing (B).**

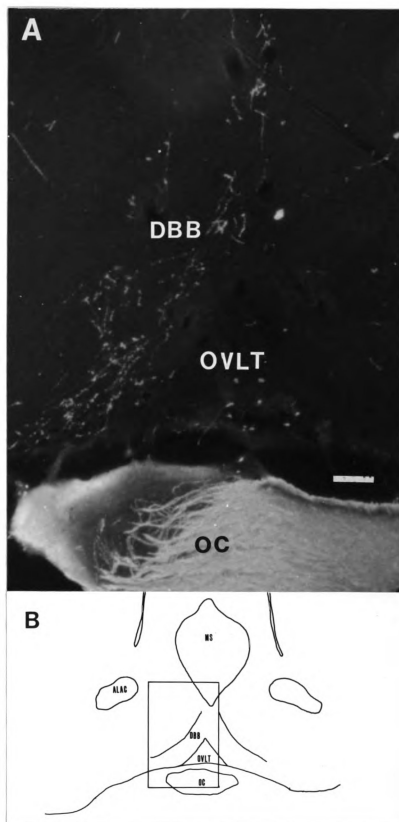


Figure 5



were similarly distributed but did not extend as far laterally and were fewer in number. The course of all rostrally projecting fibers through the POA was particularly salient in tissue sectioned in a horizontal plane and material cut in this fashion facilitated the interpretation of the trajectory of these fibers (Figure 6).

*Piriform Cortex* - Approximately 200  $\mu\text{m}$  caudal to the Tu, laterally projecting fibers emerged from the OC forming a fascicle along the ventral surface of the brain and extended laterally toward the rhinal fissure (Figures 1B-G, 7). This set of axons was generally confined to layer 1 $\alpha$  of the Pyr (Devor, 1976; Haberly & Feig, 1983). Fibers were never observed in the pyramidal cell layer of the Pyr. Moving caudally through this region of the brain, the fascicle persisted to the level of the caudal SCN. At points along the fascicle, fibers turned and entered the overlying layer 1a where many ended in terminal swellings (Figure 7B). Occasionally, individual stained fibers were observed in the medial amygdaloid nucleus and anterior amygdaloid area.

In the hypothalamus, intermingled with the fibers destined for the Pyr were other fibers that appeared to terminate in the dorsal SON. Some fibers possessed varicosities suggestive of *en passant* terminals while others appeared to give off short branches that ended in swellings (Figure 8).

*Extra-geniculate Thalamus* - The antero-medial (TAM) and antero-ventral (TAV) thalamus received direct retinal input (Figure 9). The small bundle of stained fibers reaching this level appeared as a rostral continuation of the large RGC input to the lateral geniculate nucleus (LGN; Figure 1C-F). At the level of the rostral LGN, some labeled fibers separated from those terminating in the nucleus and continued into the

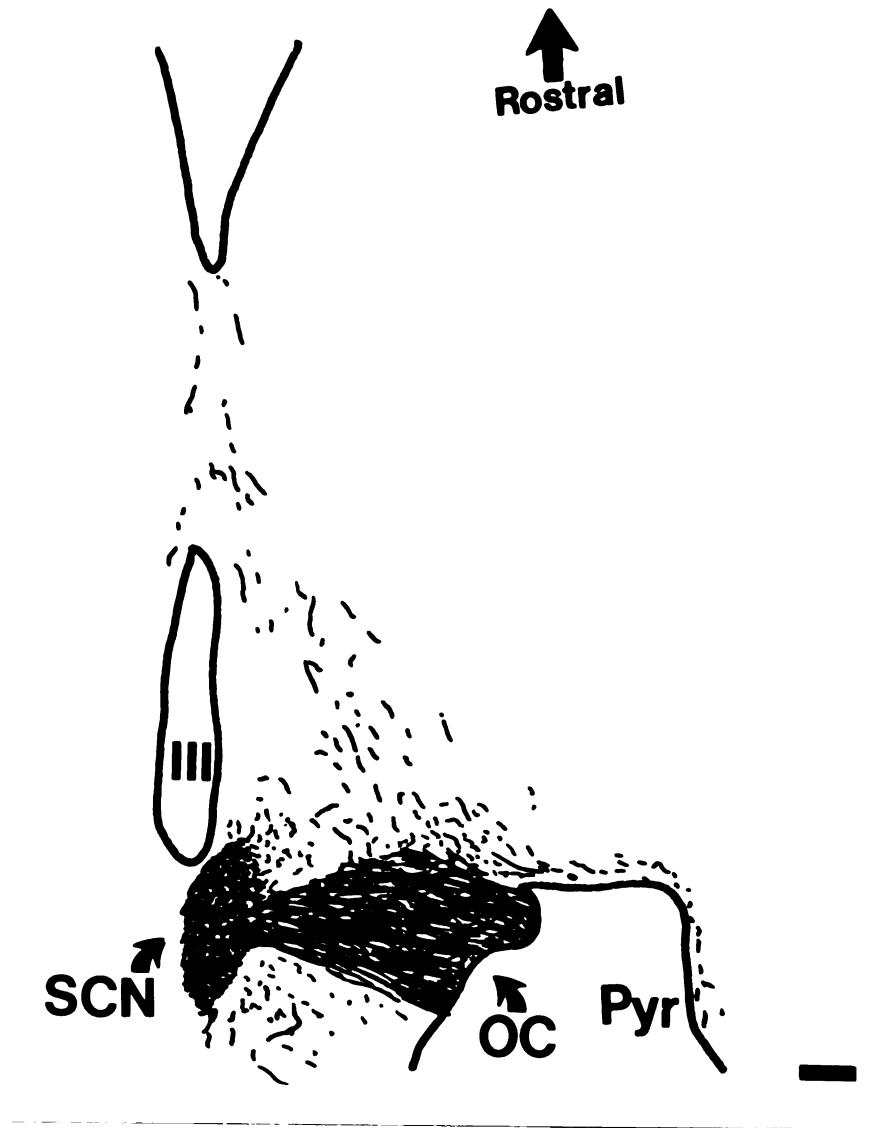


Figure 6. Camera lucida drawing of a tissue section cut in a horizontal plane and stained for CT-HRP. Some labeled fibers emerged from the lateral half of the optic chiasm and coursed rostro-medially to the level of the OVLT. (Bar = 200  $\mu$ m)

**Figure 7. A fascicle of CT-HRP labeled RGC efferents emerged from the lateral OC at the level of the caudal SCN and turned ventro-laterally, entering layer 1 $\alpha$  of the Pyr (A; Bar = 200  $\mu$ m). At higher magnification (B) individual fibers with occasional varicosities along their length were seen turning dorsally and ending in small swellings in layer 1A (Bar = 20  $\mu$ m). (brightfield illumination)**

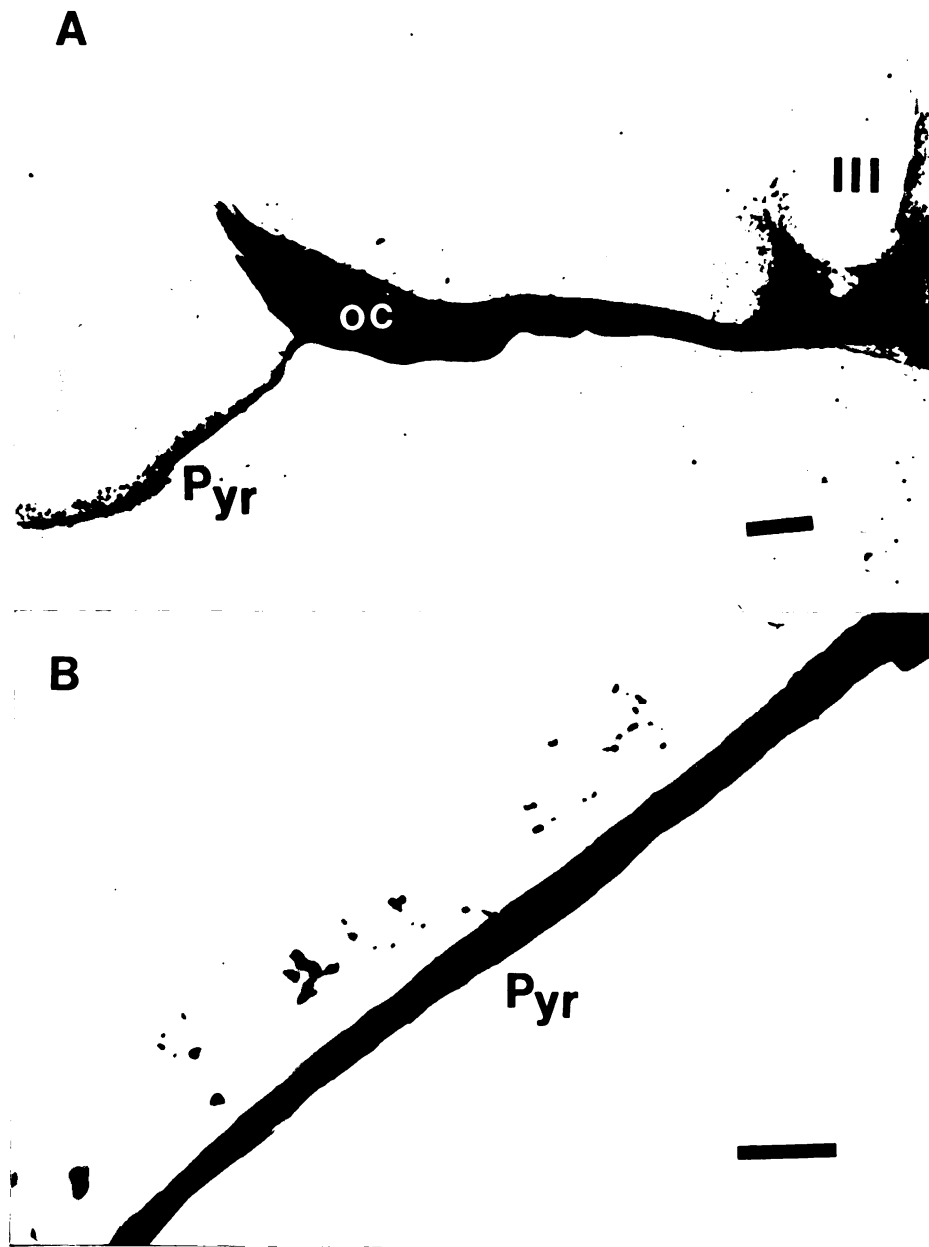


Figure 7

**Figure 8. Photomicrograph (A) of a coronal section through the SON. In the rostral hypothalamus, CT-HRP labeled fibers emerged from the lateral OC and passed laterally over the SON where some fibers terminated in the dorsal SON. This bundle of fibers extended ventro-laterally into the Pyr (darkfield illumination; Bar = 20  $\mu$ m). The box in (B) indicates the location of the fibers shown in (A).**

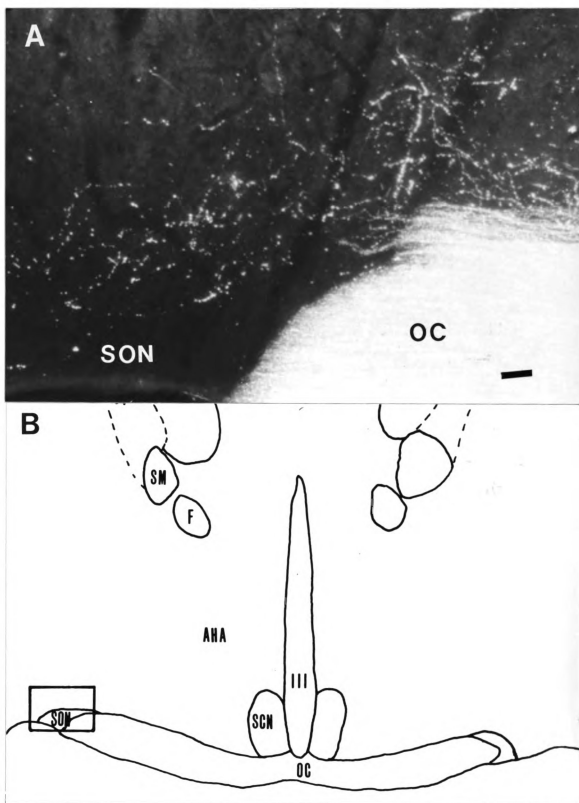


Figure 8

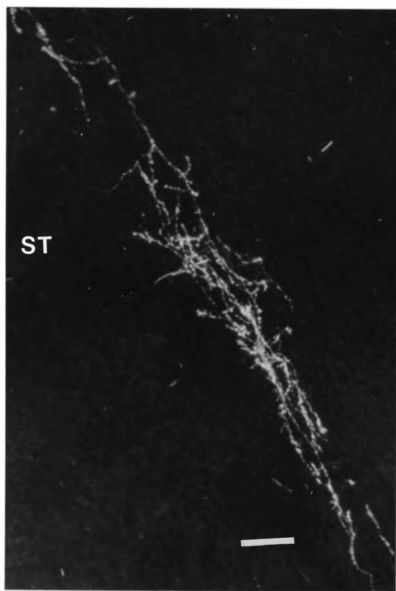


Figure 9. Photomicrograph of a coronal section through the rostral pole of the anterior thalamic nuclei. A small bundle of CT-HRP labeled fibers joined the stria terminalis (ST) as they continued from the LGN and ended in the TAM/TAV (darkfield illumination; Bar = 50  $\mu$ m; see Figure 1C for location of fibers)

medial ST taking a position near its medial border on the floor of the lateral ventricle. The small set of axons coursed forward to the rostral thalamus where it left the ST ventro-medially. The fibers terminated in a triangle of tissue, containing the TAM and TAV, formed between the ST and stria medullaris (SM).



**EXPERIMENT Ib-Retinal Efferent Projections to the Hypothalamus and Basal Forebrain: Retinal Neurons Retrogradely Labeled by Fluorescent Dye.**

As described in Experiment Ia, several areas of the medial forebrain receive direct RGC input. In the hypothalamus, the AHA, DMN, PVN and SON, in addition to the SCN, receive RHT input, as does the POA rostrally and the Pyr laterally. Dorsally, the ZI and the rostral pole of the thalamus (TAM/TAV) also receive optic input. Despite the absence of staining in the visual cortex that might indicate trans-synaptic transport, the concern remains that the observations in Experiment Ia were the result of multisynaptic transport. To corroborate these data, selected sites found to contain CT-HRP stained fibers in Experiment Ia received micropressure injections of rhodamine fluorescent dye labeled latex microspheres (RLM; Katz, *et al.*, 1984). The retinae were then examined for evidence of retrogradely labeled ganglion cells.

34  
**METHOD**

**Animals**

Animal and housing conditions were identical to Experiment Ia.

**Surgery**

Adult male (n = 8) and female hamsters (n = 5) received bilateral stereotaxically placed injections of RLM into one of several areas of the brain found to possess stained fibers in Experiment Ia. The sites chosen to receive injections were: 1) POA/DBB, 2) TAM/TAV, 3) PVN/ZI. Based on the data from Experiment Ia, each area that was selected represented the terminus of a retinal efferent path. The interpretation of the results from injections into these sites would be less likely to be confounded by RGC fibers-of-passage located near the injection taking up the tracer dye. Also, the pattern of CT-HRP labeling in the selected sites following ocular injections was relatively discrete. It was anticipated that the relatively circumscribed distribution of RGC fibers would maximize the opportunity for uptake and retrograde transport to RGC. Two of these sites (POA/DBB & PVN/ZI) were of interest as structures implicated in the control of sexual behavior and photoperiodism. In the hamster, the TAM/TAV had been found to contain RGC efferents once previously (Johnson, et al., 1988) but the trajectory of the efferents to this area of the brain had not been described until the present report (Experiment Ia). These structures received injections to confirm the retinal efferent projection to each.

In preliminary cases (n = 10 males) RLM injections spread to include other structures receiving RGC input (e.g., LGN, SON, AHA) or invaded the optic nerve or chiasm. These cases were used to assess the ability of RLM to retrogradely label ganglion cells.

Animals were anesthetized with Equithesin (4.5 ml/kg) and placed in the stereotaxic apparatus. The skull was exposed and a burr hole drilled. The stereotaxic coordinates were empirically determined for each site receiving an injection (from Bregma, POA/DBB: rostro-caudal (RC) +2.2 mm, medio-lateral (ML)  $\pm$  0.6 mm, dorso-ventral (DV) -6.7 mm; PVN/ZI: RC +0.3 mm, ML  $\pm$  0.5 mm, DV -6.4 mm; TAM/TAV: RC +0.6 mm, ML  $\pm$  1.3 mm, DV -5.3 mm; DV coordinates are from the surface of the brain with the nose bar -2.0 mm from ear-bar zero).

A 1- $\mu$ l Hamilton syringe with a glass micropipette attached (tip dia.: 40-50  $\mu$ m) to the needle was used to make the injections. The assembly was first backfilled with mineral oil to displace all air in the assembly, then backfilled with the fluorescent dye and mounted on the stereotaxic. The micropipette was lowered in the brain at the selected coordinates and, after a 5 minute delay, the tracer (60-200 nl RLM) was injected over a 5 minute period using a micrometer drive. The syringe was left in place for another 5 minutes after the injection was made, then removed. The skin wound was closed and the animal returned to the long-day photoperiod in an individual cage.

#### Perfusion and Histology

*Brain:* After survival periods of 7 to 15 days, the animals were perfused transcardially using the method described in Experiment Ia with a heparinized (2 U/ml) 0.05 M phosphate buffered (pH 7.4) physiological saline rinse followed by 4 % (v/v) formaldehyde in 0.05 M phosphate buffered (pH 7.4). The eyes were removed during the saline rinse. They were stored in petri dishes labeled for left or right side of the body, and, kept in the same rinse solution until the retinæ were removed. The brains were stored overnight at 4°C in the same fixative,

then cut (50-80  $\mu\text{m}$  sections) in a coronal plane. The sections were mounted to gelatinized slides, cleared in xylenes and coverslipped using DPX, a non-fluorescing mounting media. The injection sites were verified by microscopic examination of the tissue using an epi-fluorescent illumination attachment (510-560 nm excitation / 590 nm barrier filter).

*Retinae:* The retinae were removed from the eyes and in some cases were flattened, ganglion cell layer-side up, on gelatinized glass slides. Radial cuts were made in the tissue to reduce distortion. A coverslip was placed on top of the tissue and the slide placed in a petri dish containing 0.05 M phosphate buffered 4% formalin for 6 hours to fix the tissue. The slide was subsequently taken from the petri dish, the coverslip removed, and the tissue rinsed with physiological saline. The retinae were allowed to air-dry to the slides then cleared in xylenes and coverslipped using DPX. The retinae were then examined for evidence of retrogradely labeled ganglion cells.

Some of the retinae were fixed free-floating in the buffered fixative 6-18 hours, then mounted to gelatinized slides as described above, before allowing them to air-dry. This procedure prevented tearing of the tissue caused when the coverslip was removed following fixation.

*Evaluation:* One investigator counted the cells in each retina that were labeled by the injections. An independent observer examined selected retinae without knowledge of treatment to confirm the presence and number of retrogradely labeled cells. Photographs were made of representative labeled cells in the retinae and drawings were made of the injection sites.

## **RESULTS**

Retinal ganglion cells were consistently labeled, in either one or both retinae, with RLM following injections placed bilaterally into the three selected areas shown to receive retinal efferents (Experiment Ia). No differences between the sexes were evident. Representative retinal ganglion cells are shown in Figure 10. In all cases, the injection site was composed of a brilliantly labeled core centered on the ventral tip of the needle tract. Surrounding the core was a halo of dispersed RLM and intensely labeled glia, neurons and processes. Beyond this ring, labeled neurons and dendrites were evident but axons beyond a short, proximal portion were rarely observed except when a significant tract was included in the injection site (e.g. - anterior commissure [AC], OT or ST).

*PVN/ZI* - Injections (n = 4 animals) included in this group did not extend into the hypothalamus ventral to the PVN or laterally to the LGN by spreading through the surrounding tissue or along blood vessels (Figure 11). In each case a short line of fluorescent dye marked the needle tract through the overlying tissue but did not pass through structures believed to receive retinal input. Labeled cells were located in either one or both retinae. The total number of labeled retinal cells ranged between 2 and 12/animal and did not appear to be distributed through the tissue in any particular pattern. Nor was there an obvious pattern to the size of labeled somata (range: 10  $\mu\text{m}$  - 19  $\mu\text{m}$ ). The intensity of labeled RGC varied considerably from sparsely labeled somata to brightly labeled cells and their associated proximal dendrites. RGC axons could not be clearly identified in the retinae in any case.

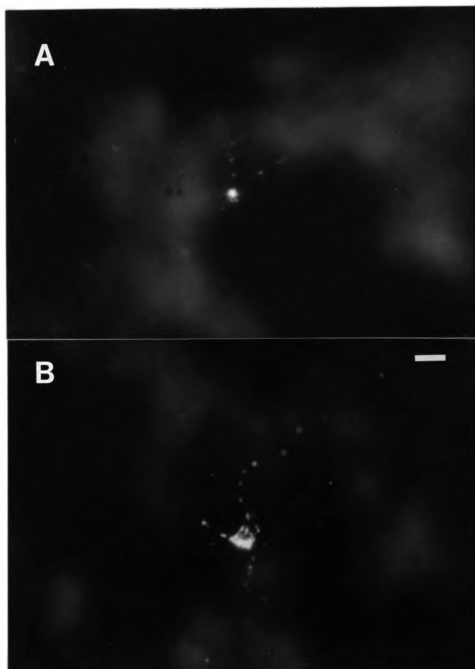


Figure 10. Photomicrograph of representative RGCs retrogradely labeled with RLM. The cells are from an animal that received a bilateral injection of RLM into the PVN (A) or POA (B) and represent the range in size of somata that were labeled. (epifluorescence illumination; Bar = 20  $\mu\text{m}$ )

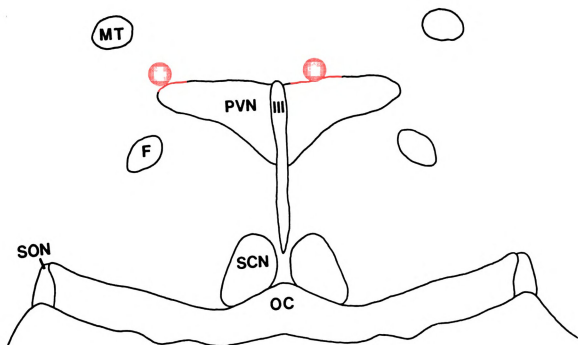


Figure 11. Camera lucida drawing of a coronal section through the hypothalamus at the level of bilateral RLM injections into the area of the PVN/ZI in a Syrian hamster. The center of each injection is marked by a dot. The total number of labeled cells counted in the retinae of each animal ranged between 2 and 12.

**POA/DBB** - Injections that were placed in the POA/DBB (n = 4 animals) rostral to the SCN and medial to the LOT, including injections that spread to the level of the OVLt, were counted in this group (Figure 12). Similar to 'PVN/ZI' injections, a small number of RGC were consistently labeled by RLM (range 3 - 15/animal). One injection was found placed particularly rostral in the brain anterior to the OVLt along the ventral surface of the brain; this injection also labeled 3 RGC in each retina. The low number of labeled cells and their bilateral distribution suggests the tip of the micropipette attached to the syringe had not pierced the ipsilateral optic nerve (ON) located medial to the injection site at this level.

**TAM/TAV**- Injections in this area labeling RGC were effective only if the rostral pole of the thalamus was included in the 'core' (Figure 13). Injections that excluded this area but that did label the medial ST (i.e. - injections of the bed nucleus of the stria terminalis [BNST]) were ineffective in labeling RGC. Few cells in the retinae were labeled (range 2 - 9/animal) and were not distributed in any obvious pattern.

*Injections outside the target regions:* Retinal ganglion cells were labeled by injections that included the LGN (n = 2 animals) or OC (n = 2 animals) or ON (n = 1 animal). These injections were associated with many (>50) labeled retinal ganglion cells in one (an injection including one ON) or both eyes (injections including the OC or LGN). Injections that were confined to areas of the brain not observed to contain CT-HRP stained fibers in Experiment Ia (e.g., lateral septum, BNST, or medial thalamus) did not label RGC.

In the remainder of the control cases the dye spread outside the target area confounding the interpretation of the data. The most



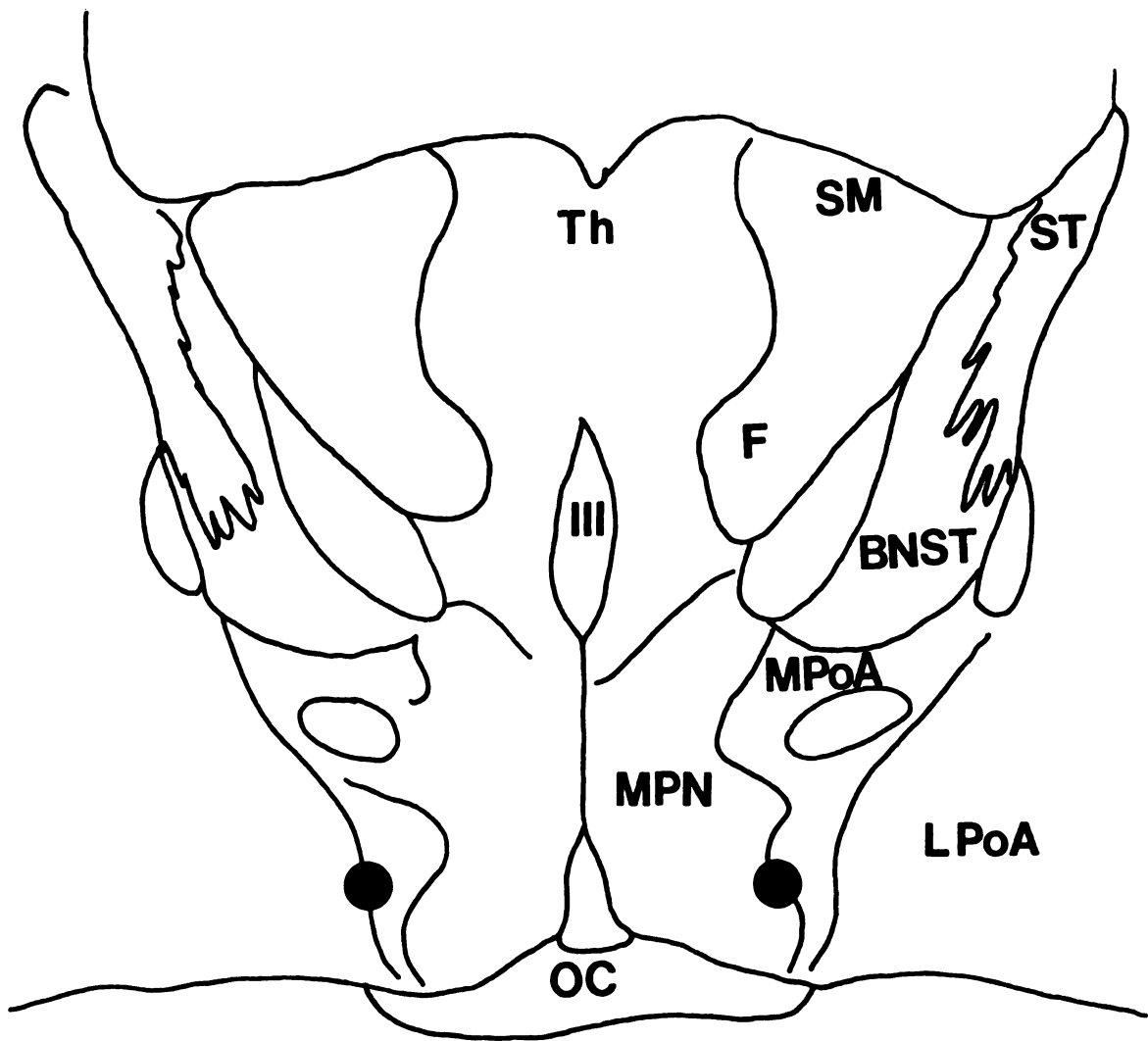


**Figure 12.** Schematic representation of the POA at the level of bilateral RLM injection into the brain of a hamster. The center of each injections is marked by a dot. The total number of cells labeled in each animal ranged between 3 and 15. (Illustration adapted from Maragos, *et al.*, 1989)

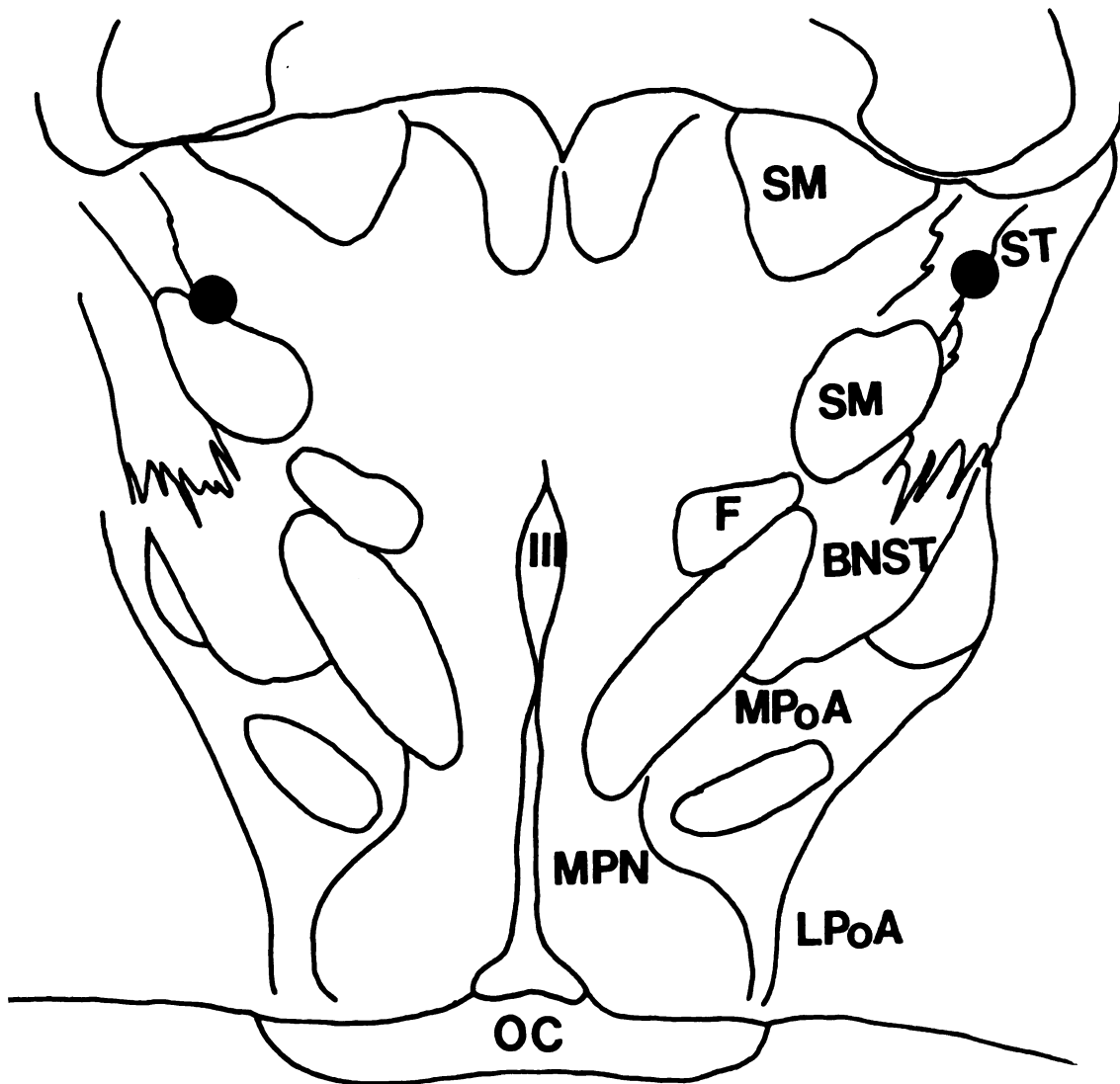


**Figure 13.** Schematic representation of the brain of a Syrian hamster at the level of bilateral RLM injections into the rostral thalamus. The center of each injection is marked by a dot. The total number of cells labeled in each animal ranged between 2 and 9. (Illustration adapted from Maragos, *et al.*, 1989)

common mechanism of spread was dye following the needle tract dorsally. But dye also spread along blood vessels passing through the vicinity of the injection site. As a result, some injections centered in or immediately dorsal to the PVN exhibited dye-spread either along the large blood vessels that also passed through or near the SON and lateral OC (n = 3 animals), or, along blood vessels that passed through the LGN and optic tract (n = 2 animals). More RGC were labeled in these cases compared to the cases in which injections were confined to the intended target. In each case the relative contribution of each of the affected areas could not be determined. Spread of the RLM was reduced or prevented by decreasing the volume of dye injected and decreasing the rate of injection.

### DISCUSSION

The results of Experiment I confirmed the bilateral RHT input to the SCN of the Syrian hamster and demonstrated the path of retinal efferents to several extra-hypothalamic structures, including the DBB, Pyr and rostral TAM/TAV. There is currently no evidence suggesting that these particular regions of the brain receive direct input from the SCN that might account for these inputs based on anterograde trans-synaptic transport of CT-HRP (Watts, *et al.*, 1987). Nor have previous studies employing CT-HRP as a tract-tracer reported evidence of such transport (Johnson, *et al.*, 1988; Levine, *et al.*, 1986). The labeling of RGC by injections of RLM into the PVN/ZI, TAM/TAV and POA/DBB provides supporting evidence that retinal input reaches these structures.

The SCN are the principal recipients of RHT input and were labeled throughout their rostro-caudal extent, including the dorso-medial crescent of each nucleus. Retinal input to this subdivision had been in doubt until recently (Card & Moore, 1984) but seems to be a consistent feature in the Syrian hamster (Experiment Ia; Johnson, *et al.*, 1988). Next in density of RHT input in the hypothalamus was the AHA; some fibers passed through this area to the PVN. In the rat, a dense SCN projection ending in the AHA has been demonstrated by injections of PHA-L while other fibers invade the PVN (Watts, *et al.*, 1987). Also, in the rat, some cells of the AHA and sub-PVN area project to the PVN (Poulain & Carette, 1987). It seems that the distribution of RHT fibers overlaps with that of some SCN projections; these inputs may interact to modulate the output of the AHA and PVN and thus influence the photoperiodic response in the hamster. Direct RGC input may act to either work in concert with SCN input to enhance the probability that a particular behavior or physiological mechanism is activated, or to inhibit further conduction of SCN-generated activity and thus prevent its activation (masking?).

The PVN is part of the multisynaptic pathway mediating the circadian rhythm of MEL production and photoperiodism, but the specific function of the PVN in this pathway is unknown. Rats and hamsters exposed to pulses of light during darkness display a precipitous decline in pineal and serum levels (Tamarkin, *et al.*, 1979; Vanecek & Illnerova, 1982; Illnerova & Vanecek, 1982a,b). In the rat, comparisons of changes in the rhythm of MEL production in animals released into constant darkness following exposure to a pulse of light at night suggests that temporary suppression of pineal MEL production

may occur in the absence of long-term changes in the rhythm of MEL production. Direct RHT input to the PVN, AHA (through its connection to the PVN) or both may bypass the clock, thus, providing a mechanism for modulating MEL production in the pineal gland at times during the night when the circadian system is relatively insensitive to light.

A number of interconnecting circuits may exist between several areas of the brain receiving retinal input. In the rat and hamster, the intergeniculate leaflet (IGL) of the LGN participates in the entrainment of circadian rhythms to the light-dark cycle (Pickard, *et al.*, 1987; Johnson, *et al.*, 1989). The IGL projects to the SCN in the hamster (Pickard, 1985), and, at least in the rat, this connection is reciprocated (Card & Moore, 1989). In addition, the AHA and retrochiasmatic area project to the IGL (Card & Moore, 1989) and receive direct retinal input (Experiment 1a) in addition to input from the SCN (Watts, *et al.*, 1987). These geniculo-hypothalamic circuits may participate in a feedback mechanism to modulate the phase relationships of other SCN-dependent rhythms to the photoperiod.

A projection to the POA labeled here and confirmed by RLM injection has been previously recognized in both the rat and the hamster (Pickard & Silverman, 1981; Johnson *et al.*, 1988). Johnson and coworkers (1988) reported labeled fibers that were traced to the DBB and to the vicinity of the OVL. These authors reported that the fibers emerged from the optic nerve to provide input to the DBB and caudally in the POA, ultimately terminating in the amygdala. The interpretation of the present results give a different picture of this path. In horizontally sectioned material the projection to the POA and DBB was seen to emerge from the lateral OC and to follow a rostro-medial

course into the POA. In the rostral POA, fibers destined for the level of the OVLt entered the horizontal limb of the DBB. A portion of the RGC input to the rostral Pyr also coursed through the POA before turning laterally.

In rodents, the POA participates in the control of sexual and maternal behaviors as well as the release of gonadotropins (Merchenthaler, *et al.*, 1984; Wiegand & Terasawa, 1982; Numan, 1988; Kalra, 1986; Napoli, *et al.*, 1972; Powers & Valenstein, 1972; Larsson, 1979). This control involves connections that have been previously described between the POA and the brainstem, 'limbic system' and hypothalamus (see Swanson, 1987; Berk & Finkelstein, 1981; Simerly & Swanson, 1986; Kevetter & Winans, 1981). Gonadectomized hamsters of both sexes, exposed to short photoperiods, are less sensitive to the behavioral effects of exogenous gonadal hormones than similarly treated animals housed in a long photoperiod (Badura, *et al.*, 1987b; Badura & Nunez, 1989; Campbell, *et al.*, 1978; Morin & Zucker, 1978). In the female, but not in the male, this effect is pineal-independent (Badura, *et al.*, 1987b). In rodents, the POA participates in the control of sexual and maternal behaviors as well as the release of gonadotropins (Merchenthaler, *et al.*, 1984; Wiegand & Terasawa, 1982; Numan, 1988; Kalra, 1986; Napoli, *et al.*, 1972; Powers & Valenstein, 1972; Larsson, 1979). This control involves connections that have been previously described between the POA and the brainstem, 'limbic system' and hypothalamus (see Swanson, 1987; Berk & Finkelstein, 1981; Simerly & Swanson, 1986; Kevetter & Winans, 1981). In the male hamster, electrolytic or chemical lesions of the medial preoptic area (MPoA) produces deficits in copulatory behavior (Powers, *et al.*,

1987). These deficits in the expression of male sexual behavior appear to be due to disruption of medial amygdaloid nucleus connections to the BNST and POA (Lehman, *et al.*, 1983; Lehman, *et al.*, 1980). In the female rat, activation of maternal behaviors involves both the medial preoptic area (MPoA) and lateral preoptic area (LPoA) and their connections to the brainstem (Numan, 1988). Pinealectomized male and female hamsters exposed to short photoperiod are reproductively competent (Reiter, 1973/74). However, the maternal behavior of these females is deficient when compared to that of females bearing litters in long days. Thus, the effects of short-days on maternal behavior may be pineal-independent. The POA and VMN are also involved in the control of lordosis in the female rat and hamster (Dornan, *et al.*, 1989; Takahashi & Lisk, 1988; Pfaff & Modianos, 1985). Thus, these structures may integrate the information about ambient light with chemosensory and endocrine input to mediate the pineal-dependent and -independent photoperiodic effects on sexual and maternal reproductive behavior.

A circadian rhythm in body temperature has been reported for rats and it is abolished by SCN lesions (Melanie & Kittrell, 1987). In the rat, some neurons of the POA and anterior hypothalamus display changes in their firing rate in response to thermal, osmotic and cardiovascular challenges (Hori, *et al.*, 1988; Knox, *et al.*, 1973; Werner & Bienck, 1985; Eisenman & Jackson, 1967). Retinal input to the POA may provide a mechanism to modulate the circadian temperature rhythm through connections with neurons responsible for the rhythm's generation.

In addition to RGC input to the VMN, retinal fibers reached the DMN. These nuclei, along with the PVN, have been implicated in the control of feeding and metabolism (Luiten, *et al.*, 1987). Recent work in the hamster has shown pineal-independent photoperiod-induced changes in various measures of energy balance and metabolism (Bartness & Wade, 1985). Therefore, photic input to these structures could be involved in the photoperiodic control of metabolic functions.

The retinal input into the piriform and periamygdaloid cortex extended from near the Tu to the level of the anterior cortical nucleus of the amygdala (Scalia & Winans, 1975). In contrast to a previous report (Johnson, *et al.*, 1988) and in agreement with Pickard and Silverman (1981), only a few fibers were evident in the amygdaloid nuclei. Like olfactory fiber input, the retinal fibers terminated in the adjacent layer Ia. In the rat and hamster, the main and accessory olfactory bulbs project to layer Ia of the piriform and periamygdaloid cortex (Devor, 1976; Haberly & Feig, 1983). Thus, direct retinal input to the Pyr may overlap olfactory projections. The olfactory cortex in turn provides some of the input to the corticomedial amygdala and amygdalo-hippocampal area (see Price, *et al.*, 1987). Fibers from these nuclei terminating in the BNST and MPoA course through the stria terminalis (Maragos, *et al.*, 1989) and modulate male sexual behavior as mentioned above. In addition, amygdala projections reach the VMN and may modulate some female sexual behaviors at this level (Krettek & Price, 1978).

Evidence of a RGC efferent projection ending in the rostral thalamus has been obtained for several mammalian species (Itaya, *et al.*, 1981; Itaya, *et al.*, 1986; Conrad & Stumpf, 1975; Johnson, *et al.*, 1988; Levine, *et al.*, 1986). The results of Experiment I confirmed the



RGC input to this thalamic region and extended our knowledge of this path in the hamster by clarifying the course taken by these fibers to the TAM/TAV. The anterior thalamic nuclei receive input from the hippocampus formation (primarily the subiculum *via* the fornix), limbic cortex and mammillary nuclei (see Jones, 1985 for a review). Recently, input to the anterior thalamic nuclei from several areas of the brainstem associated with the auditory system has been identified (Sikes & Vogt, 1987; Gabriel, *et al.*, 1980a,b). In the rabbit, the TAV have been implicated in the control of operantly conditioned responses to auditory stimuli (Gabriel, *et al.*, 1980a,b). The electrophysiological activity of the TAV and anterior cingulate cortex is positively correlated with acquisition of discriminative behavior. When the relationship of the conditional stimuli to the unconditional stimuli are reversed, only the TAV displays a reversal in the electrophysiological response to the 'new' positive versus 'old' positive stimuli. Furthermore, this reversal becomes significant only during the first session in which the training criterion is met. Although there is currently no evidence for a similar mechanism involving the control of responses to visual stimuli, the TAV may participate in the learning of conditioned discriminatory behavior through mechanisms that involve polymodal sensory input.

The combined results of Experiment Ia and Ib suggest that the retinal input to the hypothalamus and basal forebrain is more widespread than traditionally thought. While the results of RLM injections provided additional evidence in support of the extended distribution of retinal input to certain areas of the brain, the total number of retinal cells labeled per case was relatively small. The small number of labeled RGC's may simply reflect the presence of a relatively small projection

from the retina to these sites. Alternatively, the small number of labeled RGC's may indicate that the efficiency of latex microspheres to label cells retrogradely is relatively low compared to anterograde labeling of fibers by HRP conjugates. However, double-labeling studies in the visual system have demonstrated that collaterals of some cells reach widely separated terminal sites (Pickard, 1985, Giollo & Town, 1980; Jeffery, *et al.*, 1981; Yamadori, *et al.*, 1989). Thus, a subset of ganglion cells may provide input to a variety of structures in the basal forebrain simultaneously. Such input might serve to coordinate the activity of various systems in response to the prevailing photoperiod in addition to the information relayed by the SCN.

**EXPERIMENT IIa-The PVN Efferent Pathway to the Spinal Cord  
Identified by Iontophoretically Applied *Phaseolus vulgaris*-  
Leucoagglutinin.**

Lesions that destroy the PVN of the Syrian hamster prevent short-day-induced gonadal regression in males and acyclicity in females (Eskes & Rusak, 1985; Brown, *et al.*, 1988; Bartness, *et al.*, 1985; Lehman, *et al.*, 1984; Pickard & Turek, 1983). Horizontal knife-cuts placed above the PVN are similarly effective in preventing short-photoperiod induced gonadal regression in males (Nunez, *et al.*, 1985; Inouye & Turek, 1986). The model of the multisynaptic pathway mediating the expression of photoperiodism suggests that the PVN-spinal cord connection is an essential segment of the pathway. PVN efferents that course through the level of the knife cuts may be disrupted by these lesions. It is clear that the PVN projects to the spinal cord in the Syrian hamster (DonCarlos & Finkelstein, 1987; Brown, *et al.*, 1987), but the trajectory of these fibers to the spinal cord has not been described. In the rat, the course of PVN fibers terminating in the spinal cord has been examined using PHA-L (Luiten, *et al.*, 1985). Two prominent bundles arising from the PVN were described: a dorso-caudal (Tract 1) and a lateral (Tract 2) pathway. Tract 1 was comprised of a relatively small bundle of fibers formed over the third ventricle and Tract 2 developed from fibers coursing laterally from the nucleus. However, similar data are not available for hamsters. The present experiment aimed to describe the course of PVN efferents terminating in the spinal cord of the Syrian hamster utilizing iontophoretic injections of PHA-L into the PVN. The course of labeled fibers through the

diencephalon to the brain stem and spinal cord was studied in male hamsters.

## METHOD

### Animals

Adult male Syrian hamsters were housed in the same conditions as in Experiment 1.

### Surgery

Animals were anesthetized (Equithesin 4.5 ml/kg) and placed in a stereotaxic apparatus. The skull was exposed and a burr hole (dia. 3 mm) drilled through the bone. Each animal received an iontophoretic injection of PHA-L (Gerfen & Sawchenko, 1984) aimed at the lateral PVN (coordinates from Bregma: RC 0.0 mm, ML + 0.3 mm and DV —6.6 mm; nose bar —2.0 mm from ear-bar zero). Tip diameters for the glass micropipettes ranged between 12-20  $\mu$ m. The lectin was ejected from the micropipette by passing positive current through the solution using a Midguard Constant Current device set to 5  $\mu$ A and operated in the alternating on/off mode for 15 minutes. After removing the micropipette, the skin over the skull was sutured closed. Each animal was placed into an individual cage and returned to the long-day photoperiod for the remainder of the experiment.

### Perfusion and Histology

After a survival period of 6-8 days, the animals were perfused transcardially following the protocol of Gerfen and Sawchenko (1984) modified to contain buffer at 0.05 M rather than 0.1 M. This modification, in addition to the use of an infusion pump, improved the quality of the fixation. The brain and spinal cord (to the level of vertebra T<sub>2</sub>) were removed together and post fixed in the final fixative for at least 24 hours. Prior to sectioning, some of the tissue was embedded in polyethylene glycol (PEG; Smithson, *et al.*, 1983).

Immunocytochemical staining was generally improved if the tissue was embedded in this matrix prior to sectioning. Brains embedded in PEG were sectioned with a rotary microtome (15 - 35  $\mu\text{m}$ ) in a coronal or parasagittal plane and the other brains were sectioned frozen (50  $\mu\text{m}$ ) in a coronal or parasagittal plane. The tissue was processed for immunocytochemical visualization of PHA-L using a modification of the protocol of Gerfen and Sawchenko (1984). The modification included the incubation of the sections with normal rabbit serum (1:50) for hour prior to incubation of the tissue with the primary antibody (1:500). The tissue was mounted on gelatinized slides, lightly counterstained with cresylecht violet and coverslipped.

### Evaluation

The tissue from each case was examined with brightfield illumination for evidence of uptake of the lectin and anterograde transport. Cases possessing PHA-L stained cells and fibers were assigned to three groups: Group 1-included cases with the injection sites confined to the PVN. Group 2-injection sites included the PVN plus tissue outside the PVN. Group 3 cases contained injection sites located exclusively outside the PVN and were designated 'controls' for this experiment. Camera lucida drawings of the tissue containing labeled cells and processes were made of selected cases from each group.

## RESULTS

The centers of representative injections are shown in schematic drawings in Figure 14. Four injections were centered in the PVN,

**Figure 14. Schematic drawings of the center of PHA-L injections to show their location in the brain. The numbers in the lower left corner refer to the case number (Cor - coronal section; Sag - sagittal section).**

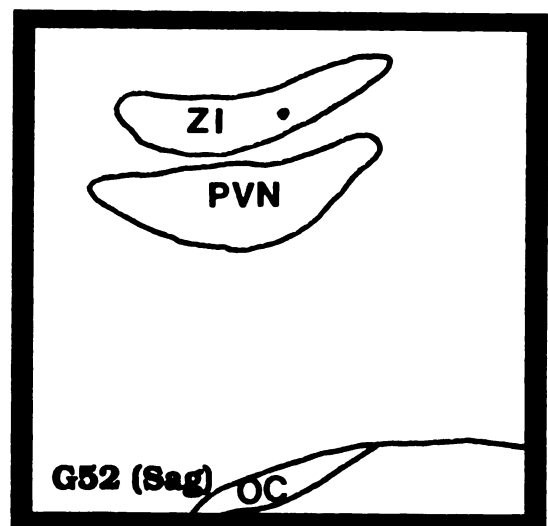
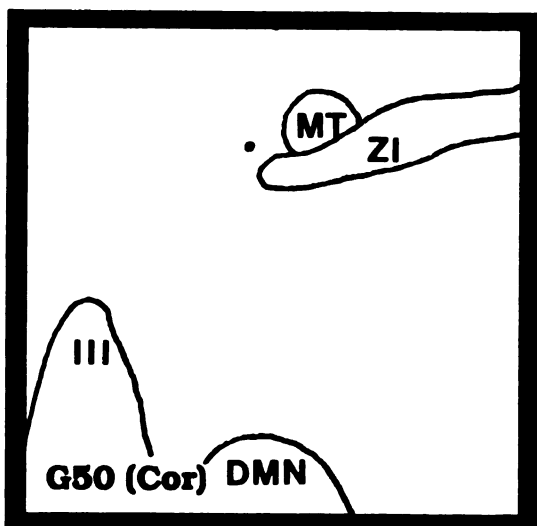
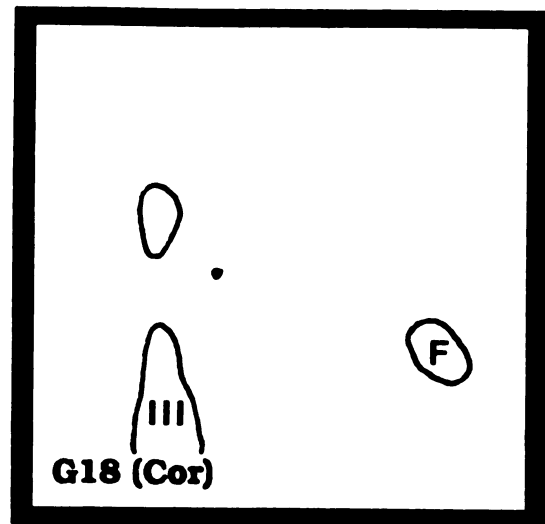
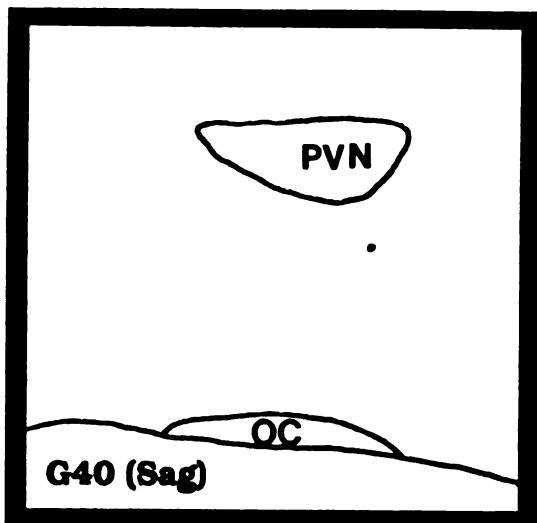


Figure 14— (continued)



including two into the lateral PVN (G10 and G16) and one each into the ventro-medial PVN (G28) and medial PVN (G67). Other injections (Group 2) spread to include the PVN and adjacent structures, such as the ZI (G133) and AHA (G39, G40). The remaining injections (Group 3) pictured in Figure 14 were centered outside the PVN and did not spread into the PVN (G18, G50, G52).

There were few differences in the overall pattern of staining in the diencephalon and mesencephalon regardless of the injection's location. The distribution of labeling obtained from the injections included in Group 1 will be presented first, followed by a brief description of particular variations that were evident in cases included in Groups 2 & 3. Animal G16 received an injection into the proximal lateral PVN and will be used to present the description of PVN efferents because of the relatively large number of cells and fibers stained by this injection that was confined to the PVN (Figure 15). Additional detail will be provided from G10 which was sectioned in a sagittal plane.

Labeled cells were found in the caudal two thirds of the PVN with few cells located in the medial subdivision of the nucleus. Numerous darkly stained fibers emanated from the vicinity of the injection, oriented predominantly medio-laterally. Near the PVN these fibers were relatively thick, with few varicosities. Shorter labeled fiber segments emanated from the PVN in all directions, but the largest number were distributed throughout the medial two-thirds of the hypothalamus between the PVN and base of the brain. These segments were thin with occasional clusters of swellings along the fibers or individual short branches ending in swellings. The density of labeled fibers was generally lower in the medial PVN than in immediately adjacent tissue



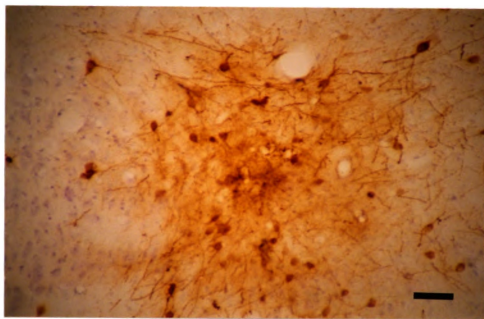


**Figure 15 . Photomicrograph of a coronal section through the center of a PHA-L injection site confined to the PVN (G16). (brightfield illumination; Bar = 50  $\mu$ m)**

(Figure 15, 16A,B). The fibers present in the medial PVN were fine caliber with few branches.

Areas of the brain receiving PVN efferents are identified in Table 2. A fiber bundle of PVN origin was seen dorsal to the third ventricle. Fibers contributing to this bundle (labeled 1a in Figure 16) coursed medially over the PVN, then turned dorsally and traversed the thalamus until reaching the thalamic paratenial (PT) and paraventricular nuclei (PVT). Few varicosities or branches were evident on these fibers until they entered these thalamic nuclei where some fibers appeared to terminate in short branches with terminal swellings. The majority of the fibers continued into the ipsilateral lateral habenula (LH in Figure 16) where short branches contained increased numbers of putative terminals (Figure 16C). Occasional fibers were evident in the medial habenula (MHa). A smaller number of fibers entered the contralateral habenula. Data obtained from G10 indicate that some fibers followed a rostro-dorsal course over the anterior pole of the thalamus before entering the PVT and habenula. Caudal to the PVN, few fibers of this bundle were present in the thalamic and subthalamic region between the habenula and hypothalamus. Some fibers in this path continued caudally to the level of the posterior commissure (PC) and subcommissural organ (SO; Figure 16D). The increased branching of labeled fibers and the number of swellings suggested this was also a terminal field for this path. A ventral continuation of this path entered the PAG where some of the fibers terminated. It is not clear whether any fibers in this path continued on to the spinal cord.

A second dorsal, midline path (1b in Figure 16) was confined closer to the roof of the third ventricle (Figure 16 A-C). At the level of

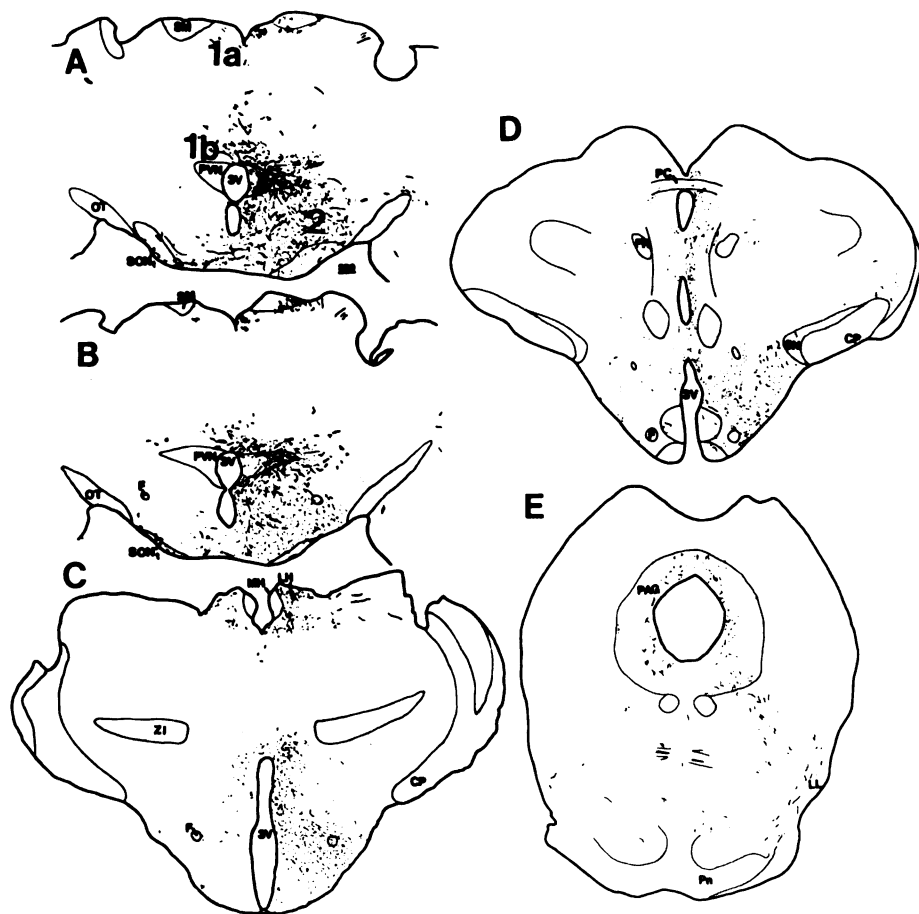


**Figure 16.** Camera lucida drawings of coronal sections through the brain of a hamster (G16) that received an iontophoretic injection of PHA-L into the lateral PVN. Some fibers emerging dorsally (1a & 1b) and ventro-laterally (2) from the PVN and formed tracts that followed separate trajectories to the periaqueductal grey (PAG). (Bar = 300  $\mu$ m)

Table 2

## Areas of the CNS Containing PHA-L Stained PVN Efferents

**AMYGDALA**

Central Nucleus  
Corticomедial Nucleus

**BRAIN STEM/SPINAL CORD**

Area Postrema  
Periaqueductal Grey  
Dorsal Nucleus of the  
Vagus  
Intermediolateral Cell  
Column  
Locus Coeruleus  
Nucleus of the Solitary  
Tract  
Parabrachial Nucleus

**HYPOTHALAMUS/PREOPTIC**

Anterior Preoptic Area  
Anterior Hypothalamic  
Area  
Dorsomedial Nucleus  
Lateral Hypothalamic  
Area

Medial Preoptic Area  
Septohypothalamic  
Nucleus  
Supraoptic Nucleus  
pars anterior  
pars tuberal  
Ventromedial Nucleus

**SEPTAL AREA**

Lateral Septum  
dorsal  
intermediate  
Medial Septum  
Triangular Septum

**THALAMUS/EPITHALAMUS**

Lateral Habenula  
Paraventricular Nucleus  
Nucleus Reuniens

the mammillary bodies the fibers turned dorsally along the midline to enter the PAG (Figure 16D). Some labeled fibers in the ventral, medial and dorsal PAG branched into fine caliber short branches tipped by stained swellings. A minority of these fibers then turned ventro-laterally to join a lateral fascicle (described below) of stained fibers near the lateral surface of the brain stem at the level of the parabrachial nucleus (PB; Figure 16E). In the brain stem some midline fibers terminated in the AP, locus coeruleus (LC), nucleus of the solitary tract (NST) or dorsal nucleus of the vagus (DNV; Figure 17). While individual fibers were observed near the midline caudal to the AP, there was no evidence of a terminal field. Labeling was not detected near the midline caudal to the raphe obscurus (RPO) or in the central grey of the spinal cord.

At the level of the PVN, diffusely distributed fibers were located primarily in the medial two-thirds of the hypothalamus ventral to the PVN (Figure 16A,B). Caudally, at the level of the VMN, a group of fibers clustered near the fornix (bundle 2 in Figure 16C) and other fibers were evident in both layers of the median eminence. Further caudally, the fibers in the ventro-lateral hypothalamus remained near the surface of the brain. At the level of the mammillary bodies, fibers in the medial hypothalamus provided input to the mammillary nuclear complex. Fibers of the ventro-lateral bundle turned dorso-laterally taking a position over the substantia nigra (SN). This group formed the fascicle which joined with the dorsal path near the PB. Some of these fibers terminated in the PB while the remainder appeared to continue into the spinal cord. In the spinal cord, fibers were found in the lateral funiculus (Figure 17). In the lower cervical spinal cord, labeled thin

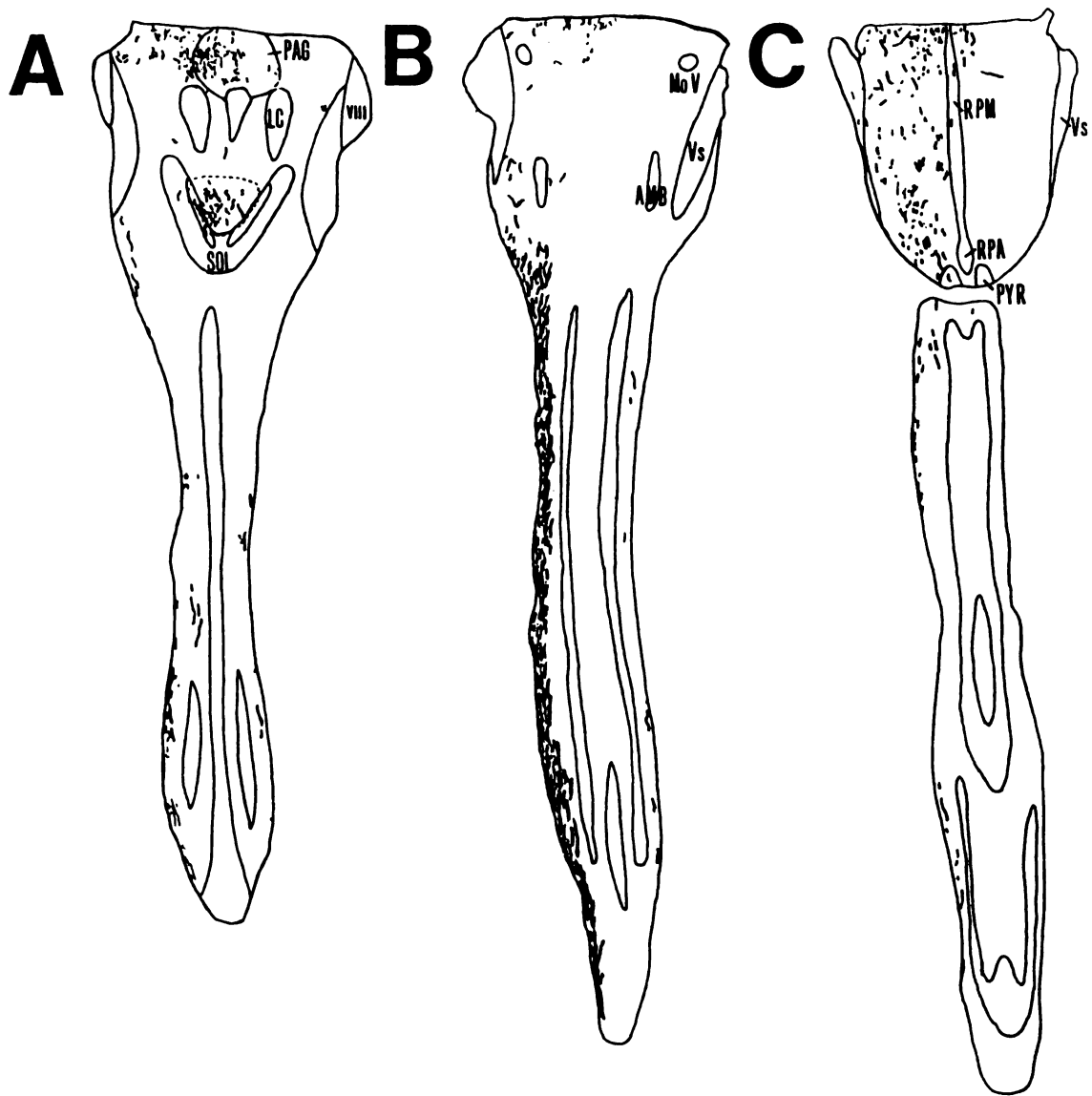


**Figure 17. Schematic drawings of horizontal sections of the caudal brainstem and spinal cord (cervical and rostral thoracic) from an animal that received an iontophoretic injection of PHA-L into the left (L) PVN (G16). Drawings are arranged dorsal (A) to ventral (C) and are composites of 4 sections taken from each third of the spinal cord.**



collateral branches could be traced medially to the IML. Some fibers in the IML terminated in small clusters of swellings while others divided again into several fine branches that surrounded individual cell bodies. The pattern of labeling in tissue sections taken from other animals in Group 1 was similar to that observed in G16.

Several differences in the distribution of staining were noted in cases included in Groups 2 and 3 compared to the cases in Group 1. The dorsal bundles were more salient after injections that encompassed both the dorsal PVN and ZI (G133) or AHA (G39, G40). In contrast, few stained fibers were found in the habenula following injections restricted to the ZI (G52), the hypothalamus ventro-caudal to the PVN (G18), or near the mammillo-thalamic tract (MT) dorso-caudal to the PVN (G50). Injections into the AHA (G39, G40) and ZI (G52) labeled some fibers in the PVN, but the density of labeling in the nucleus proper was clearly less than in the hypothalamus immediately ventral to it. Staining was not evident in the median eminence when the injection was confined to the ZI (G52). All of the injections resulted in labeled fibers in the spinal cord with the exception of G40, in which no stained fibers could be found in the spinal cord and G39 in which only one stained fiber was found in the spinal cord. In three cases (G133, G18 & G52) stained fine caliber fibers branched and surrounded individual cells in the IML ipsilateral to the injection site.

**EXPERIMENT I Ib-The PVN Efferent Pathway to the Spinal Cord:  
Retrograde labeling of Neurons and Fibers in the PVN and  
LHA.**

Evidence suggesting that a direct paraventriculo-spinal projection terminates in the IML was described for male hamsters in Experiment I Ia. The data indicated that PVN efferents to the spinal cord may follow several pathways, including the possibility of a dorsal tract passing through the habenula. There is functional evidence to suggest a possible sex difference in the circuit mediating the gonadal response to photoperiod in Syrian hamsters. In males, horizontal knife cuts placed above the PVN block testicular regression when the animals were placed in a short-day photoperiod (Nunez, *et al.*, 1985; Inouye & Turek, 1985). In contrast, similar cuts made in females were ineffective in preventing uterine regression and acyclicity (Badura, *et al.*, 1989). One interpretation of these results suggests that an anatomical difference exists between the sexes in the path taken by PVN efferent fibers terminating in the spinal cord that are involved in the control of photoperiodism. However, knife-cuts dorsal to the PVN in male hamsters have been associated with elevated serum levels of FSH (Badura, *et al.*, 1989). Regularly fluctuating levels of FSH are normal in the female (Lisk, 1985) and persistently elevated levels of FSH resulting from knife cuts placed dorsal to the PVN may be ineffective in maintaining estrous cyclicity.

PHA-L offered several advantages over other anterograde tract-tracing techniques (e.g. - autoradiography). The lectin is taken up by a limited number of neurons and dendrites located at the injection site but not by intact fibers-of-passage (Gerfen & Sawchenko, 1984). Thus

the extent of the effective injection site may be assessed. The resulting Golgi-like filling of the stained cells and fibers, including fibers some distance from their parent cells, permits easy identification of the labeled fibers and putative terminals that can then be related to the set of labeled neurons. However, in the present context the PHA-L technique could not answer several questions regarding the PVN-spinal cord connection in the hamster. Injections of PHA-L labeled cells projecting to other areas of the brain in addition to those terminating in the spinal cord. A distinction between those labeled paraventricular fibers terminating prior to the spinal cord relative to those terminating in the spinal cord was not possible. Also, there was no assurance that the labeled cells were representative of the paraventriculo-spinal cord connection. Retrograde tract-tracers can complement the results of anterograde techniques such as PHA-L by providing information regarding the source of input to the spinal cord. Conjugates of HRP can retrogradely fill the neurons by way of fibers that extend into the injection site as well as the fibers themselves, thus, permitting identification of the source neurons and the tracing of the fiber's course from the parent cell toward the injection site. However, when several sources of input exist, labeling of structures near the injection site can be relatively dense and indiscriminate, reducing the possibility of discerning the pattern of fiber termination in the vicinity of the injection site.

The present experiment sought to confirm the path of axons of PVN neurons that terminate in the spinal cord in male and female hamsters, and to determine if sex differences exist in the anatomy of these connections, using pressure injections of either WGA-HRP or CT-

HRP aimed at the level of segments C<sub>7</sub>-T<sub>1</sub> of the spinal cord to retrogradely label PVN neurons.

**METHOD****Animals**

Animal and housing conditions were identical to EXPERIMENT Ia.

**Surgery**

Animals were anesthetized with Equithesin (4.5 ml/kg). Each animal received unilateral or bilateral pressure injections of an HRP conjugate between C<sub>7</sub> and T<sub>2</sub>. Multiple injections (totaling 3  $\mu$ l/side) of WGA- or CT-HRP were aimed at the IML. The conjugates were prepared in the laboratory of Dr. R.R. Miselis (Univ. of Pennsylvania). In some early cases a laminectomy was performed (n = 5 males) at the level of C<sub>7</sub> to T<sub>1</sub> and the dura mater incised. To enhance uptake of CT-HRP the spinal cord was hemisected (unilateral injection; n = 3) and the CT-HRP injected just rostral to the area of insult. In cases where bilateral injections were made, the lateral spinal cord was intentionally damaged (crushed or cut transversely; n = 2) in the area which received the injection.

In the remaining cases (n = 19 males & 3 females), an incision was made on the dura and pia mater after the spinal column was exposed, and a glass tipped 1- $\mu$ l Hamilton syringe was used to place 3-1  $\mu$ l injections of one of two HRP conjugates into the lateral spinal cord (see Figure 18 and METHOD-Experiment Ib for details). Either WGA-HRP or CT-HRP, prepared with the assistance of Dr. M.L. Weiss at M.S.U., was used. The protocol followed in the preparation of the conjugates was essentially the same as used for Experiment Ia. In most cases, the conjugate and free HRP mixture was used for injections into the animals without first separating the conjugates from the precursors. Prior

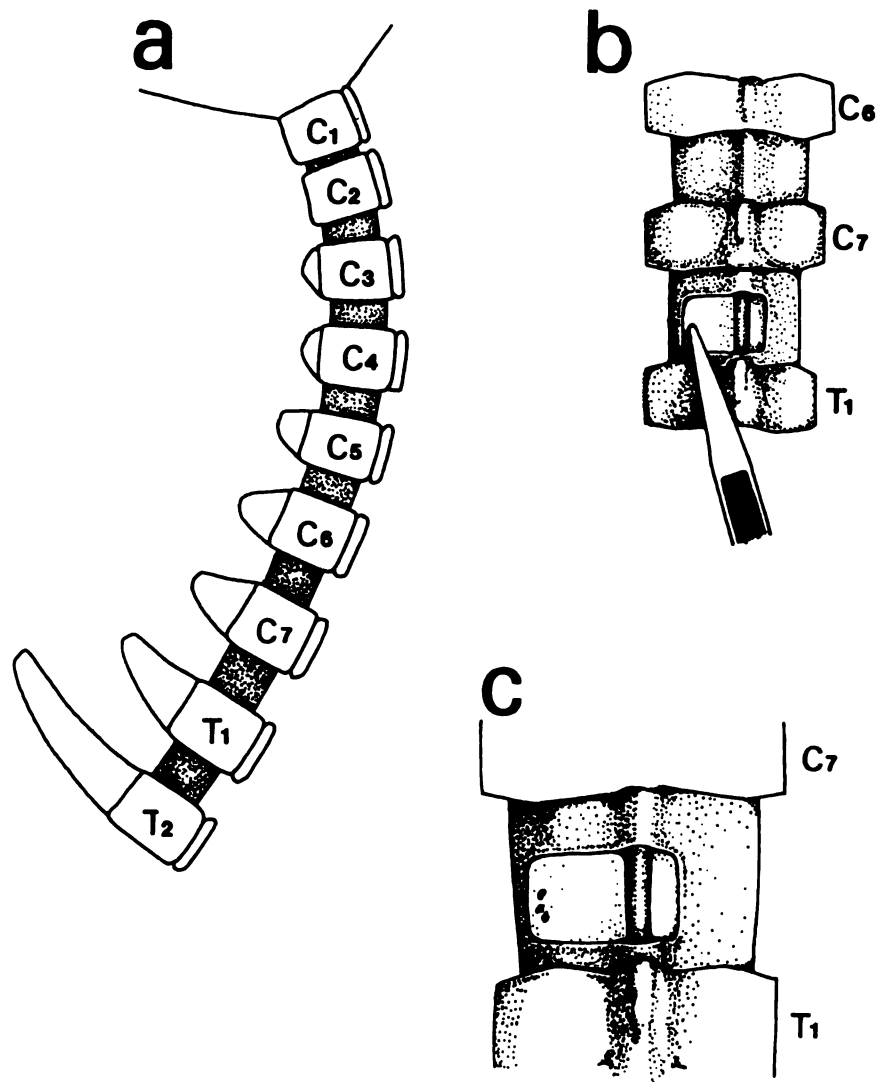


**Figure 18.** Schematic drawing demonstrating the vertebra, dorsal spines and spinal cord of the upper thoracic and cervical spinal column (a) of a Syrian hamster depicting the location of the glass pipette-tipped 1- $\mu$ l Hamilton syringe (b) used to inject the HRP conjugates into the lateral spinal cord (c).

to its use, a portion of the WGA-HRP was separated from the free HRP on an FPLC column (Superose 12) provided by Dr. J Kaguni, Dept. of Biochemistry, M.S.U. prior to its use. The various solutions produced similar patterns of labeling in the hypothalamus. Following the injections, the musculature and overlying skin was sutured closed. The animals were individually housed and returned to the long-day photoperiod following surgery until the time of sacrifice.

#### Perfusion and Histology

The animals were sacrificed after 2-3 days and the tissue processed following the protocol described in Experiment Ia. The brains were sectioned in either a coronal (n = 24) or sagittal (n = 3 males) plane.

#### Evaluation

The sections were examined with bright- and dark-field optics immediately after the reacted tissue was mounted and coverslipped. Photographs were taken for documenting the presence of labeled fibers and neurons within the PVN and lateral hypothalamus. Camera lucida drawings of representative tissue sections were made during the same examination of the tissue and stained fibers and retrogradely filled neurons were plotted.

### RESULTS

The pattern of labeling was similar in male and female hamsters. The intensity of labeling increased with increased survival time but the pattern was not altered. Further, manipulation of the spinal cord near the injection site did not alter the distribution of labeling. In addition to the labeling in the hypothalamus that is reported below, an

occasional neuron ( $N < 4/\text{animal}$ ) in the SON ipsilateral to the injection site was observed. Labeling was not evident in the preoptic area or hypothalamus rostral to the PVN, and no labeled cells were found in the SCN. A list of sites in the brain that contained retrogradely labeled cells is presented in Table 3.

The injections were clustered approximately half-way between the midline and lateral edge of the spinal cord (Figure 18) and extended approximately 1 mm rostro-caudally, spreading laterally to the surface of the spinal cord. After unilateral injections a small amount of intra- and extracellular reaction product was evident in the spinal cord contralateral to the injection site. However, the contribution of this staining to the results described below appeared to be minor based upon the relatively sparse labeling found in the contralateral hypothalamus.

Case 88-G84, an animal receiving a unilateral injection of WGA-HRP, was representative of the results obtained and will be described in detail. The hypothalamic projection to the spinal cord was predominantly ipsilateral (Figure 19). Near the rostral pole of the PVN, labeled cells and processes were scattered throughout the PVN ipsilateral to the injection (Figure 19A, 20). At this level, the labeled cells were generally small to medium sized, ranging between 9.5 and 16  $\mu\text{m}$  on their long axis. An occasional cell was evident in the dorsal and lateral hypothalamus. Moving caudally approximately 200  $\mu\text{m}$  from this level, the cluster of stained cells in the ventro-lateral PVN expanded laterally. The smaller cluster of cells in the dorsal PVN (Figure 19B) was intensely labeled. Some horizontally directed fibers from this group were traced to the midline (Figure 21).



Table 3

**Areas of the Brain Containing Retrogradely Labeled Neurons Following  
Injections of CT- and WGA-HRP into the Spinal Cord.**

**Telencephalon**

Basal Nucleus of Meynert  
Pyramidal Cells  
Parietal Cortex  
Sensory Cortex  
Substantia Innominata

**Diencephalon**

Dorsal Hypothalamus  
Lateral Hypothalamus  
Paraventricular Nuclei  
Posterior Hypothalamus  
Retrochiasmatic Area  
Zona Incerta

**Mesencephalon**

Dorsal Raphe Nucleus  
Lateral Dorsal Tegmentum  
Nucleus of Darkschewitsch  
Periaqueductal Grey  
Red Nucleus

**Metencephalon**

Locus Coeruleus  
Medial Parabrachial Nucleus  
Pontine Reticular Nucleus,  
Ventral  
Subcoeruleus  
Reticulotegmental Nucleus,  
Pons  
Pedunculo pontine Tegmental  
Nucleus

**Myelencephalon**

Nucleus Ambiguus  
Reticular Nucleus of the  
Medulla, ventral part  
Nucleus of the Solitary  
Tract  
Raphe Caudal Linear Nucleus  
Ventral Gigantocellularis  
Nucleus  
Ventral Medullary Reticular  
Nucleus

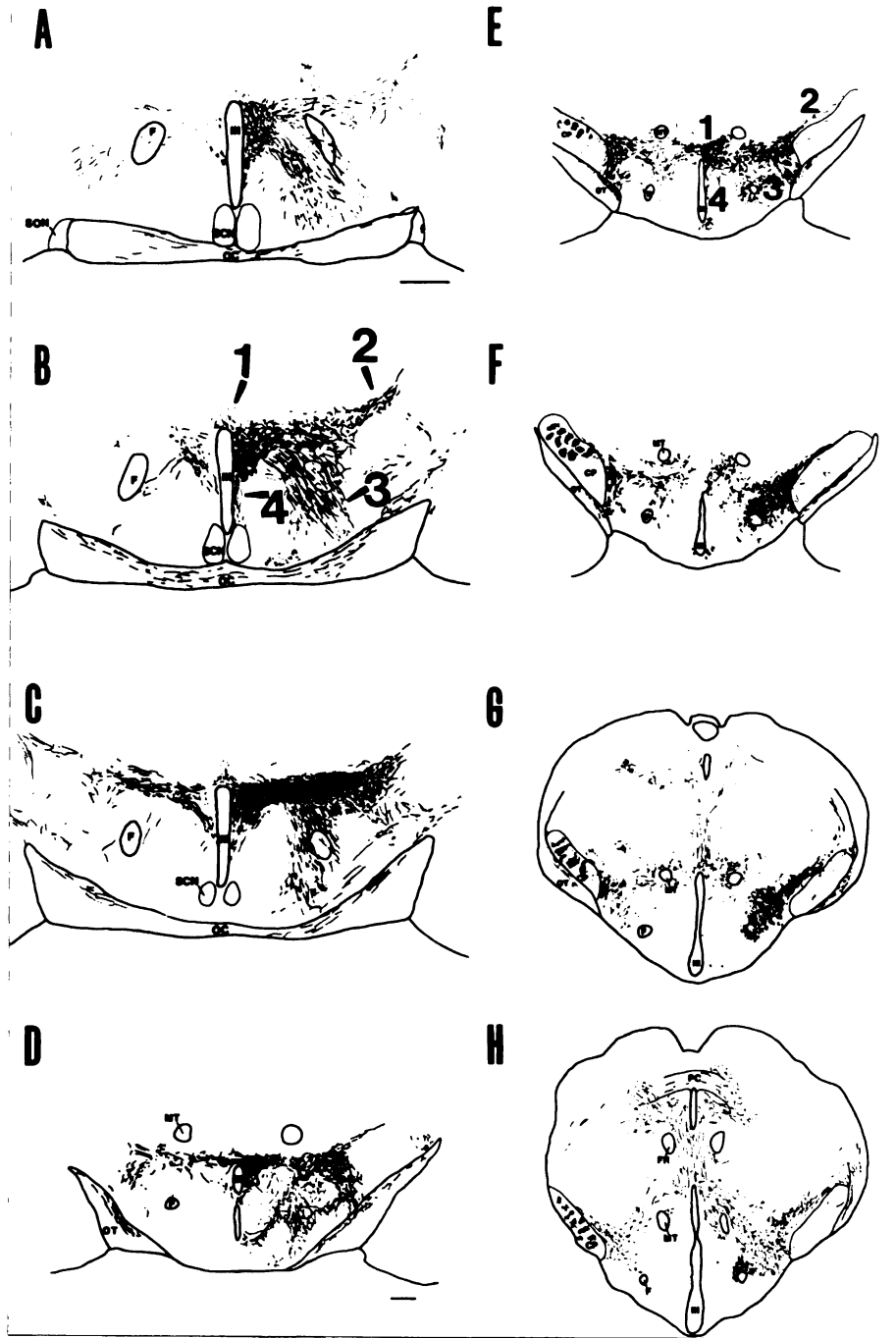


**Figure 19.** Camera lucida drawings of coronal sections through the brain of a male Syrian hamster that received a unilateral injection of WGA-HRP into the spinal cord between vertebra C<sub>7</sub> and T<sub>1</sub>. Labeling in the brain was predominantly ipsilateral to the injection site. Four tracts (labeled '1', '2', '3' & '4' in [B]) of stained fibers were seen to emanate from the PVN. (Bar [A & D] = 500  $\mu$ m)

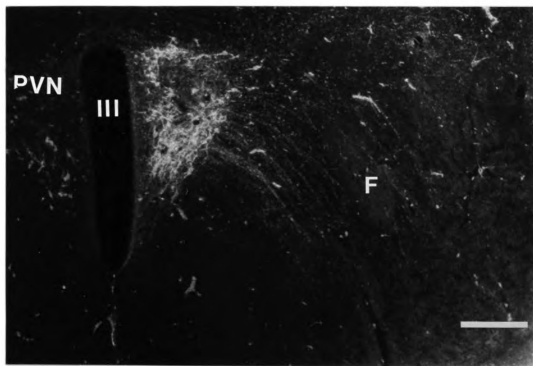


Figure 20. Photomicrograph of a coronal section through the rostral PVN of a Syrian hamster. The dorsal and ventro-lateral PVN ipsilateral to an injection of WGA-HRP into the spinal cord contained retrogradely labeled neurons and fibers. Tract 3 was prominent as fibers from the PVN course ventro-laterally around the fornix. A few fibers were seen over the roof of the third ventricle (Tract 1), lateral to the PVN (Tract 2) and ventral to the PVN (Tract 4). Scattered labeled cells were also seen in the ipsilateral hypothalamus and contralateral PVN. (darkfield illumination; Bar = 200  $\mu$ m)

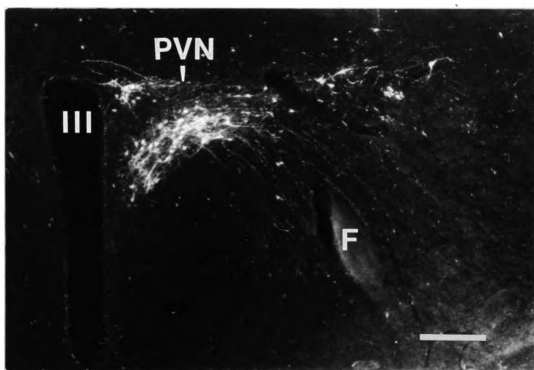


Figure 21. Photomicrograph of a coronal section near the middle of the PVN. A collection of retrogradely labeled cells were observed in the dorsal and ventro-lateral PVN. Fibers of Tract 3 remained evident around the fornix. Some fibers of the dorsal cell group were traced to the area over the third ventricle. (darkfield illumination; Bar = 200  $\mu$ m)

In the caudal third of the PVN, the lateral subdivision extending over the fornix was so densely stained that individual features were difficult to discern (Figure 19C, 22). Those cell bodies which could be distinguished from the background of dense staining were large (25 - 35  $\mu\text{m}$  on their long axis), fusiform and oriented in a horizontal plane. At the same level, the number of labeled cells in the medial PVN declined while the density of labeled fibers appeared to remain similar to the previous level.

Near the posterior limit of the PVN, labeled cells were scattered bilaterally and were more numerous in the dorsal half (Figure 19D, 23). Contralateral to the injected side, the number of stained PVN cells and fibers was quite small and mirrored the location of labeled cells in the ipsilateral nucleus. Some fibers crossed the midline dorsally, but it was not obvious from which half of the hypothalamus they originated (Figure 19D,E).

Outside the PVN, stained fibers were generally located within one of four bundles (see Figure 19 for a summary of the paths taken by these bundles). Two minor bundles, one above and one below the PVN remained near the midline, while two larger bundles emerged laterally. One immediately turned ventro-laterally approaching the lateral OC and the other continued lateral over the fornix. To facilitate comparison with Experiment IIa and the work of Luiten, *et al.*, (1985) in the rat, the individual bundles will be identified as Tracts 1 through 4 with the dorsomedial bundle as Tract 1, the lateral bundle as Tract 2, the ventro-lateral bundle as Tract 3 and the ventro-medial bundle as Tract 4.

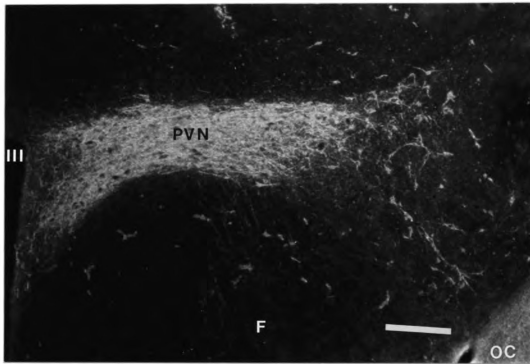


Figure 22. Photomicrograph of a coronal section through the caudal third of the PVN showing the nucleus ipsilateral to the injection site. The lateral parvocellular subdivision (as defined for the rat by Swanson & Kuypers[1980]) was intensely labeled and few individual cells could be seen distinctly from the background of labeling. The ventro-medial portion of the PVN contained fewer labeled cells than the lateral division while the fewest number of cells were observed in the medial PVN. (darkfield illumination; Bar = 200  $\mu$ m)

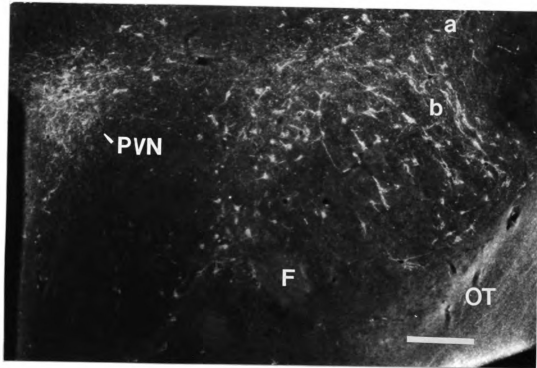


Figure 23. Photomicrograph of a coronal section through the caudal PVN. WGA-HRP labeled cells were present in the PVN and scattered through the LHA. At this level, fibers of Tract 2 split into two bundles. One fascicle turned ventrally (b) to join Tract 3 in the caudal hypothalamus while the second turned dorso-laterally over the CP (a). (darkfield illumination; Bar = 200  $\mu$ m)

Tract 1 remained within 200  $\mu\text{m}$  of the roof of the ventricle through much of the caudal hypothalamus. Additional PVN fibers joined Tract 1 from the posterior levels of the nucleus. Near the caudal pole of the PVN, the tract became less salient. Comparison of coronal sections with those cut in a sagittal plane suggests this tract continued caudally through the posterior hypothalamus, where the bundle turned dorsally. A dense cluster of labeled cells was grouped near the ventro-medial MT and dorsal hypothalamus and fibers from these cells mingled with Tract 1 fibers as they continued into the PAG (Figure 19E-H). Retrogradely labeled cells were present in the PAG and the addition of labeled fibers from these cells to those just described prevented tracing Tract 1 further caudally.

Tract 2 arched dorsally over the fornix and continued into the LHA (Figure 19A,B, 20 & 21). At the level of the caudal PVN, it divided into two paths, a dorso-lateral and a ventro-lateral component (Figure 19D, 23). This division anticipated the appearance of the CP present in subsequent caudal sections. Labeled cells were abundant from the ZI ventrally to the OT (Figure 19D-F, 22). Retrogradely labeled cells were also scattered in the ZI ipsilateral to the injection site and their axons contributed to the dorsal limb of Tract 2. The dorsal component continued caudally above the CP and SN while the ventral branch merged with Tract 3 (described below) in the posterior hypothalamus.

Fibers in Tract 3 emerged from the lateral and ventro-lateral PVN (Figure 24), surrounding and passing through the fornix then entered the MFB as the tract coursed through the caudal hypothalamus (Figure 19). A few retrogradely labeled cells (3-4/sections) were present in the fornix and contributed to Tract 3. At the level of the caudal SCN, a



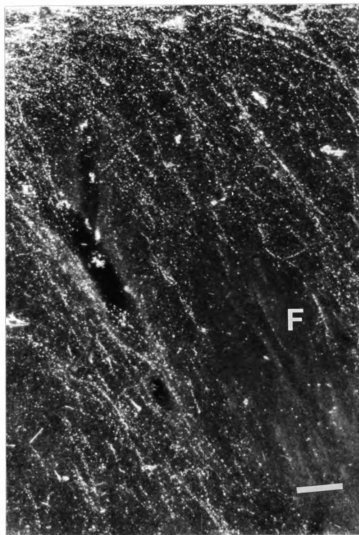


Figure 24. Photomicrograph of a coronal section near the level of Figure 21. The PVN is just out of the field depicted dorsally and to the viewer's left. Numerous fibers emerged from the ventral border of the PVN and surrounded or passed through the fornix. (darkfield illumination; Bar = 50  $\mu$ m)

small group of cells and fibers were situated near the OC lateral to the SCN (Figure 19B). Stained fibers from this cluster appeared to course dorso-laterally to meet Tract 3. A second group of retrogradely labeled cells was clustered in the retrochiasmatic hypothalamus adjacent to the floor of the third ventricle further caudally (Figure 19D). Fibers from this cluster also rose dorso-laterally to meet Tract 3. About 300  $\mu\text{m}$  further posterior in the hypothalamus, Tract 3 collected around the fornix (especially the ventromedial quadrant). Approximately 250  $\mu\text{m}$  posterior, Tract 3 moved to a position lateral to the fornix, merging with fibers of the ventral limb of Tract 2 and other fibers from the labeled lateral hypothalamic neurons. Labeling in the LHA began at the level of the caudal SCN and persisted through caudal sections. At the level of the caudal PVN, labeled cells of the LHA formed a ventro-lateral continuum with those labeled PVN neurons of the lateral subdivision (Figure 23). Fibers were consistently seen in the OC crossing the midline. Neurons of the LHA contributed some of these fibers and the possibility of LHA contribution to Tract 2 or Tract 3 fibers cannot be ruled out. In the posterior hypothalamus, at the level of the mammillary bodies, Tract 3 moved dorso-laterally over the SN (Figure 19G,H). Fibers of this tract may have joined with fibers from the dorsal limb of Tract 2 in this region.

The ventro-medially directed Tract 4, emerged from the ventral PVN and following the wall of the third ventricle, tapering medially toward the wall (Figure 25). The tract was first evident in sections containing the SCN. The tract approached this nucleus, but did not invade it. Additional fibers joined the tract at intervals from the PVN but beyond the posterior PVN they turned caudally and could not be

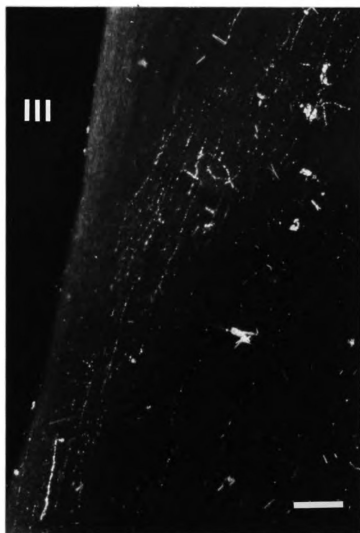


Figure 25. Photomicrograph of a coronal section near the level of Figure 20, showing labeled fibers of Tract 4 near the wall of the third ventricle. (darkfield illumination; Bar = 50  $\mu\text{m}$ )

detected in coronally sectioned material. Labeling in tissue sectioned in a sagittal plane suggests these fibers continued caudally to the posterior hypothalamus where fibers adjacent to the third ventricle wall turned dorsally and were joined by fibers from retrogradely labeled cells located nearby. It is possible that fibers of Tract 4 merged with fibers of Tract 1 as they coursed through the rostral mesencephalon.

### DISCUSSION

The PVN neurons terminating in the spinal cord were located through the rostro-caudal extent of the nucleus (Experiment IIb). The projections of the PVN are primarily uncrossed as reported previously for the hamster (DonCarlos & Finkelstein, 1987) and rat (Swanson and Kuyper, 1980). Most of the cells retrogradely labeled were in areas corresponding to the parvocellular subdivisions described for the rat (Swanson & Kuyper, 1980), however, a few labeled cell were located in the magnocellular subdivision. Cell sizes ranged from those generally considered parvocellular to magnocellular and, thus are not a good predictor of neurons that terminate in the spinal cord.

The fibers of PVN neurons terminating in the spinal cord formed 4 descending tracts. Similar to the results obtained in Experiment IIa, the WGA- or CT-HRP injections revealed the presence of fibers of PVN origin that extended dorsally over the third ventricle (Tract 1) and ventro-laterally in the hypothalamus (Tract 3). A small bundle of laterally projecting PVN fibers had been discerned after PHA-L injections to the nucleus. While individual fibers were detected in PHA-L labeled material, the quantity of labeling was not suggestive of a fiber path. In material stained with HRP conjugates, additional fibers in this

bundle were observed (Tract 2). This tract is similar in trajectory to the Tract 2 described for the rat (Luiten, *et al.*, 1985). The presence of a dorsal PVN-spinal cord projection passing through the habenula was suggested by the pattern of labeled fibers after injections of PHA-L. This projection was not confirmed by the results obtained with the HRP injections. Following spinal injections, stained fibers were rarely observed in the habenula or PVT. The method used detected a number of paths originating in the PVN, including one that has not been previously reported for PVN efferent fibers to the spinal cord (Tract 4). In addition, the injections were capable of labeling other structures previously reported to terminate in the spinal cord (Table 3), suggesting this dorsal projection probably would have been labeled if it was present. Thus the PVN projection passing through the thalamus and epithalamus of the hamster appears to terminate prior to the level of the spinal cord receiving the injections.

Of the two PHA-L labeled tracts, the injections predominantly labeled fibers that appear to correspond to Tract 3 identified in Experiment IIb. This may have been due to the placement of the PHA-L injection within the proximal portion of the lateral PVN. Many of the fibers in Tract 3 emerged from the medial and ventro-lateral PVN.

The ventro-medial tract (i.e., Tract 4) near the ventral wall of the third ventricle was not detected in Experiment IIa. This may have been because the tract was obscured by the staining found through much of the medial hypothalamus after the PHA-L injections. Fibers of this tract remained near the third ventricle through the caudal hypothalamus. Horizontal knife cuts placed between the SCN and PVN prevent gonadal regression in both male and female hamsters (Eskes & Rusak, 1985;

Nunez, *et al.*, 1985; Badura, *et al.*, 1987). These results have been attributed to the disruption of SCN input to the PVN. But, Tract 4 may provide supplemental input to the circuit mediating the circadian rhythm of melatonin production. It is not possible at this time to selectively sever this spinal cord connection as it emerges from the ventral PVN without disruption of the SCN-PVN connection and thus, it may prove difficult to isolate this tract and assess its contribution. However, knife cuts made in a coronal plane and aimed ventro-caudal to the PVN may be effective in severing this tract without damaging SCN-PVN projections.

Tract 1 remained relatively close to the roof of the third ventricle throughout most of the hypothalamus. In male hamsters, horizontal knife cuts placed dorsal to the PVN have been reported effective in preventing gonadal regression in response to exposure to a short photoperiod (Nunez, *et al.*, 1985; Inouye & Turek, 1986). However, these same knife cuts do not prevent retrograde HRP labeling of PVN neurons (Brown, 1986). Such lesions would likely have disrupted Tract 1 but would probably not have caused major damage to Tract 2 or little damage to Tracts 3 and 4. But, some of these cuts appeared to be located in the thalamus dorsal to Tract 1 and thus would not have disrupted the tract (Inouye & Turek, 1986). In castrated male hamsters, these knife cuts dorsal to the PVN produce a rise in plasma levels of FSH in excess of castrates receiving sham lesions (Badura, *et al.*, 1988). BLX and lesions of the olfactory system also cause elevated levels of FSH and LH in male hamsters housed in a long photoperiod (Clancy, *et al.*, 1986; Pieper, *et al.*, 1989). Long-term exposure of BLX animals to a short photoperiod reduces the level of serum FSH, but to a

level that remains above that measured in long-day control animals, and BLX males retain large testes. In the hypophysectomized rat, infusions of FSH that produce serum levels in the physiological range significantly reduces the decline in testicular weight and supports spermatogenesis (Bartlett, *et al.*, 1989). Thus, large testes in short-day housed males that have received knife cuts dorsal to the PVN may be attributable to elevated levels of FSH. Although the knife cuts that produce the persistent increase in FSH in males are generally found near the PVN, there is no evidence to indicate that the PVN, *per se*, is involved in the mechanism mediating the increase in serum levels of FSH. These knife cuts may disrupt fibers-of-passage that course near the PVN. Thus far, a systematic examination of this question has not been conducted.

Coronal knife cuts aimed caudal to the PVN have also been employed to examine the role of PVN efferents of Tract 1 in the pathway mediating photoperiodism (Johnson, *et al.*, 1989; Smale, *et al.*, 1989). Such knife cuts in male hamsters did not prevent gonadal regression. Coronal knife cuts would have disrupted fibers of Tract 1 while sparing most of the fibers oriented in a dorso-ventral plane that were damaged by horizontal knife cuts suspected of being responsible for the rise in serum FSH and large testes. These data support the notion that Tract 1 is not an essential part of the pathway mediating photoperiodism in the male hamster.

Bilateral parasagittal knife cuts in male and female hamsters that are placed lateral to the PVN and that disrupt most or all of Tracts 2 & 3 are effective in preventing gonadal regression and acyclicity in short-photoperiod housed animals (Badura, *et al.*, 1989; Smale, *et al.*, 1989;

Johnson, *et al.*, 1989). In males, other parasagittal knife cuts that do not extend far enough ventrally so as to lesion Tract 3 and little, if any, of Tract 2, do not prevent these short-photoperiod-induced effects (Johnson, *et al.*, 1989). However, the interpretation of these results are confounded by the placement of the cuts. SCN efferent fibers may project directly onto lateral PVN neurons or participate in a circuit that involves AHA neurons acting as intermediaries to lateral PVN neurons. Those knife cuts found to be 'effective' may have disconnected such a circuit as well as disrupted most or all of Tract 2 & 3. Whereas, 'ineffective' knife cuts may have damaged only a portion of these tracts but failed to interrupt SCN input to the lateral PVN, and thus, allowed the circuit to the pineal gland to remain intact. In the future, the results of Experiment II might be used to guide the placement of lesions in the path of each lateral tract and assist in evaluating gonadal responses to exposure to short photoperiods.



### **EXPERIMENT III-Do Extrahypothalamic Lesions of a PVN to Spinal Cord Pathway (Tract 1) Block the Testicular Response to Photoperiod?**

Data from Experiment II indicated that some fibers originating in the PVN passed through the PAG in their course to the spinal cord. These fibers project dorsally from the PVN before turning caudally, and may correspond to Tract 1 as described in the rat (Luiten, *et al.*, 1985). In the hamster, this tract (Tract 1 of Experiment IIB) follows the roof of the posterior hypothalamic portion of the third ventricle caudally and, at the level of the posterior hypothalamus, rises dorso-caudally to penetrate the PAG. In the male hamster, knife cuts placed dorsal to the PVN prevent gonadal regression in animals exposed to short-photoperiods (Nunez, *et al.*, 1985, Inouye & Turek, 1986). Thus, interruption of the dorsal efferent projections of the PVN, destined to terminate in the spinal cord appears to block photoperiodic responses in male hamsters. However, similar knife-cuts result in elevated serum levels of FSH (Badura, *et al.*, 1988) thus complicating the interpretation of the effects of such knife cuts on photoperiodism.

This experiment was completed prior to the inception of Experiment IIB and those recent studies describing the effects of parasagittal knife cuts on the reproductive system of Syrian hamsters. Thus it was designed to further investigate the importance of Tract 1 in photoperiodism, by assessing the effects of electrolytic lesions aimed at the rostral PAG on short-day induced testicular regression. Tract 1 and the lateral efferents achieve maximum separation in the diencephalic-mesencephalic transition where the fibers of Tract 1 are restricted to the rostral PAG. Such lesions would interrupt Tract 1 at an extra-

**hypothalamic site separated by some distance from the laterally projecting PVN efferents and, presumably, from those connections involved in mediating FSH release.**

## METHOD

### Animals

Adult male Syrian hamsters were initially group housed (n = 5 or 6/cage) and placed in a long photoperiod of 16 hours light and 8 hours dark. Food and water were available *ad libitum*.

### Procedures

At the end of the first week after their arrival to the colony, all animals were separated into individual plastic cages. The right testis width and body weight of each animal were measured at the end of the second week. Testicular width has been shown to be positively correlated with the ability to produce sperm in the male hamster (Turek & Losee, 1978; Berndtson & Desjardins, 1974). Animals were then randomly assigned to three groups: lesion (n = 24), short day sham (n = 12) and long day sham (n = 12).

### Surgery

*Tract 1 Lesion (LES):* Animals were anesthetized with Equithesin (4.5 ml/kg) and placed in the stereotaxic apparatus. The skull was exposed and two burr holes (coordinates from Lambda: RC +1.5 mm, ML  $\pm$  0.3 mm, DV -5.3 mm, DV taken from surface of the brain; nose bar 2 mm below earbar zero) were made bilaterally in the skull over the PAG. A steel insect pin (#00) insulated with Epoxy-lite, except for approximately 0.2 mm of the tip, was used to make the lesions. The electrode was aimed at the rostral portion of the PAG surrounding the fourth ventricle bilaterally. An cathodal current (positive terminal of the lesion maker attached to the electrode) of 2 mA was passed for 10 seconds. The electrode was immediately withdrawn and the skin sutured closed. The animals were returned in individual cages to the

long-photoperiod room for at least two weeks after recovery from anesthetic.

A large proportion of the animals with lesions (n = 19 of 24) did not survive beyond 2 weeks post-surgically. Therefore, 7 animals originally assigned to either sham group were reassigned to the lesion group. The transfer of animals to the short-day room was delayed so that additional surgeries could be performed to increase the number of surviving animals with lesions (final n = 8).

*Long day sham (LDS):* Animals in this group (n = 6) were treated in a similar manner as the lesioned animals. Sham surgery consisted of lowering the electrode into each side of the brain using the same set of coordinates. The electrode was left in place for 30 second, however the lesioning device was not turned on.

*Short day sham (SDS):* Animals in this group (n = 8) were treated in a similar manner as long-day sham animals.

*Measurements:* Animals assigned to the short-day photoperiod (sham and lesion) were transferred to a room set to a LD schedule of 6L:18D after a minimum of two weeks postsurgical recovery. The right testis width and length and body weights of all animals were obtained at the time of transfer to the final photoperiod and every 1-2 weeks thereafter for 13 weeks. The animals were lightly anesthetized with ketamine (1 mg/kg) to measure testicular size. At the end of the experiment, all short-day animals were anesthetized with an initial injection of Equithesin (4.5 ml/kg) and the testes removed. Final testes weight, length and width were determined at this time. The animals were then sacrificed by an overdose of Equithesin administered within 15 minutes of the first injection.

### Perfusion and Histology

Animals with lesions were perfused transcardially with heparinized (2 U/ml) 0.1 M phosphate buffered (pH 7.4) physiological saline rinse followed by 0.1 M phosphate buffered (pH 7.4) 4 % (v/v) formaldehyde. The brains were stored in cold fixative at least overnight, then sectioned in a coronal plane into distilled water. Sections were mounted to gelatinized slides, counterstained with cresylecht violet and coverslipped with Permount. The location of the lesion site was verified by examining the tissue with brightfield optics.

### Evaluation

Camera lucida drawings of the lesion sites were made from the counterstained tissue. Some of the drawings were traced onto photocopies of an atlas of the rat brain (Paxinos & Watson, 1982). The atlas plates used were selected by comparing structures that could be identified in the sections obtained from the hamster brain to those structures pictured in the atlas. The extent of damage to the PAG was assessed by two observers who examined the counterstained sections with brightfield illumination on a microscope. Complete lesions were defined as the absence of tissue corresponding to the rostral PAG in several sections containing the rostral mesencephalon. Incomplete lesions left some portion of the rostral of the PAG intact.

### Statistics

Group body weights and right testicular widths obtained at the end of the experiment were analyzed by one-way ANOVA. Pair-wise comparisons of mean testicular widths were made using the Least Squares Difference test.

## RESULTS

A total of three animals (1 short-day sham and 2 long-day shams) died prior to the completion of the experiment and thus were not included in the data reported here. Examination of cresylecht violet stained tissue obtained from the lesioned animals revealed that the rostral PAG was destroyed in 3 cases and extensively damaged in the other cases. Periaqueductal grey lesions (complete or incomplete) did not prevent gonadal regression in animals maintained in the short photoperiod compared to long-photoperiod-housed shams (Figure 26). The onset of regression (statistically significant decline in mean width of right testes as compared to the LDS group) in each of the two groups housed in the short photoperiod was not different from one another and occurred by Week 8. At the completion of the experiment the mean testicular width of lesioned animals was not significantly different from SDS animals (LES  $7.29 \text{ mm} \pm 0.29 \text{ mm}$  [mean  $\pm$  sem] vs SDS  $7.45 \text{ mm} \pm 0.18 \text{ mm}$ ,  $p > 0.05$  [Table 4]) while the testes width of the sham-operated animals in the long photoperiod ( $13.72 \text{ mm} \pm 0.20 \text{ mm}$ ) was significantly greater than both short photoperiod-housed groups ( $p < 0.05$ ; Table 4). There was no evidence of recrudescence in either group at the end of 13 weeks in the short photoperiod. The body-weight of animals in both groups housed in the short photoperiod displayed a non-significant decline ( $p > 0.10$ ) over the course of the experiment compared to long photoperiod-housed shams (Figure 27).

## DISCUSSION

Electrolytic lesions that destroyed the PAG did not prevent short-day induced gonadal regression in male Syrian hamsters. Nor did these lesions appear to alter the time course of gonadal regression compared

Table 4

Final Mean Width ( $\pm$  sem) of Right Testis of Male Syrian Hamsters in  
Experiment III

Group	<u>n</u>	Testes Width (mm)
Lesioned	8	7.29 $\pm$ 0.29 <sup>a</sup>
Short-day Sham	7	7.54 $\pm$ 0.18 <sup>b</sup>
Long-day Sham	4	13.72 $\pm$ 0.20

<sup>a</sup> Significantly different from long-day sham operated group  
( $p < 0.001$ ,  $df = 10$ )

<sup>b</sup> Significantly different from long-day sham operated group  
( $p < 0.001$ ,  $df = 9$ )

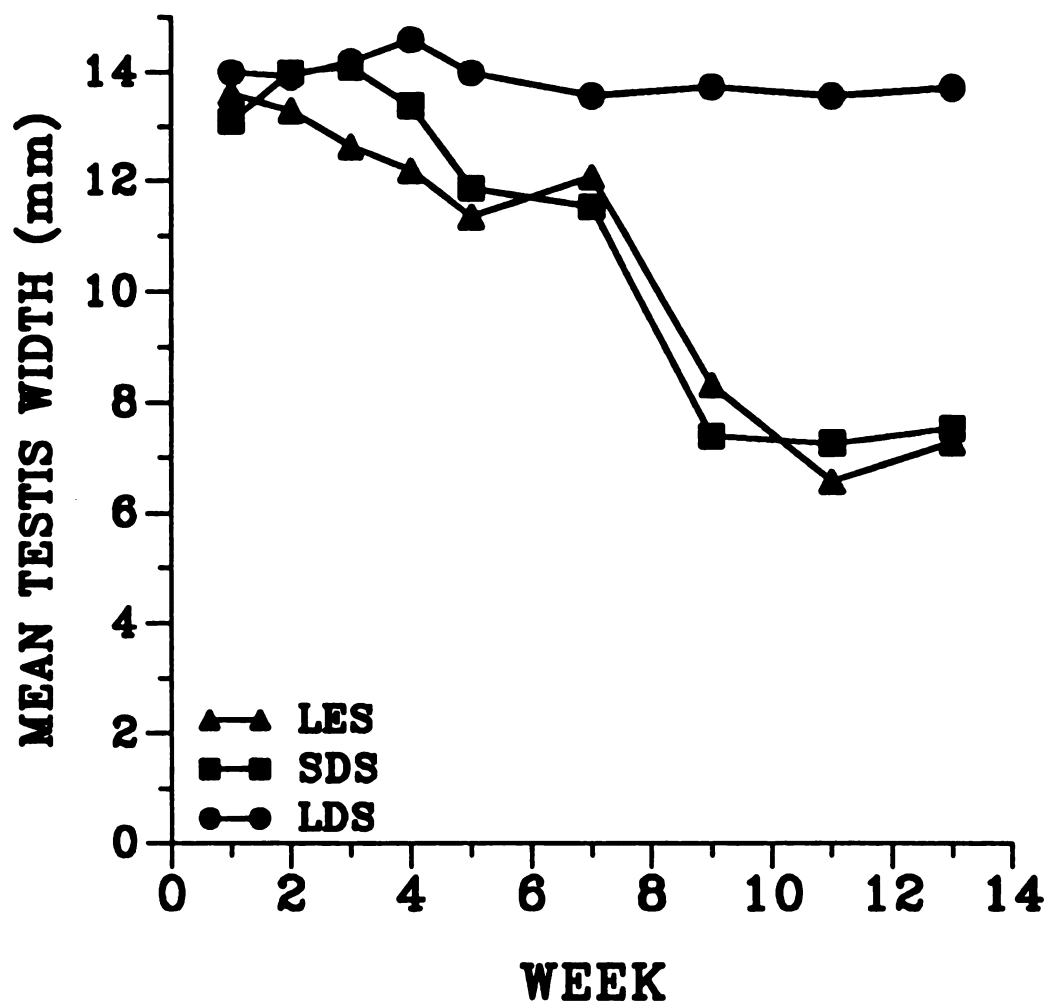


Figure 26. Mean width of the right testis (measured trans-scrotally) of animals receiving electrolytic lesions aimed at the PAG or sham-lesioned. Animals were lesioned (LES;  $n = 8$ ) or sham lesioned (SDS;  $n = 7$ ) and placed in a 8L:16D photoperiod, or sham lesioned and placed in a 16L:8D photoperiod (long-day sham [LDS];  $n = 4$ ). The mean testicular width for each short photoperiod housed groups was significantly smaller than that of the LDS group by the end of Week 8 and remained so until the end of the experiment.



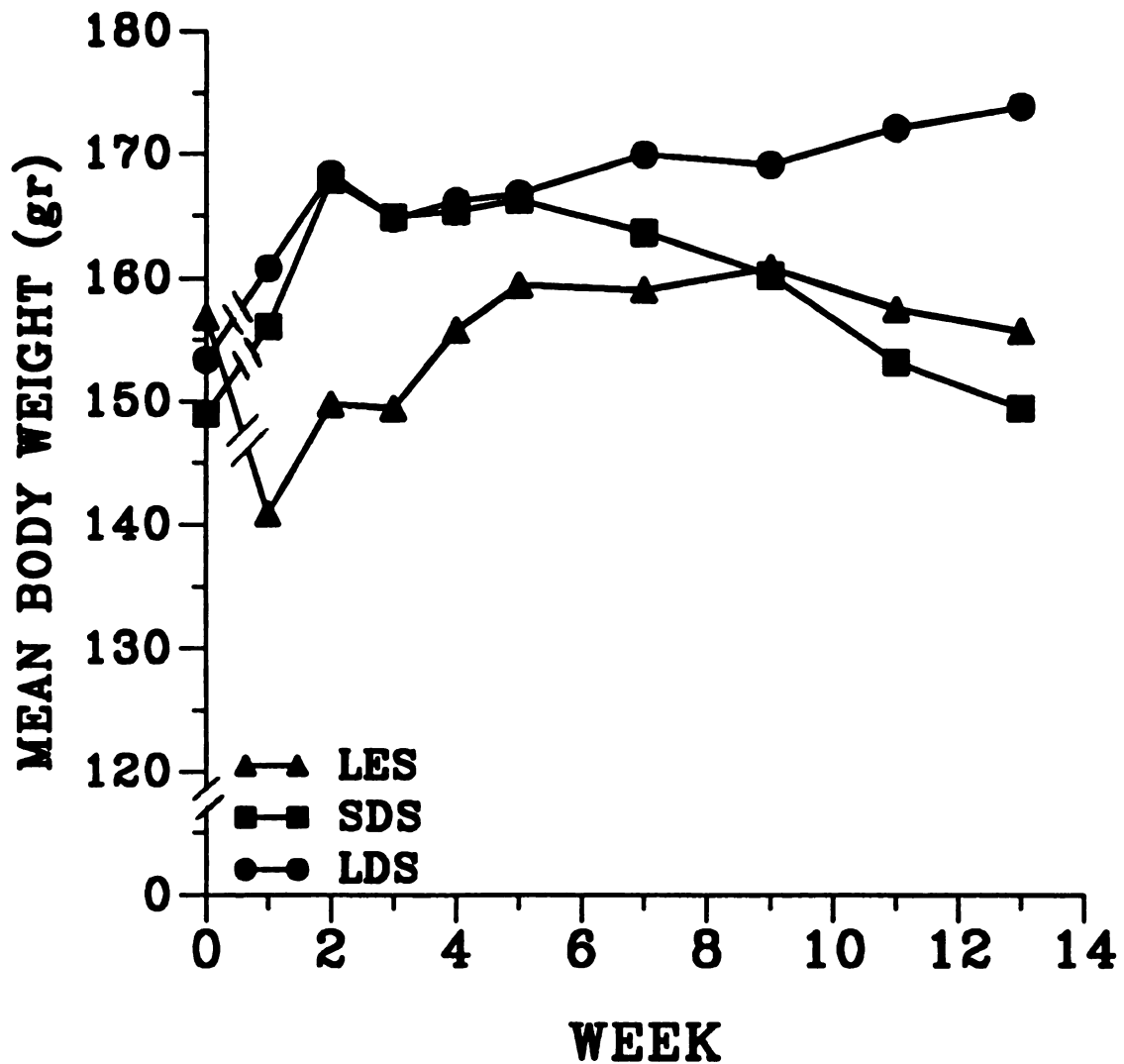


Figure 27. Mean body weight of animals receiving electrolytic lesions aimed at the PAG or sham-lesioned. Animals were lesioned (LES;  $n = 8$ ) or sham lesioned (SDS;  $n = 7$ ) and placed in a 8L:16D photoperiod, or sham lesioned and placed in a 16L:8D photoperiod (long-day sham [LDS];  $n = 4$ ). A nonsignificant decline in the mean body weight was observed in both short-photoperiod housed groups. Week zero represents the mean presurgical body weight of each group.

to SDS animals. The lesions were severely debilitating to many of the animals and were associated with a noticeable but non-significant postsurgical weight loss. The present data indicate that the animals with lesions tended to increase their body weight over most of the experiment, appearing to match the rate of gain in body weight made by the long photoperiod group. In the latter half of the experiment, however, both short photoperiod group displayed a non-significant loss of body weight. This trend is in contrast to reports of increased weight gain shown by hamsters kept in short days (Wade, 1983; Bartness & Wade, 1985; Hoffman, *et al.*, 1982). An explanation for the weight loss is not available and may be due to differences in diet and housing conditions between laboratories.

The results of Experiments IIa and IIb suggest that one or more of the brainstem sites receiving PVN input (i.e. - PAG, PB, SOL and area adjacent to the LC) and also containing neurons possessing axons reaching the level of C<sub>7</sub>-T<sub>1</sub> of the spinal cord, are in a position to participate in the pathway mediating the reproductive system's response to photoperiod. However, because PVN input to the PAG, LC area and SOL would likely have been disrupted by rostral PAG lesions, the direct involvement of these structures in the pathway appears remote. The PVN efferent fibers projecting directly to the spinal cord via a tract passing through the PAG (Tract 1) also do not appear essential for the display of gonadal response to short-day photoperiod. In the female Syrian hamster, in contrast to the results in the male, horizontal knife cuts placed above the PVN do not prevent the reproductive system response to short-day photoperiod. Bilateral parasagittal knife cuts, on the other hand, are effective in preventing gonadal regression in both

sexes when the animals are exposed to short-days. Taken together with the results of Experiment II, these results suggest that the effectiveness of horizontal knife-cuts above the PVN to prevent testicular regression may not depend on disruption of dorsal PVN-spinal cord projections, but may instead be due to elevated levels of FSH associated with this type knife-cut. This rise in FSH levels may involve PVN efferents not involved in the generation of the pineal melatonin rhythm. Thus, Tracts 2 and 3 (Experiment II) seem to provide an essential connection between the PVN and the spinal cord in the pathway mediating photoperiodism in male and female Syrian hamsters.

## GENERAL DISCUSSION

### PHOTOPERIODISM

The present experiments examined the anatomical connections in the Syrian hamster between the retina and forebrain, and between the PVN and spinal cord, two segments of what is believed to be a multisynaptic circuit ultimately controlling MEL secretion by the pineal gland important for the display of photoperiodism (Tamarkin, *et al.*, 1985). Photoperiodism is commonly associated with the seasonal reproductive cycles of mammals such as the Syrian hamster. In the hamster, seasonal cycles are eliminated by pinealectomy and mimicked by timed infusions or injections of MEL (Elliott & Goldman, 1981; Tamarkin, *et al.*, 1976; Watson-Whitmyre & Stetson, 1983). Seasonal fluctuations in reproductive physiology, however, represent only one aspect of mammalian photoperiodism.

Other aspects of the animal's physiology and behavior are influenced by photoperiod in ways that prepare the animal for the anticipated change in the environment. In the Syrian hamster, exposure to a short photoperiod is associated with a number of metabolic changes that are independent of gonadal secretions (see Bartness & Wade, 1985). The feed efficiency (i.e., weight gain/calories consumed), thermogenic capacity, brown adipose tissue mass and body weight (primarily lipid content) are increased in short-day housed animals with little change in their caloric intake. Further, thyroid hormone levels and presumably metabolic activity, are reduced (Vaughan, *et al.*, 1982). In Siberian hamsters, changes in pelage and the onset of daily bouts of torpor are also associated with exposure to

short photoperiods (Bartness & Wade, 1985). All of these changes in non-reproductive functions can be induced in animals kept in long days by administration of timed daily injections of MEL (Bartness & Wade, 1984; Bartness & Wade, 1988). However, different from the effects of photoperiod on reproductive physiology, neither the pineal gland nor MEL is necessary for the expression of some of these changes. For example, Wade, Bartness and others have presented evidence that the short-day effect on body weight, energy balance and lipid content can be expressed in the pinealectomized Syrian hamster (Bartness & Wade, 1984; Hoffman, *et al.*, 1982).

The display of reproductive behavior is partially pineal-independent in a sex-specific manner. Ovariectomized female hamsters, kept in a short photoperiod, are less sensitive to activational effects of estrogen and progesterone on sexual behavior than long day housed animals, and, as in the case of changes in energy balance, pinealectomy does not abolish this effect of photoperiod (Badura, *et al.*, 1987; Badura & Nunez, 1989). In contrast to the female, however, the short-photoperiod-associated reduced behavioral sensitivity of the male hamster to testosterone is pineal-dependent (Miernicki, *et al.*, 1987). Prolactin (PRL) release is also sensitive to changes in photoperiod (Blask, *et al.*, 1986). Serum levels of PRL, a hormone associated with reproductive and non-reproductive systems, fall in both males and females when the animals are placed in short days, however, in the female, pinealectomy is only partially effective in reversing the short-photoperiod induced decline in the production and storage of PRL by the anterior pituitary gland.

### RGC INPUT TO THE BASAL FOREBRAIN

The RHT-SCN connection is considered an important component of the circadian system and of the mechanism controlling photoperiodism in reproductive physiology. But, as was seen in Experiment I, the SCN is not the only area of the forebrain receiving retinal efferents. A number of regions of the brain (in both sexes) thought to be involved in the control of many of the regulatory and behavioral functions that are affected by photoperiod (e.g. - POA, Pyr, AHA, PVN) receive direct retinal input (Experiment I; Johnson, *et al.*, 1988). The extra-SCN retinal inputs, thus, may mediate some of the effects of photoperiod on physiology and behavior that are independent of the pineal gland. Photoperiodic responses in the Syrian hamster may be pineal-dependent, -independent or some point in between and in some instances there is a gender difference. It is not obvious why the hamster should exhibit different degrees of involvement for MEL in the control of photoperiodic responses in physiology and behavior. But, the changes in physiology examined thus far appear to be adaptive to the anticipated changes in the environment (the onset of "winter-like" conditions).

Comparison of the target sites of SCN efferent projections and the sites that receive RGC input in the hamster reveals a large degree of overlap. It is, therefore, possible that this anatomical overlap provides a basis for interactions between these two sources of light-dark information. Direct retinal input might override the circadian control provided by the SCN to a site, thus forming the basis of 'masking'. This phenomenon occurs, for instance, when acute exposure to light causes a decline in pineal MEL release at night while the SCN may or may not

be phase shifted by the same pulse of light (Illnerova & Vanecek, 1982a,b). A similar effect of light may be present in the phenomenon of masking of locomotor activity and drinking rhythms observed during transients when an animal is exposed to phase shifts of the LD cycle (Sisk & Stephan, 1981).

Direct RGC input may interact with the SCN input to produce pineal-independent photoperiodic effects. Thus, direct photic input may affect different neural systems only during periods of photosensitivity modulated in a circadian fashion by inputs from the SCN. Such overlapping of inputs may provide an explanation for the pineal-independent response to photoperiod noted in the production and secretion of PRL, the behavioral sensitivity to steroids and the control of metabolic functions in the hamster. The gender differences observed with respect to the effect of pinealectomy on some of these photoperiodic responses may be due to sexually-dimorphic anatomical or functional mechanisms in the regions receiving SCN and RHT input or that are sensitive to MEL.

#### PARAVENTRICULO-SPINAL CORD CONNECTIONS

In contrast to what appears to be fundamental differences between the sexes with respect to the degree that the pineal gland participates in the behavioral and endocrine responses to photoperiod mentioned above, the differential response by males and females to horizontal knife cuts dorsal to the PVN does not appear to be due to a sexual dimorphism in the anatomical pathways that mediate photoperiodism. The anatomy of the paraventriculo-spinal connections are similar in males and females (Experiment IIb). Also, Experiment III demonstrated that lesions in the PAG that presumably disrupt Tract 1,

but do not damage fibers at the level of the PVN, do not prevent gonadal regression in males. Other evidence suggests that the large testes observed in animals with cuts dorsal to the PVN are the result of elevated FSH levels (Badura, *et al.*, 1988). In hypophysectomized rats, FSH replacement to physiological levels is sufficient to prevent complete testicular regression even though spermatogenesis is incomplete (Bartlett, *et al.*, 1989). Thus, the apparent sexually dimorphic response to photoperiod after cuts dorsal to the PVN may be due to an increase in FSH secretion that is sufficient to maintain large testicular size but not female estrous cycles.

A number of questions remain to be answered regarding the pathway mediating photoperiodism. While dorsally projecting PVN efferents may not participate in the control of photoperiodism, the course of PVN-spinal efferents that do remains to be clarified. Recent evidence obtained in the male and female hamster suggests that lateral PVN projections participate in this circuit (Badura, *et al.*, 1989; Smale, *et al.*, 1989; Johnson, *et al.*, 1989). Discrete lesions placed in the path of Tracts 2 or 3 may reveal that one or both of these tracts is essential to the expression of photoperiodism. When these tracts are disrupted in this manner particular care should be given to avoid damage to the adjacent tract. The parasagittal cuts used in the previous studies may have produced damage to both sets of PVN lateral projections, thus preventing the evaluation of the role of each bundle in the control of photoperiodic responses.

Since the pineal gland and MEL are intimately involved in the expression of photoperiodism in the reproductive physiology of the hamster, future studies involving effects of knife cuts and lesions on



photoperiodism should evaluate the effects of such insults upon the rhythm of MEL production. Measurements of MEL levels in the serum, ideally over a 24-hour period, should serve to establish whether the circadian rhythm of MEL secretion has been disrupted by the brain damage. Given the effects of knife cuts dorsal to the PVN and that of damage to olfactory pathways, on the levels of serum FSH, it seems important that the serum levels of FSH and LH be measured and the histology of the gonads examined in addition to the use of testicular size in males or cyclicity in females as indices of responsiveness to photoperiodic changes.

#### NEURAL CONTROL OF THE CIRCADIAN RHYTHM OF PINEAL MEL SYNTHESIS

A neurophysiological question also remains regarding the circuit mediating the circadian rhythm of MEL production and photoperiodism. Experiment II demonstrated a direct projection from the PVN to the spinal cord and IML. But, the electrophysiological activity of the SCN compared to pineal gland activity displays an inverse relationship. In the rat, extracellular recordings of electrical activity in the SCN reveals an increase in SCN activity during the day or when the optic nerve is stimulated (Inouye & Kawamura, 1979, Shibata, *et al.*, 1984a,b). In contrast, pineal gland activity (and melatonin production) is normally reduced during the day or following acute exposure to light (Hudson & Menaker, 1984; Tamarkin, *et al.*, 1979; Vanecek & Illnerova, 1982). Also in the rat, activation of the SCG results in increased production of MEL (Bowers & Zigmond, 1982; Bowers, *et al.*, 1984). Thus, at some point in the pathway controlling the circadian rhythm of MEL

production, exposure of the animal to light must inhibit activity of the SCG.

The PVN and AHA receive direct RGC input as well as input from the SCN (Experiment I; Johnson, *et al.*, 1988). In the rat, electrical activity in the AHA, isolated with the SCN in a 'hypothalamic island', is low during the day and high at night (Inouye & Kawamura, 1979). This observation is in contrast to the SCN which displays increased activity during the day. Bilateral enucleation has no effect either on SCN or AHA activity within the island but the lesions producing the islands sever most or all RGC efferents, thus preventing light information from reaching the isolated tissue. It would be informative to measure the electrical activity of the same sites following acute exposure to light at night in similarly prepared hamsters, providing the optic fibers were preserved intact. AHA cells, in the hamster, receiving SCN input may be similarly influenced by direct RGC input and participate, through its connections to the PVN, in mediating the acute effects of light at night on the rhythm of pineal MEL synthesis.

The PVN projects to the IML (Experiment II; Luiten, *et al.*, 1985) and could serve to inhibit further transmission of SCN output to distal segments of the circuit. In the Guinea pig, a number of neurotransmitters and peptides are present in the IML (Chiba & Masuko, 1987). Among these is enkephalin, which has been reported to produce inhibitory effects in the CNS (Zieglansberger, 1982). In the rat, some PVN neurons projecting to the spinal cord contain enkephalin-like immunoreactivity and may provide inhibitory input to the IML (Cechetto & Saper, 1988). Thus, the PVN is in a position to

mediate inhibitory influences on the rest of the pathway. However, in the rat, stimulation of the PVN for an extended period (3 hours) during the day, but not during the night, results in a significant increase in the concentration of the MEL metabolite, 6-hydroxymelatonin in the urine (Yanovski, *et al.*, 1987). This suggests that the inhibition of MEL production at night due to acute exposure to light is due to inhibition of the PVN or another structure at a point in the circuit prior to the PVN.

Experiment II also revealed a number of nuclei in the brain that receive PVN input and that, in the rat, terminate in the IML. Among these nuclei are the locus coeruleus, nucleus of the solitary tract and parabrachial nucleus (Tucker & Saper, 1985; Westlund, *et al.*, 1981; Chiba & Masuko, 1987). The LHA and dopaminergic cells in the posterior hypothalamus-rostral mesencephalon (A11) also project to the IML (Chiba & Masuko, 1987; Lindvall, *et al.*, 1983; Tucker & Saper, 1985). Similar connections appear to be present in the hamster and one or several of these nuclei may act to modulate the activity of neurons in the IML. The results of Experiment III suggest the parabrachial nucleus would be the most likely candidate as a brainstem relay in the circuit. The possibility also exists that interneurons present at one or more level of the pathway are responsible for this phenomenon.

#### SPECIES SPECIFIC ANATOMY

The model of the multisynaptic pathway mediating the circadian rhythm of pineal MEL secretion first obtained much of its anatomical supporting evidence in data for the rat (Tamarkin, *et al.*, 1985). Studies that have addressed the functional anatomy of this circuit in the hamster have, in the main, also supported this model but have had to

rely upon the anatomical data for the rat to guide the interpretation of the results (Inouye & Turek, 1985; Nunez, *et al.*, 1985; Eskes & Rusak, 1985; Lehman *et al.*, 1984; Pickard & Turek, 1983). However, the present data and those from other studies suggest that differences exist between neuroanatomical connections of the rat and hamster (Experiments I & II; Johnson, *et al.*, 1988; Levine, *et al.*, 1986; Youngstrom & Weiss, unpublished results). Differences exist in the pattern of labeling between the rat and hamster following intraocular injections of HRP conjugates. The hypothalamus of the Syrian hamster is more densely stained at every level compared to the rat. In addition, the input to the anterior thalamus and Pyr observed in the hamster was absent in the rat. Other differences in the anatomy of these two species with respect to the trajectory of PVN efferents to the spinal cord were observed in Experiment II. Thus, four fiber tracts originating in the PVN were counted in the hypothalamus of the hamster following spinal cord injections of HRP conjugates. In contrast, iontophoretic injections of PHA-L labeled two tracts in the rat. These differences with respect to paraventriculo-spinal connections must be viewed cautiously, given the different tract-tracing techniques used and the results of Experiment IIa compared to IIb. Nevertheless, it seems essential that the neuroanatomy of the hamster be further addressed. Photoperiodism is the product of an interaction between a circadian system displaying a circadian rhythm of photoperiodic photosensitivity and the external photoperiod (Elliott & Goldman, 1981). If we are to fully understand this phenomenon it seems only reasonable that the anatomy of the underlying structures in the hamster and other photoperiodic species receive the same attention that the physiological responses associated

with photoperiodism have received. Otherwise the interpretation of the results of functional studies using photoperiodic species will continue to rest upon the neuroanatomical descriptions available for the essentially non-photoperiodic rat.

## **BIBLIOGRAPHY**

## **BIBLIOGRAPHY**

- Badura, L.L., Sisk, C.L. & Nunez, A.A. Neural Pathways Involved in the Photoperiodic Control of Reproductive Physiology and Behavior in Female Hamsters (*Mesocricetus auratus*). *Neuroendocrinol.*, **46**:339-344, 1987a.
- Badura, L.L., Yant, W.R & Nunez, A.A. Photoperiodic Modulation of Steroid-Induced Lordosis in Golden Hamsters. *Physiol. Behav.*, **40**:551-554, 1987b.
- Badura, L.L., Sisk, C.L. & Nunez, A.A. Knife Cuts Dorsal to the Hypothalamic Paraventricular Nucleus Disinhibit Gonadotrophin Secretion in Male Golden Hamsters Kept in Long or Short Days. *Soc. Neur. Abstr.*, **14**:52, 1988
- Badura, L.L & Nunez, A.A. Photoperiodic Modulation of Sexual and Aggressive Behavior in Female Golden Hamsters (*Mesocricetus auratus*): Role of the Pineal Gland. *Horm. Behav.*, **23**:27-42, 1989.
- Badura, L.L., Kelly, K.K. & Nunez, A.A. Knife Cuts Lateral but not Dorsal to the Hypothalamic Paraventricular Nucleus Abolish Gonadal Responses to Photoperiod in Female Hamsters (*Mesocricetus auratus*). *J. Biol. Rhythms*, **4**:79-91, 1989.
- Bartlett, J.M.S., Weinbauer, G.F. & Nieschlag, E. Differential Effects of FSH and Testosterone on the Maintenance of Spermatogenesis in the Adult Hypophysectomized Rat. *J. Endocrinol.*, **121**:49-58, 1989
- Bartness, T.J. & Goldman, B.D. Peak Duration of Serum Melatonin and Short Day Responses in Adult Siberian Hamsters. *Am. J. Physiol.*, **255**:R812-R822, 1988
- Bartness, T.J. & Wade, G.N. Photoperiodic Control of Body Weight and Energy Metabolism in Syrian Hamsters (*Mesocricetus auratus*): Role of Pineal Gland, Melatonin, Gonads and Diet. *Endocrinol.*, **114**:492-498, 1984.
- Bartness, T.J. & Wade, G.N. Photoperiodic Control of Seasonal Body Weight Cycles in Hamsters. *Neurosci. Biobehav. Revs.*, **9**:599-612, 1985

- Bartness, T.J., Bittman, E.L. & Wade, G.N. Paraventricular Nucleus Lesions Exaggerate Dietary Obesity but Block Photoperiod-Induced Weight Gains and Suspension of Estrous Cyclicity in Syrian Hamsters. *Brain Res. Bull.*, **14**:427-430, 1985.
- Berk, M.L & Finkelstein, J.A. Afferent Projections to the Preoptic Area and Hypothalamic Regions in the Rat Brain. *Neurosci.*, **6**:1601-1624, 1981.
- Berndtson, W.E. & Desjardins, C. Circulating LH and FSH Levels and Testicular Function in Hamsters During Light Deprivation and Subsequent Photoperiodic Stimulation. *Endocrinol.*, **95**:195-205, 1974
- Bittman, E.L. & Karsch, F.J. Nightly Duration of Pineal Melatonin Secretion Determines the Reproductive Response to Inhibitory Day Length in the Ewe. *Biol. Reprod.*, **30**:585-593, 1984.
- Bittman, E.L. Melatonin and Photoperiodic Time Measurement: Evidence from Rodents and Ruminants. In: Reiter, R.J. (Ed.), *The Pineal Gland*. New York. Raven Press. pp. 155-192. 1984.
- Bittman, E.L., Dempsey, R.J. & Karsch, F.J. Pineal Melatonin Secretion Drives the Reproductive Response to Daylength in the Ewe. *Endocrinol.*, **113**:2276-2283, 1983.
- Bittman, E.L., Kaynard, A.H., Olster, D.H., Robinson, J.E., Yellon, S.M. & Karsch, F.J. Pineal Melatonin Mediates Photoperiodic Control of Pulsatile Luteinizing Hormone Secretion in the Ewe. *Neuroendocrinol.*, **40**:409-418, 1985
- Bittman, E. L. & Lehman, M.N. Paraventricular Neurons Control Hamster Photoperiodism by a Predominantly Uncrossed Descending Pathway. *Brain Res. Bull.*, **19**: 687-694, 1987.
- Blask, D.E., Leadem, C.A., Orstead, K.M. & Larsen, B.R. Prolactin Cell Activity in Female and Male Syrian Hamsters: An Apparent Sexually Dimorphic Response to Light Deprivation and Pinealectomy. *Neuroendocrinol.*, **42**:15-20, 1986.
- Bowers, C.W., Baldwin, C. & Zigmond, R.E. Sympathetic Reinnervation of the Pineal Gland After Postganglionic Nerve Lesion Does Not Restore Normal Pineal Function. *J. Neurosci.*, **4**:2010-2015, 1984.
- Bowers, C.W. & Zigmond, R.E. The Influence of Frequency and Pattern of Sympathetic Nerve Activity on Serotonin N-acetyltransferase in the Rat Pineal Gland. *J. Physiol.*, **330**:279-296, 1982.
- Broadwell, R.D. & Brightman, M.W. Entry of Peroxidase into Neurons of the Central and Peripheral Nervous Systems from Extracerebral and Cerebral Blood. *J. Comp. Neurol.*, **166**:257-284, 1976.



- Brown, M.H. Hypothalamic Neural Pathways that Mediate Photoperiodic Control of Reproduction in the Syrian Hamster (*Mesocricetus auratus*). A Dissertation, Michigan State University, 1986.
- Brown, M.H., Badura, L.L. & Nunez, A.A. Evidence that Neurons of the Paraventricular Nucleus of the Hypothalamus with Projections to the Spinal Cord are Sensitive to the Toxic Effects of N-Methyl Aspartic Acid. *Neurosci. Lett.*, **73**:103-108, 1987.
- Brown, M.H., Badura, L.L. & Nunez, A.A. Axon-Sparing Lesions of the Hypothalamic Paraventricular Nucleus Abolish Gonadal Responses to Photoperiod in Male Syrian Hamsters. *J. Biol. Rhythms.*, **3**:59-69, 1988.
- Campbell, C.S., Finkelstein, J.S. & Turek, F.W. The Interaction of Photoperiod and Testosterone on the Development of Copulatory Behavior in Male Hamsters. *Physiol. Behav.*, **21**:409-415, 1978.
- Card, J.P. & Moore, R.Y. Organization of Lateral Geniculate-Hypothalamic Connections in the Rat. *J. Comp. Neurol.*, **284**:135-147, 1989.
- Card, J.P. & Moore, R.Y. The Suprachiasmatic Nucleus of the Golden Hamster: Immunohistochemical Analysis of Cell and Fiber Distribution. *Neurosci.*, **13**:415-431, 1984.
- Carter, D.S. and B.D. Goldman. Antigonadal Effects of Timed Melatonin Infusion in Pinealectomized Male Djungarian Hamsters (*Phodopus sungorus sungorus*): Duration is the Critical Parameter. *Endocrinol.*, **113**:1261-1267, 1983.
- Cassone, V.M, Speh, J.C., Card, J.P. & Moore, R.Y. Comparative Anatomy of the Mammalian Hypothalamic Suprachiasmatic Nucleus. *J. Biol. Rhythms.* **3**:71-91, 1988.
- Cechetto, D.F. & Saper, C.B. Neurochemical Organization of the Hypothalamic Projection to the Spinal Cord in the Rat. *J. Comp. Neurol.*, **272**:579-604, 1988.
- Chiba, T. & Masuko, S. Synaptic Structure of the Monoamine and Peptide Nerve Terminals in the Intermediolateral Nucleus of the Guinea Pig Thoracic Spinal Cord. *J. Comp. Neurol.*, **262**:242-255, 1987.
- Clancy, A.N., Goldman, B.D., Bartke, A. & Macrides, F. Reproductive Effects of Olfactory Bulbectomy in the Syrian Hamster. *Biol. Reprod.*, **35**:1202-1209, 1986.
- Conrad, C.D & Stumpf, W.E. Direct Visual Input to the Limbic System: Crossed Retinal Projections to the Nucleus Anterodorsalis Thalami in the Tree Shrew. *Exp. Brain Res.*, **23**:141-149, 1975.
- Devor, M. Fiber Trajectories of Olfactory Bulb Efferents in the Hamster. *J. Comp. Neurol.*, **166**:31-48, 1976.

- Don Carlos, L.L. & Finkelstein, J.A. Hypothalamo-Spinal Projections in the Golden Hamster. *Brain Res. Bull.*, **18**:709-714, 1987.
- Dornan, W.A., Block, G.J., Priest, C.A & Micevych, P.E. Microinjections of Cholecystokinin into the Medial Preoptic Nucleus Facilitates Lordosis Behavior in the Female Rat. *Physiol. Behav.*, **45**:969-974, 1989
- Eisenman, J.S & Jackson, D.C. Thermal Response Patterns of Septal and Preoptic Neurons in Cats. *Exp. Neurol.*, **19**:33-45, 1967.
- Elliott, J.A. & Goldman, B.D. Seasonal Reproduction: Photoperiodism and Biological Clocks. In: Adler, N.T. (Ed), *Neuroendocrinology of Reproduction*, New York, Plenum Press, pp. 377-423, 1981.
- Eskes, G.A. & Rusak, B. Horizontal Knife Cuts in the Suprachiasmatic Area Prevent Gonadal Responses to Photoperiod. *Neurosci. Lett.*, **61**:261-266, 1985.
- Gabriel, M., Foster, K., Orona, E., Saltwick, Se. & Stanton, M. Neuronal Activity of Cingulate Cortex, Anteroventral Thalamus, in Hippocampal Formation and Discriminative Conditioning: Encoding and Extraction of the Significance of Conditional Stimuli. In: Sprague, J.M. & Epstein, A.N. (Eds.), *Progress in Psychobiology and Physiological Psychology*, Vol. 9. New York, Academic Press, pp. 125-232, 1980a.
- Gabriel, M., Orona, E., Foster, K. & Lambert, R.W. Cingulate Cortex and Anterior Thalamic Neuronal Correlates of Reversal Learning in Rabbits. *J. Comp. Physiol. Psych.*, **94**:1087-1100, 1980b.
- Gaston, S. & Menaker, M. Photoperiodic Control of Hamster Testes. *Sci.*, **158**:925-928, 1967
- Gerfen, C.R. & Sawchenko, P.E. An Anterograde Neuroanatomical Tracing Method that Shows the Detailed Morphology of Neurons, Their Axons and Terminals: Immunohistochemical Localization of an Axonally Transported Plant Lectin, Phaseolus vulgaris, Leucoagglutinin (PHA-L). *Brain Res.*, **290**:219-238, 1984.
- Giolli, R.A. & Town, L.C. A Review of Axon Collateralization in the Mammalian Visual System. *Brain Behav. Evol.*, **17**:364-390, 1980.
- Goldman, B.D. & Darrow, J.M. The Pineal Gland and Mammalian Photoperiodism. *Neuroendocrinol.*, **37**:386-396, 1983.
- Goldman, B.D., Hall, V., Hollister, C., Reppert, S., Roycurdhury, P., Yellon, S.M. & Tamarkin, L. Diurnal Changes in Pineal Melatonin Content in Four Rodent Species: Relationship to Photoperiodism. *Biol. Reprod.*, **24**:778-783, 1981.

- Haberly, L.B & Feig, S.L. Structure of the Piriform Cortex of the Opossum. II. Fine Structure of Cell Bodies and Neuropil. *J. Comp. Neurol.*, **216**:69-88, 1983.
- Hastings, M.H. & Herbert, J. Neurotoxic Lesions of the Paraventriculo-Spinal Projection Block the Nocturnal Rise in Pineal Melatonin Synthesis in the Syrian Hamster. *Neurosci. Lett.*, **69**:1-6, 1986.
- Hoffman, R.A., Davidson, K. & Steinberg, K. Influence of Photoperiod and Temperature on Weight Gain, Food Consumption, Fat Pads and Thyroxine in Male Golden Hamsters. *Growth*, **46**:150-162, 1982.
- Hori, T., Nakashima, T, Koga, H., Kiyohara, T & Inoue, T. Convergence of Thermal, Osmotic and Cardiovascular Signals on Preoptic and Anterior Hypothalamic Neurons in the Rat. *Brain Res. Bull.*, **20**:879-885, 1988.
- Hudson, D.J. & Menaker, M. Pineal Melatonin Synthesis in the Hamster: Sensitivity to Light. *Soc. Neurosci. Abstr.*, **10**:820, 1984.
- Illnerova, H. & Vanecek, J. Complex Control of the Circadian Rhythm in N-Acetyltransferase Activity in the Rat Pineal Gland. In: Aschoff, J., et al., (Eds.), *Vertebrate Circadian Systems*. Berlin. Springer-Verlag. pp. 285-296, 1982a.
- Illnerova, H. & Vanecek, J. Two-Oscillator Structure of the Pacemaker Controlling the Circadian Rhythm of N-Acetyltransferase in the Rat Pineal. *J. Comp. Physiol.*, **145**:539-548, 1982b.
- Illnerova, H. Vanecek, J. Effect of Light on the N-Acetyltransferase Rhythm in the Rat Pineal Gland. In: Reiter, R.J. & Karasek, M. (Eds.), *Advances in Pineal Research*. London. John Libbey & Co Ltd., pp. 69-76, 1986.
- Inouye, S.-I. & Kawamura, H. Persistence of Circadian Rhythmicity in a Mammalian Hypothalamic "Island" Containing the Suprachiasmatic Nucleus. *Proc. Natl. Acad. Sci.*, **76**:5962-5966, 1979.
- Inouye, S.-I. & Turek, F.W. Horizontal Knife Cuts Either Ventral or Dorsal to the Hypothalamic Paraventricular Nucleus Block Testicular Regression in Golden Hamsters Maintained in Short Days. *Brain Res.* **370**:102-107, 1986
- Itaya, S.K. & VAN Hoesen, G.W. WGA-HRP as a Transneuronal Marker in the Visual Pathways of Monkey and Rat. *Brain Res.*, **236**:199-204, 1982.
- Itaya, S.K. VAN Hoesen, G.W & Benevento, L.A. Direct Retinal Pathways to the Limbic Thalamus of the Monkey. *Exp. Brain Res.*, **61**:607-613, 1986.

- Itaya, S.K., VAN Hoesen, G.W. & Jenq, C.-B. Direct Retinal Input to the Limbic System of the Rat. *Brain Res.*, **226**:33-42, 1981.
- Jeffery, G. Cowey, A. & Kuypers, H.G.J.M. Bifurcating Retinal Ganglion Cell Axons in the Rat, Demonstrated by Retrograde Double Labeling. *Exp. Brain Res.*, **44**:34-40, 1981.
- Johnson, R.F., Morin, L.P. & Moore, R.Y. Retinohypothalamic Projections in the Hamster and Rat Demonstrated Using Cholera Toxin. *Brain Res.*, **462**:301-312, 1988.
- Johnson, R.F., Moore, R.Y. & Morin, L.P. Lateral Geniculate Lesions Alter Circadian Activity Rhythms in the Hamster. *Brain Res. Bull.*, **33**:422-422, 1989.
- Johnson, R.F., Smale, L. Moore, R.Y. & Morin, L.P. Paraventricular Nucleus Efferents Mediating Photoperiodism in Male Golden Hamsters. *Neurosci. Lett.*, **98**:85-90, 1989.
- Jones, E.G. The Thalamus. Plenum Press, New York, pp. 673-698, 1985.
- Kalra, S.P. Neural Circuitry Involved in the Control of LHRH Secretion: A Model for Preovulatory LH Release. In: Ganong, W.F. and Martini, L. (Eds.), *Frontiers in Neuroendocrinology*, **9**:31-75, 1986.
- Kappers, J.A. The Development, Topographical Relations and Innervation of the Epiphysis Cerebri in the Albino Rat. *Z. Zellforsch.*, **52**:163-215, 1960.
- Katz, L.C., Burkhalter, A. & Dreyer, W.J. Fluorescent Latex Microspheres as a Retrograde Neuronal Marker for In Vivo and In Vitro Studies of Visual Cortex. *Nature*, **310**:498-500, 1984.
- Kevetter, G.A. & Winans, S.S. Connections of the Corticomедial Amygdala in the Golden Hamster. I. Efferents of the "Vomeronasal Amygdala". *J. Comp. Neurol.*, **197**:81-98, 1981.
- Klein, D.C. & Moore, R.Y. Pineal N-Acetyltransferase and Hydroxyindole-O-Methyltransferase. Control by the Retinohypothalamic Tract and the Suprachiasmatic Nucleus. *Brain Res.*, **174**:245-262, 1979.
- Klein, D.C. Circadian Rhythms in the Pineal Gland. In: Krieger, D.T., (Ed.), *Endocrine Rhythms*. Raven Press, New York, pp. 203-223, 1979.
- Knox, G.V., Campbell, C. & Lomax, P. Cutaneous Temperature and Unit Activity in Hypothalamic Thermoregulatory Centers. *Exp. Neurol.*, **40**:717-726, 1973.
- Krettek, J.E. & Price, J.L. Amygdaloid Projections to Subcortical Structures Within the Basal Forebrain and the Brainstem in the Rat and Cat. *J. Comp. Neurol.*, **178**:225-254, 1978.

- Larsson, K. Features of the Neuroendocrine Regulation of Masculine Sexual Behavior. In: Beyer, C. (Ed.), *Endocrine Control of Sexual Behavior*, Raven Press New York, pp. 77-163, 1979.
- Lehman, M.N., Bittman, E.L. & Winans-Newman, S. Role of the Hypothalamic Paraventricular Nucleus in Neuroendocrine Responses to Daylength in the Golden Hamster. *Brain Res.*, **308**:25-32, 1984.
- Lehman, M.N., Powers, J.B. & Winans, S.S. Stria Terminalis Lesions Alter the Temporal Pattern of Copulatory Behavior in the Male Golden Hamster. *Behav. Brain Res.*, **8**:109-128, 1983.
- Lehman, M.N., Winans, S.S. & Powers, J.B. Medial Nucleus of the Amygdala Mediates Chemosensory Control of Male Hamsters Sexual Behavior. *Sci.*, **210**:557-560, 1980.
- Levine, J.D., Weiss, M.L., Gosin, D., Rosenwasser, A.L. & Miselis, R.R. Re-Examination of the Retino-Hypothalamic Projections of the Rat Using HRP Conjugated to Cholera Toxin (CT-HRP). *Soc. Neurosci. Abstr.*, **12**:549, 1986.
- Lindvall, O., Björklund, A. & Skagerburg, G. Dopamine-Containing Neurons in the Spinal Cord: Anatomy and Some Functional Aspects. *Ann. Neurol.*, **14**:255-260, 1983.
- Lisk, R.D. The Estrous Cycle. In: Siegel, H.I. (Ed.), *The Hamster: Reproduction and Behavior*. Plenum Press, New York, pp. 23-51, 1985.
- Luiten, P.G.M., TER Horst, G.J., Karst, H. & Steffens, A.B. The Course of Paraventricular Hypothalamic Efferents to Autonomic Structures in Medulla and Spinal Cord. *Brain Res.*, **329**:374-378, 1985.
- Luiten, P.G.M., TER Horst, G.J. & Steffens, A.B. The Hypothalamus, Intrinsic Connections and Outflow Pathways to the Endocrine System in Relation to the Control of Feeding and Metabolism. *Prog. Neurobiol.*, **28**:1-54, 1987.
- Maragos, W.F., Newman, S.W., Lehman, M.N. & Powers, J.B. Neurons of Origin and Fiber Trajectory of Amygdalofugal Projections to the Medial Preoptic Area in Syrian Hamsters. *J. Comp. Neurol.*, **280**:59-71, 1989.
- Melanie, E. & Kittrell, W. Lesions of the Suprachiasmatic Nuclei and Surrounding Basal Hypothalamus Abolish the Circadian Rhythms of Activity, Drinking, and Body Temperature in Female Rats. *Soc. Neurosci. Abstr.*, **13**:419, 1987.
- Merchenvaler, I., Gores, T., Setalo, G., Petrusz, P. & Flerko, B. Gonadotropin-Releasing Hormone (GnRH) Neurons and Pathways in the Rat Brain. *Cell Tiss. Res.*, **237**:15-29, 1984.



- Mesulam, M.-M. Principles of Horseradish Peroxidase Neurohistochemistry and Their Applications for Tracing Neural Pathways-Axonal Transport, Enzyme Histochemistry and Light Microscopic Analysis. In: Mesulam, M.-M., (Ed.), *Tracing Neural Connections with Horseradish Peroxidase*. New York. John Wiley & Sons Ltd., pp. 1-151, 1982.
- Miernicki, M., Pospichal, M., Karp, J. & Powers, B. Photoperiodic Effects on Male Hamster Sexual Behavior. *Con. Reprod. Behav. Abstr.*, 1987.
- Morin, L.P. & Zucker, I. Photoperiodic Regulation of Copulatory Behavior in the Male Hamster. *J. Endocrinol.*, **77**:249-258, 1978.
- Moore, R.Y. Central Neural Control of Circadian Rhythms. In: Ganong, W.F. & Martini, L., (Eds.), *Frontiers in Neuroendocrinology*. New York. Raven. Vol. 5, pp. 185-206, 1978.
- Napoli, A., Powers, V.B. & Valenstein, E.S. Hormonal Induction of Behavioral Estrus Modified by Electrical Stimulation of Hypothalamus. *Physiol. Behav.*, **9**:115-117, 1972.
- Numan, M. Neural Basis of Maternal Behavior in the Rat. *Psychoneuroendocrinol.*, **13**:47-62, 1988.
- Nunez, A.A., Brown, M.H. & Youngstrom, T.G. Hypothalamic Circuits Involved in the Regulation of Seasonal and Circadian Rhythms in Male Golden Hamsters. *Brain Res. Bull.*, **15**:149-153, 1985.
- Paxinos, G. & Watson, C. The Rat Brain in Stereotaxic Coordinates. New York. Academic Press. 1982.
- Pfaff, D.W. & Modianos, D. Neural Mechanisms of Female Reproductive Behavior. In: Adler, N., Pfaff, D. & Goy, R.W. (Eds.), *Handbook of Behavioral Neurobiology & Reproduction*. Plenum Press, New York, pp. 423-480, 1985.
- Pickard, G.E. & Silverman, A.J. Direct Retinal Projections to the Hypothalamus, Piriform Cortex, and Accessory Optic Nuclei in the Golden Hamster as Demonstrated by a Sensitive Anterograde Horseradish Peroxidase Technique. *J. Comp. Neurol.*, **196**:155-172, 1981.
- Pickard, G.E. & Turek, F.W. The Hypothalamic Paraventricular Nucleus Mediates the Photoperiodic Control of Reproduction But Not the Effects of Light on the Circadian Rhythm of Activity. *Neurosci. Lett.*, **43**:67-72, 1983.
- Pickard, G.E. Bifurcating Axons of Retinal Ganglion Cells Terminate in the Hypothalamic Suprachiasmatic Nucleus and the Intergeniculate Leaflet of the Thalamus. *Neurosci. Lett.*, **55**:211-217, 1985.

- Pickard, G.E., Ralph, M.R. & Menaker, M. The Intergeniculate Leaflet Partially Mediates Effects of Light on Circadian Rhythms. *J. Biol. Rhythms*, **2**:35-56, 1987.
- Pieper, D.R., Newman, S.W., Lobocki, C.A. & Gogola, G. Bilateral Transection of the Lateral Olfactory Tract but not Removal of the Vomeronasal Organs Inhibit Short-Photoperiod-Induced Testicular Regression in Golden Hamster. *Brain Res.*, **485**:382-390, 1989.
- Poulain, P. & Carette, B. Low-Threshold Calcium Spikes in Hypothalamic Neurons Recorded Near the Paraventricular Nucleus In Vitro. *Brain Res. Bull.*, **19**:453-460, 1987.
- Powers, B. & Valenstein, E.S. Sexual Receptivity: Facilitation by Medial Preoptic Lesions in Female Rats. *Sci.*, **175**:1003-1005, 1972.
- Powers, J.B., Newman, S.W. & Bergondy, M.L. MPOA and BNST Lesions in Male Syrian Hamsters: Differential Effects on Copulatory and Chemoinvestigative Behaviors. *Behav. Brain Res.*, **23**:181-195, 1987.
- Price, J.L., Russchen, F.T. & Amaral, D.G., The Limbic Region. II: The Amygdaloid Complex. In: Bjorklund, A., Hokfelt, T. & Swanson, L.W., (Eds.), *Handbook of Chemical Neuroanatomy*. Vol. 5: *Integrated Systems of the CNS, Part I. Hypothalamus, Hippocampus, Amygdala, Retina*. Elsevier, New York, pp. 279-388, 1987.
- Reuss, S., Johnson, R.F., Morin, L.P. & Moore, R.Y. Localization of Spinal Cord Preganglionic Neurons Innervating the Superior Cervical Ganglion in the Golden Hamster. *Brain Res. Bull.*, **22**:289-293, 1989.
- Rollag, M.D. & Niswender, G.D. Radioimmunoassay of Serum Concentrations of Melatonin in Sheep Exposed to Different Light Regimens. *Endocrinol.*, **98**:482-489, 1976.
- Rollag, M.D., O'Callaghan, P.L. & Niswender, G.D. Serum Melatonin Concentrations During Different Stages of the Annual Reproductive Cycle in Ewes. *Biol. Reprod.*, **18**:279-285, 1978.
- Scalia, F. & Winans, S.S. The Differential Projections of the Olfactory Bulb and Accessory Olfactory Bulb in Mammals. *J. Comp. Neurol.*, **161**:31-56, 1975.
- Seegal, R.F. & Goldman, B.D. Effects of Photoperiod on Cyclicity and Serum Gonadotropins in the Syrian Hamster. *Biol. Reprod.*, **12**:223-231, 1975.
- Shapiro, R. E. & Miselis, R.R. The Central Neural Connections of the Area Postrema in the Rat. *J. Comp. Neurol.*, **234**:344-364, 1985.



- Shibata, S., Liou, S.Y., Ueki, S., Oomura, Y. Influence of Environmental Light-Dark Cycle and Enucleation on Activity of Suprachiasmatic Neurons in Slice Preparations. *Brain Res.*, **302**:75-81, 1984a.
- Shibata, S., Oomura, Y., Hattori, K. & Kita, H. Responses of Suprachiasmatic Nucleus Neurons to Optic Nerve Stimulation in Rat Hypothalamic Slice Preparation. *Brain Res.*, **302**:83-89, 1984b.
- Sikes, R.W. & Vogt, B.A. Afferent Connections of Anterior Thalamus in Rats: Sources and Association with Muscarinic Acetylcholine Receptors. *J. Comp. Neurol.*, **256**:538-551, 1987.
- Simerly, R.B. & Swanson, L.W. The Organization of Neural Inputs to the Medial Preoptic Nucleus of the Rat. *J. Comp. Neurol.*, **246**:312-342, 1986.
- Sisk, C.L. & Stephan, F.W. Phase Shifts of Circadian Rhythms of Activity and Drinking in the Hamster. *Behav. Neural Biol.*, **33**:334-344, 1981
- Smale, L., Cassone, V.M., Moore, R.Y. & Morin, L.P. Paraventricular Nucleus Projections Mediating Pineal Melatonin and Gonadal Responses to Photoperiod in the Hamster. *Brain Res. Bull.*, **22**:263-269, 1989
- Smithson, K.E., MacVicar, B.A. & Hatton, G.I. Polyethylene Glycol Embedding: a Technique Compatible with Immunocytochemistry, Enzyme Histochemistry, Histofluorescence, and Intracellular Staining. *J. Neurosci. Meth.*, **7**:27-41, 1983.
- Swanson, L.W. & Kuypers, H.G.J.M. The Paraventricular Nucleus of the Hypothalamus: Cytoarchitectonic Subdivisions and Organization of Projections to the Pituitary, Dorsal Vagal Complex, and Spinal Cord as Demonstrated by Retrograde Fluorescence Double-Labeling Methods. *J. Comp. Neurol.*, **194**:555-570, 1980.
- Swanson, L.W. The Hypothalamus. In: Bjorklund, A., Hokfelt, T. & Swanson, L.W., (Eds.), *Handbook of Chemical Neuroanatomy. Vol. 5: Integrated Systems of the CNS, Part I. Hypothalamus, Hippocampus, Amygdala, Retina*. Elsevier, New York, pp. 1-124, 1987.
- Takahashi, L.K. & Lisk, R.D. Dual Progesterone Action in Diencephalon Facilitates the Induction of Sexual Receptivity in Estrogen-Primed Golden Hamsters. *Physiol. Behav.*, **44**:741-747, 1988.
- Tamarkin, L., Baird, C.J. & Almeida, O.F.X. Melatonin: A Coordinating Signal for Mammalian Reproduction. *Sci.*, **227**:714-720, 1985.
- Tamarkin, L., Reppert, S.M. & Klein, D.C. Regulation of Pineal Melatonin in the Syrian Hamster. *Endocrinol.*, **104**:385-389, 1979.

- Tamarkin, L., Westrom, W.K., Hamill, A.I. & Goldman, B.D. Effect of Melatonin on the Reproductive Systems of Male and Female Syrian Hamsters: A Diurnal Rhythm in Sensitivity to Melatonin. *Endocrinol.*, **99**:1534-1541, 1976.
- Tucker, D.C. & Saper, C.B. Specificity of Spinal Projections From Hypothalamic and Brainstem Areas which Innervate Sympathetic Preganglionic Neurons. *Brain Res.*, **360**:159-164, 1985.
- Turek, F.W. & Losee, S.H. Melatonin-Induced Testicular Growth in Golden Hamsters Maintained on Short Days. *Biol. Reprod.* **18**:299-305, 1978.
- Vanecek, J. & Illnerova, H. Effect of Light at Night on the Pineal Rhythm in N-Acetyltransferase Activity in the Syrian Hamster *Mesocricetus auratus*. *Experientia*, **38**:513-514, 1982.
- Vaughan, M.K., Powanda, M.C., Brainard, G.C., Johnson, L.Y. & Reiter, R.J. Effects of Blinding or Afternoon Melatonin Injections on Plasma Cholesterol, Triglycerides, Glucose, TSH and Thyroid Hormone Levels in Male and Female Syrian Hamsters. In: Reiter, R.J. (Ed.), *The Pineal and Its Hormones*. Alan R. Liss, Inc., New York, pp. 177-186, 1982.
- Wade, G.N. Dietary Obesity in Golden Hamsters: Reversibility and Effects of Sex and Photoperiod. *Physiol. Behav.*, **30**:131-137, 1983.
- Watson-Whitmyre, M. & Stetson, M.H. Simulation of Peak Pineal Melatonin Release Restores Sensitivity to Evening Melatonin Injections in Pinealectomized Hamsters. *Endocrinol.*, **112**:763-765, 1983.
- Watts, A.G., Swanson, L.W. and Sanchez-Watts, G. Efferent Projections of the Suprachiasmatic Nucleus: I. Studies Using Anterograde Transport of Phaseolus vulgaris-Leucoagglutinin in the Rat. *J. Comp. Neurol.* **258**:204-229, 1987.
- Werner, J & Bienck, A. The Significance of Nucleus Raphi Dorsalis and Centralis for Thermoafferent Signal Transmission to the Preoptic Area of the Rat. *Exp. Brain Res.*, **59**:543-547, 1985.
- Westlund, K.N., Bowker, R.M., Ziegler, M.G. & Coulter, J.D. Origins of Spinal Noradrenergic Pathways Demonstrated by Retrograde Transport of Antibody to Dopamine- $\beta$ -Hydroxylase. *Neurosci. Lett.*, **25**:243-249, 1981.
- Wiegand, S.J. & Terasawa, I. Discrete Lesions Reveal Functional Heterogeneity of Suprachiasmatic Structures in Regulation of Gonadotropin Secretion in the Female Rat. *Neuroendocrinol.*, **34**:395-404, 1982.



- Wurtman, R.J., Axelrod, & Fischer, J.F. Melatonin Synthesis in the Pineal Gland: Effect of Light Mediated by the Sympathetic Nervous System. *Sci.*, **143**:1328-1329, 1964.
- Yamadori, T., Nakamura, T. & Takami, K. A Study on the Retinal Ganglion Cell which has an Uncrossed Bifurcating Axon in the Albino Rat. *Brain Res.* **488**:143-148, 1989.
- Yanovski, J., Witcher, J., Adler, N., Markey, SP. & Klein, DC. Stimulation of the Paraventricular Nucleus Area of the Hypothalamus Elevates Urinary 6-Hydroxymelatonin During Daytime. *Brain Res. Bull.*, **19**:129-133, 1987.
- Yellon, S.M., Bittman, E.L., Lehman, M.N., Olster, D.H., Robinson, J.E. & Karsch, F.J., Importance of Duration of Nocturnal Melatonin Secretion in Determining the Reproductive Response to Inductive Photoperiod in the Ewe. *Biol. Reprod.*, **32**:523-529, 1985.
- Youngstrom, T.G. & Nunez, A.A. Neurons in the Suprachiasmatic Area are Labelled After Intravenous Injections of Horseradish Peroxidase. *Exp. Brain Res.*, **67**:127-130, 1987.
- Zieglansberger, W. Actions of Amino Acids, Amines and Neuropeptides on Target Cells in the Mammalian Central Nervous System. In: Buijs, R.M., Pevet, P. & Swaab, D.F. (Eds.), *Chemical Transmission in the Brain. The Role of Amines, Amino Acids and Peptides. Prog. Brain Res.*, Elsevier, Biomed. Press, Amsterdam, **55**:297-320, 1982.

MICHIGAN STATE UNIV. LIBRARIES



31293007903234